A modelling tool for dynamic simulation of task based solution crystallization processes

Master Thesis

L.C. Clement

Student number: 1256041

August 2012

P&E-2545

Faculty of Applied Sciences

Chemical Engineering

Process & Energy Department, Faculty of 3mE

Section Intensified Reaction & Separation Systems

Graduation Committee

Prof.ir. J. Grievink

Dr.ir. H.J.M. Kramer

Dr. R. Lakerveld MSc

A. Soare MSc

Prof.dr.ir. A.I. Stankiewicz

Abstract

The design of current industrial crystallizers is strongly focused on optimisation of known types of crystallization equipment. To get a better control over the physical events governing crystalline product quality the TU Delft started with the development of a task based design (TBD) strategy, which is an example of a phenomena based approach. Task-based design uses physical phenomena to construct tasks, which are used as building blocks for design. In this research, a modelling tool for dynamic simulation of task based solution crystallization processes is developed. This is an important step towards the long term aim of model-based optimisation driven process synthesis.

The developed TBD model can be applied to a wide range of crystallization processes: various crystallization methods, operation modes, configurations and a variety in number of streams, compartments and crystallization tasks. The modelling structure is based on compartmental modelling. A new way to connect tasks to this compartment model is developed. This framework supports rapid generation of consistent process models and facilitates analysis of the influence of individual tasks. The model is implemented in gPROMS.

To show the ability to quickly construct networks of units representing all kinds of crystallization processes, three different cases are simulated with the new model. Already existing innovative task based equipment from the TU Delft is also implemented, such as an airlift crystallizer, a membrane unit for solvent removal and an ultrasound vessel for the creation of primary nuclei.

The first case simulates batch cooling crystallization experiments of ammonium sulphate in an airlift crystallizer with tasks Growth and Seeding and a cooling curve. The results are in agreement with experimental values. Case 2 shows the effect of individual tasks on a batch adipic acid crystallization system using a membrane unit for solvent removal. To demonstrate the future potential of TBD, in the third case a crystallization process is modelled which is never experimentally tested: continuous crystallization of adipic acid in a cascade of airlift crystallizers. Influence of the crystallizers in series on the CSD width is investigated. As expected, more larger crystals with a narrower CSD are produced in the cascade of airlifts.

The results show that the developed structure works well. Using the task-function framework, newly developed tasks can be easily added, such that innovative Process Intensifications can be included in the model. The developed TBD model offers potential for model based process design of innovative task based crystallizers.

Special thanks to my supervisors

Prof.ir. Johan Grievink, Dr.ir. Herman J.M. Kramer and Anamaria Soare MSc

Table of Contents

Introduction

Crystallization is one of the most important separation processes in process, fine chemical, pharmaceutical and food industry. A large, still growing number of products rely on crystallization as a separation, purification or particle formation step. The development of industrial crystallization processes is however hampered by the existing design approach, which is strongly focussed on optimisation of known types of crystallization equipment. These crystallizers harbour various physical phenomena, which are strongly entangled. As a result major problems like limited flexibility and off spec and varying product quality cannot be addressed and solved adequately. A shift from equipment-based to phenomena based design is required to address these fundamental problems in industrial crystallization.

Recently the TU Delft started with the development of a task based design (TBD) strategy, which is an example of a phenomena based approach. The crystallization tasks, representing fundamental changes needed to arrive at desired product quality, are used as building blocks rather than existing equipment. The representation of process alternatives in terms of physical tasks is a suitable approach to achieve Process Intensification (PI). The main goal of PI is to make substantial improvements to the efficiency of chemical processes and plants with respect to the use of physical resources (mass, energy, …), processing times, equipment and lot size and the resulting economic and ecological resources. This can only be accomplished with truly innovative solutions, such as new task based crystallizers. (Lakerveld, Kramer en Stankiewicz, et al. 2010)

As the task based crystallizer can be built from an arbitrary number of crystallization tasks, the design of the integrated crystallization process will be complicated. Therefore a modelling and optimisation tool is needed which can be used to quickly analyse the different process alternatives. The model system should contain a library for the different crystallization tasks and a framework to build a network of these crystallization tasks to represent the final crystallization process. This MSc thesis project is meant to get a feel for the complexity of this modelling assignment.

The objective of this thesis is to develop a modelling tool for dynamic simulation of task based solutions crystallizers. With this model, it should be easy to rapidly generate consistent process models for a wide range of crystallization processes. This research is essential for the long term goal of model-based optimisation driven process synthesis. Part of this research is the construction of a relatively simple pilot task-based synthesis problem, such that this problem can be solved by simulation over a predefined connectivity structure between a fixed set of tasks. The model framework is implemented in general PROcess Modelling System (gPROMS Modelbuilder 3.5.1, Process Systems Enterprise Ltd., London, UK). The scope of this research is as follows:

- The crystallization step in the crystallization process is of interest here. The upstream part of the overall process (the origin of the feed) and the downstream solids processing after the crystallization system (slurry solid/liquid separation, washing, drying, granulation, grinding, etc.) are out of scope.

- Regarding the crystallization method, only solution crystallization is considered.
- This project is concentrated on dynamic simulation; not on optimisation.
- The focus of this research is on the generic modelling framework of a TBD model, hence complex kinetics are not a main concern.
- It should be possible to model both batch and continuous operations.
- The model should enhance easy creation of flowsheets using one basic building block (a so called compartment). An arbitrary number of crystallizers, number of feed streams and interconnectivity should be possible.
- The chemical systems modelled are ammonium sulphate and adipic acid from water.

The development of a model contains several steps, which are depicted in Figure 1 (Grievink 2012). This work is built on this principle. First the problem definition and modelling goal should be clear, so definitions regarding crystallization and task based design need to be known. In chapter 1 crystallization fundamentals are covered and chapter 2 introduces task based design for crystallization processes. Since the model will be used to quickly construct networks of units, representing all kinds of crystallization processes, a general structure should be developed. Chapter 3 introduces a general terminology and structure and a way to implement tasks in a compartment structure with conservations equations. The most important tasks are identified and tested. Chapter 4 is the task library, which lists the functional dependencies and the used rate laws of all tasks in the developed model. Chapter 5 covers the implementation of the TBD model using gPROMS. In chapter 6 model verification and validation are covered. Three task-based synthesis problem cases are worked out and discussed, that show the facilities of the TBD model and test individual tasks. The first case simulates experiments of batch solution crystallization of ammonium sulphate in an airlift crystallizer. Case 2 is designed to validate trends found in batch crystallization of adipic acid. The third case is a crystallization process that is not experimentally tested yet and shows the potential of TBD: continuous crystallization of adipic acid in a cascade of airlift crystallizers.

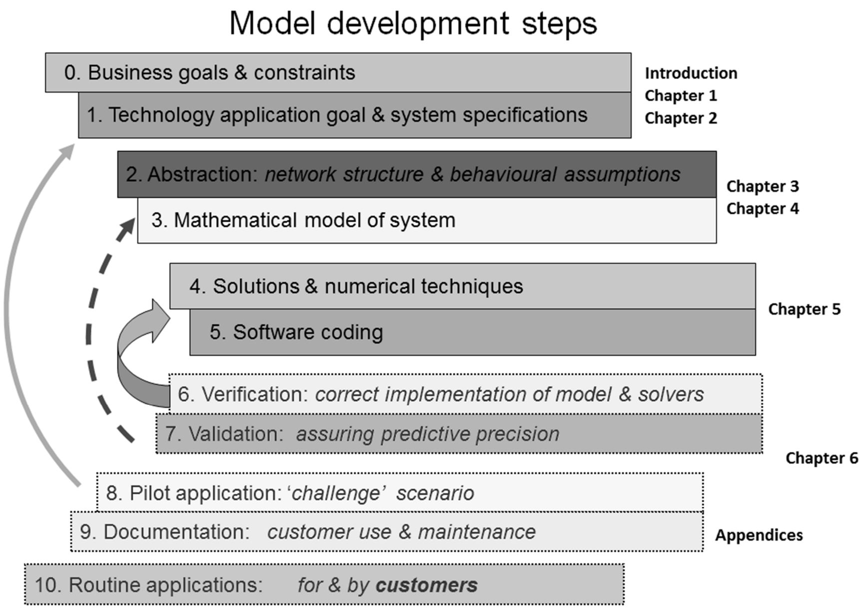

Figure 1: General model development steps (Grievink 2012) and connection to chapters of report

1 Crystallization Fundamentals

Before crystallization processes can be understood, a number of crystallization fundamentals need to be known. Below the driving force for crystallization, occurring physical processes and the aspects of product quality are covered. At the process level the population balance is important, which describes the control of crystal size and size distribution.

1.1 Definition and application of crystallization

Crystallization from solution is a separation technique where a solid crystalline phase is formed from a supersaturated mother liquor. The power of crystallization arises from the reproducibility of this process. Because the constituent atoms, ions or molecules of a crystal are arranged in a regular infinite manner, crystal surfaces only allow similar molecular-scale growth units to attach themselves to the crystal lattice. As a result crystals are highly effective in their separating power. Because 70% of the products sold by the process industry and the pharmaceutical industry - as bulk products, intermediates, fine chemicals, biochemicals, food additives and pharmaceutical products - are solids, crystallization in its widest definition is the largest separation process after distillation. (Kramer and van Rosmalen, Crystallization 2000) (Davey and Garside 2000)

1.2 Methods of Supersaturation Generation

Supersaturation

Crystallization only occurs when supersaturation is created, which acts as the driving force. Formally the supersaturation can be defined in thermodynamic terms as the dimensionless difference in chemical potential between a molecule in equilibrium state, and a molecule in supersaturated state. However, chemical engineers often write supersaturation in terms of concentration, known as the *concentration driving force*. In this thesis, relative supersaturation is used, which is defined as

$$\sigma = \frac{w - w_{sat}}{w_{sat}} \tag{1.1}$$

The saturation concentration, w_{sat}, depends on the system and is a function of temperature.

Supersaturation is a prerequisite for nucleation and growth, which are decisive not only for the formation of a solid phase but also for its occurrence; size distribution of crystals and their shape. The degree of supersaturation is determined by the flows of materials and energies, on the one hand, and by crystallization kinetics, such as nucleation and growth, on the other hand.

The solubility diagram

There are several ways to represent the *phase diagram*, showing the relation between temperature *T*, pressure *p*, composition *x* and the crystal structure of solid phases. For evaporative and cooling crystallization a *solubility diagram* is mostly used, in which the solubility of the compound is expressed as a function of temperature. Figure 1.1 shows a hypothetical solubility curve. A solution whose composition lies below the solubility curve is undersaturated and existing crystals will dissolve. A solution lying above the solubility curve is called supersaturated, since the amount of dissolved solute is greater than the equilibrium saturation value. At low supersaturations, although existing crystals will grow, it is difficult to create new crystals. Once some critical level of supersaturation is exceeded, new crystals form spontaneously and the solution is now called labile. The region between equilibrium and labile states is called the metastable zone.

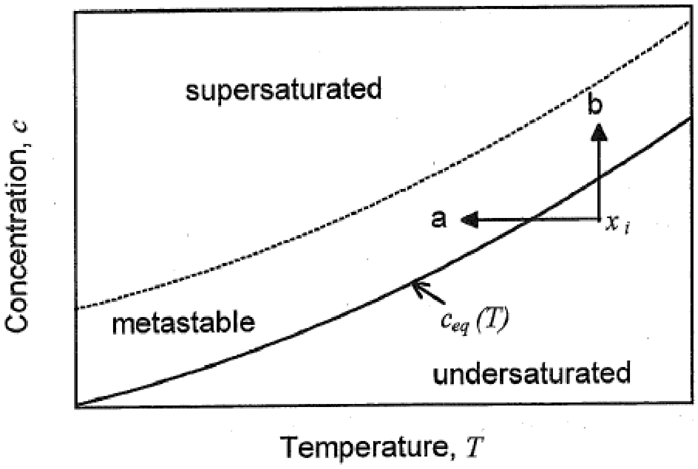

Figure 1.1: The solubility diagram (Davey en Garside 2000)

Crystallization methods

The crystallization method is mainly chosen on the basis of the thermodynamic and physical properties of the compound and the solvent, as well as on the required purity of the product. The nature of the external action to change the state of a solution from undersaturated to supersaturated determines the crystallization method:

- *Melt crystallization*: a melt is cooled below its melting point
- Crystallization from solution
    - *Cooling*: Decrease solubility by decreasing temperature
    - *Evaporative*: Increase concentration by evaporating solvent
    - *Precipitation*: Mix two well-soluble reactants to give a poorly soluble product
    - *Anti-solvent*: The solute is well-soluble in the original solvent, but is slightly soluble in the solvent/anti-solvent mixture

(Kramer and van Rosmalen, Crystallization 2000), (Rosmalen van, et al. 2003), (Kramer 2011)

1.3 Physical processes during crystallization

Below is a short overview of the most important physical processes occurring in crystallization. For a more in-depth description of the kinetics of these phenomena, the reader is referred to Chapter 4.

Primary Nucleation

Primary nucleation is the formation of a new solid phase from a clear liquid. This type of nucleation can be further subdivided into homogeneous and heterogeneous nucleation. In heterogeneous nucleation, nucleation starts on foreign substrates of mostly microscopic particles; dust or dirt particles. If such substrates are absent, new phase formation takes place by statistical fluctuations of solute entities clustering together, a mechanism referred to as homogeneous primary nucleation. Homogeneous nucleation rarely occurs in practice, as the presence of small quantities of microscopic particles is usually unavoidable.

Crystal growth and dissolution

Crystal growth is the addition of solute molecules from a supersaturated solution to the crystal lattice. Besides increasing crystal size, crystal growth also largely determines crystal morphology, surface structure and purity of the crystal. Crystal growth is a three-step process consisting of mass transfer, surface integration and heat transfer. Mass transfer and surface integration occur sequentially and in parallel with heat transfer. Mass transfer involves the diffusion of growth units (molecules, atoms or ions) to the crystal surface. Surface integration consists of surface diffusion, orientation and the actual incorporation into the lattice. Heat transfer is often a rate-limiting step in melt crystallization, but this is practically never the case in solution crystallization.

Crystals will dissolve if the concentration falls below the saturation level, which can happen due to dilution or temperature changes. The mechanism of crystal *dissolution* is not the exact opposite of growth. The release of solute molecules from the crystal lattice is generally speaking not a limiting step in the dissolution process. Therefore, the dissolution rate is typically governed by mass transport limitations only. Much faster dissolution rates compared to growth rates are measured in practice.

Mixing/Suspension

As a rule, crystals have a higher density than that of the surrounding liquid, which results in settling. Therefore a certain upflow current is needed in all crystallizers to compensate settling. As a result, crystallizers are equipped with rotors, such as stirrers or pump impellers, which induce *mixing*. Mixing is also used to minimize gradients in the bulk to enhance transport processes.

Secondary Nucleation

Nucleation of new crystals induced only because of the prior presence of crystals of the material being crystallized is termed *secondary nucleation*. This nucleation mechanism generally occurs at much lower supersaturations then primary nucleation. There are various types of secondary nucleation, but the most important source of secondary nuclei in crystallization is attrition. *Attrition*, also referred to as contact nucleation, occurs as a result of crystal-pump, crystal-vessel wall or crystal-crystal collisions.

Agglomeration and Breakage

An *agglomerate* is defined as the mass formed by the cementation of individual particles, probably by chemical forces (Randolph and Larson 1988). Agglomerates are usually undesirable because they contain mother liquor between the primary crystals that form the agglomerate. This liquor is hard to remove during drying, and promotes caking of the product during storage. Agglomeration first of all requires the collision of two or more crystals. The collision mechanism depends on the sizes of the crystals involved. Next, these crystals must form an aggregate as a result of interparticle forces. Finally, cementation of these crystals as a result of growth, before the aggregate is disrupted, is required to create an agglomerate.

Similar to attrition, *breakage* can occur as a result of crystal-pump, crystal-vessel wall or crystal-crystal collisions. The difference between breakage and attrition is not a distinct one. The fracture of a particle into one slightly smaller particle and many much smaller fragments is defined as attrition. Breakage involves the fracture of a particle into two or more pieces. The total fracture of a particle requires considerably more energy than attrition.

(Bermingham 2003), (Lakerveld 2010), (Mersmann 2001)

1.4 Product Quality

The requirements of the product rather than the method of creating supersaturation are decisive when selecting a crystallizer. The main product quality characteristics are:

- *Crystal Form & Shape* - The external appearance of a crystal is described in terms of morphology (the periodic structure of the crystal lattice) and habit (general shape of a crystal given by the relative length to width of the crystal faces). It is extremely difficult to predict the shape of crystals.
- *Crystal Size* - The crystal size and the width of the crystal size distribution. Crystal size influences performance characteristics such as filterability, settling behaviour, caking behaviour, bulk density and dissolution rates.
- *Purity* - Mechanisms affecting purity are inclusion of mother liquor in the lattice, entrapment of mother liquor in cracks, processes and agglomerates, incorporation of impurities in the crystal lattice and adsorption of impurities or solvent on crystal surfaces. Impurities increase the caking tendency, may lead to further reactions and incorrect chemical composition.

The quality components of the product are strongly influenced by the geometry and type of the crystallizer, the operating conditions, and the properties of the liquid and solid phases.

1.5 The Population Balance Equation

When one is purely interested in the yield and energy consumption of a certain crystallization process, solving the mass balances for the solvent, solutes and the solids together with the enthalpy balance will be sufficient. However, these balances provide no information on the number and size of the particles over which the crystal mass is distributed. When the crystal size distribution (CSD) of the solid phase is of interest, one needs to turn to the *population balance equation* (PBE). The PBE describes the way in which the size distribution of a crystal population develops in time as a result of various kinetic processes. This equation was introduced by Randolph in 1962 (Randolph and Larson 1988).

The PBE is encountered in many forms. The amount of particles can be expressed in terms of number, volume or mass densities, whereas particle size is usually expressed in terms of length or volume. The formulation of the PBE is based on the number density *n(L)*, which is derived from the number of particles per unit volume *N*. The number density n then derived as the limiting value of the number of particles per unit volume in the crystal size interval *ΔL*:

$$n = \lim_{\Delta L \to 0} \frac{\Delta N}{\Delta L} \tag{1.2}$$

The PBE arises by examining the particle numbers in a differential crystal size interval *dL*, as depicted in Figure 1.2. This interval can be entered by crystals that are in the feed. Crystals that are smaller than L_i can grow into the size interval to $L_i + dL$, and crystals ranging from L_i to $L_i + dL$ can grow out of the interval. Finally, effects such as crystal attrition, breakage, agglomeration, and dissolution occur. All these effects can be considered in a birth rate *B(L)* and a death rate *D(L)* for the interval concerned. For example, if a crystal in the interval breaks down into several fragments of roughly the same size, the original particle disappears or is eliminated from the interval. This is known as the death rate, *D(L)*. This effect can also occur when several crystals agglomerate; the agglomerate that has been formed belongs to a large particle size interval. If crystals that are larger than $L_i + dL$ break down, they may enter the interval in question and cause what is generally known as a birth rate, *B(L)*. If very small crystals are completely dissolved in an undersaturated area, they disappear from the interval concerned and no longer reappear in any other grain size interval.

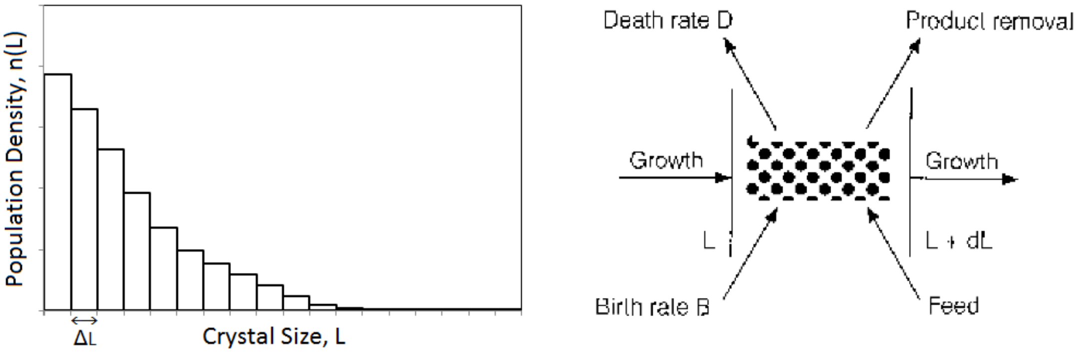

Figure 1.2: Left: Population density distribution, right (Mersmann 2001): zoom-in on one size domain *dL*

The PBE of particles in a specific volume can thus be described by the relationship:

Particle density accumulation = Particle inflow - Particle outflow + Net number of births

Mathematically in the most general form, the population balance is:

$$\frac{\partial n}{\partial t} + \nabla(\mathbf{v} \cdot n) + D(L) - B(L) = 0 \tag{1.3}$$

The vector ***v*** comprises an internal part ***v****$_i$* and an external part ***v****$_e$*:

$$\frac{\partial n}{\partial t} + \nabla \mathbf{v}_e \cdot n + \nabla \mathbf{v}_i \cdot n + D(L) - B(L) = 0 \tag{1.4}$$

The vector ***v****$_e$* is given by the external particle velocity in an external coordinate system (e.g., the crystallizer) and can be determined using a force balance of the individual particle. The internal velocity ***v****$_i$* orientates itself along an internal coordinate system (e.g., the particle). In a supersaturated solution the linear growth rate *G = dL/dt* of a crystal yields the most important factor for the internal velocity.

In practice the crystallizer is often considered to be well mixed, given the fact that roughly the same particle size distribution is found throughout the entire volume. Therefore, on the condition that the system is well mixed, the distributed model can be transformed in a lumped model, where there are no spatial variations in the external coordinates. In such cases, a suitable volume *V(t)* of external phase space can be chosen. The population balance can then be transformed into a balance over a macroscopic external coordinate region, by integration over *V(t)*. The resulting PBE is:

$$\int_V \left(\frac{\partial n}{\partial t} + \nabla \mathbf{v}_e \cdot n + \nabla \mathbf{v}_i \cdot n + D(L) - B(L) \right) dV = 0 \tag{1.5}$$

The following relations for the internal and external velocities can now be used:

$$\int_V \nabla \mathbf{v}_e \cdot n dV = \sum_k \phi_{V,k} n_k + n \frac{dV}{dt} \tag{1.6}$$

$$\nabla \mathbf{v}_i \cdot n = \frac{\partial}{\partial L}(Gn) \tag{1.7}$$

The general equation for the PBE of a crystallizer having constant volume *V* becomes:

$$\frac{\partial nV}{\partial t} + V \frac{\partial (Gn)}{\partial L} + VD(L) - VB(L) - \sum_j \phi_{V,in,j} \cdot n_{in,j} + \sum_j \phi_{V,out,j} \cdot n_{out,j} = 0 \tag{1.8}$$

If there is a difference in flow pattern of the liquid and solid phase due to particle slip, or there is fines or product classification to increase the average crystal size and/or stabilise the crystallizer with respect to the CSD, classification functions *h_j* can be added to the outgoing stream (see paragraph 4.10):

$$n_{out,j} = n \cdot h_j(L) \tag{1.9}$$

As the PBE is a partial differential equation with respect to time *t* and crystal length *L*, two boundary conditions are needed to solve it. As primary and secondary nucleation typically involve the birth of small crystals, nucleation is often presented as the birth of nuclei at zero size. Instead of a birth term in the PBE for the nucleation event that happens over a size range from 0 to L_{max}, the birth rate B_0 given by the boundary equation is used. For the second boundary condition, a seed population or a population formed by the outgrowth of primary nuclei can be substituted.

$$\begin{aligned} n(L=0,t)\left[\frac{\#}{m^3 m}\right] &= \frac{B_0(t)}{G(L=0,t)} \\ n(L,t=0) &= \text{ Initial distribution} \end{aligned} \tag{1.10}$$

(Mersmann 2001) (Kramer and van Rosmalen, Crystallization 2000) (Rosmalen van, et al. 2003)

2 Task Based Design

In this chapter, task based design for crystallization processes is introduced. It covers how current crystallization process design can be improved, the task concept, novel processing units and model based optimisation of a task based crystallization unit. This chapter is based on previous work from Bermingham (2003), Menon (2006) and Lakerveld (2010).

2.1 Current status crystallization process design

Crystallization is one of the older unit operations in the chemical industry, but severe problems are still frequently encountered during the design and operation of crystallization processes. These problems may be related to product quality requirements, such as filterability, caking behaviour and purity, and process requirements, such as production capacity and plant availability. A number of the above-mentioned problems are related to decisions taken during the design stage. The selection of crystallization equipment is traditionally done from a limited number of state-of-art industrial crystallizers followed by optimisation of that particular type of equipment. The design of the crystallizer unit itself receives less attention. This way of design leads to (Lakerveld, Kramer and Stankiewicz, et al. 2010):

- **Limited flexibility**. Optimisation is limited to the options the selected type of equipment offers. Multiple physical phenomena (including mixing, mass and heat transfer, various forms of crystal nucleation, crystal growth, generation of supersaturation, and dissolution) take place simultaneously, which makes the optimisation with respect to individual phenomena practically impossible due to the strong entanglement between them. Therefore there is limited flexibility to produce different grades of product.
- **Limited predictive capabilities of state-of-art models**. Crystalline products are more complicated compared to liquid products, because besides composition and purity also typical solid phase properties like shape, polymorphic form and size distribution have to be taken into account. Prediction of product quality is difficult because of the unclear entanglement between physical phenomena, which also strongly depends on scale of operation.
- **Process instability and dynamics**. The entanglement of physical phenomena results in strongly non-linear process behaviour, giving rise to long start up times due to oscillations or even sustained oscillations. This also reduces the window of available combinations of operational parameters for stable operation. As a result of these instabilities and response dynamics, a significant amount of off-spec product can arise.
- **Limited controllability**. The options for actuation are also limited to what is offered by the equipment. There is limited control over physical phenomena.

2.2 Task Based Design Philosophy

A shift in thinking is necessary to drastically improve on the design of crystallization processes. Process intensification by making significant reduction in the size of chemical plants, amount of off-spec products and the utilization of resources is wanted. To facilitate such principles, a design approach is needed which considers the important phenomena as starting point for design rather than the equipment itself. The physical phenomena are of key importance as in the end they determine the properties of the crystalline product. This fact has been the starting point of a task-based design strategy for industrial crystallization which is a novel approach for the conceptual design of crystallization process units. Task-based design uses physical phenomena to construct tasks, which are used as building blocks for design. The order of task-based design is as follows (Menon 2006):

1. Establishing specifications for the final (product) state and for the initial (feed related) states
2. Setting up a sequence of tasks in going from initial to final state
3. Identifying the proper physical phenomena to perform such tasks
4. Establishing the internal rate processes to enhance the tasks and grouping these in (new) operational units by selecting compatible operating conditions and space-time requirements
5. Finding spatial arrangements for selected, feasible combinations of tasks in equipment

Figure 2.1 shows the comparison between the current design method and task based design.

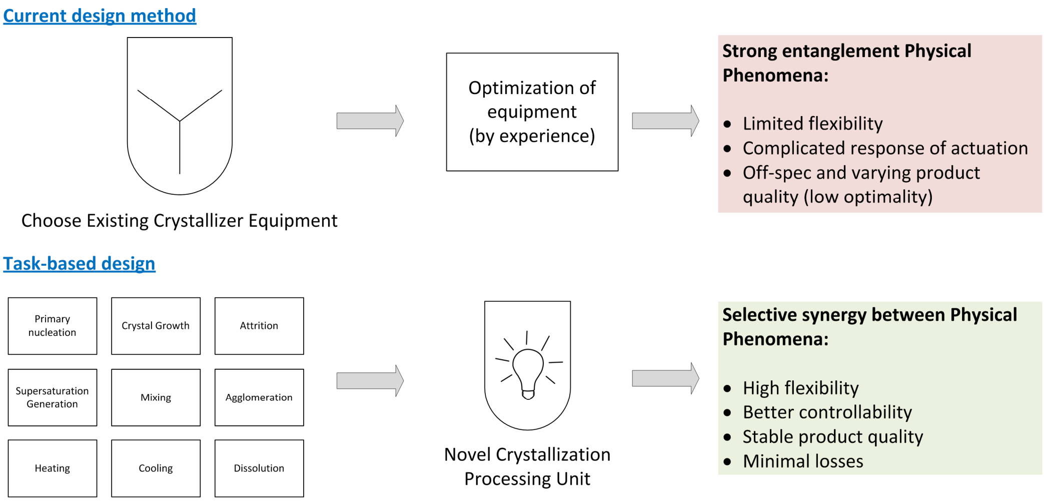

Figure 2.1: Current design method and task based design

2.3 The Task Concept

The new building block for process synthesis is the task. A **task** aims to accomplish the transition of a target process variable (composition, temperature, phase, supersaturation, size distribution,…) from an initial state to a desired state, enabled by suitable physical phenomena. The tasks to be designed are characterized by physical events that are driven by forces resulting in rate processes towards thermodynamic equilibrium. The forces are the result of deviations from equilibrium, which can be classified as

1. Thermal (temperature difference)
2. Mechanical (pressure, shear force)
3. Chemical (composition)
4. Electrical (potential difference)
5. Gravitational

The **rate processes** of tasks, which move the state variables, can be expressed as

$$r(t) = J \cdot A = k \cdot \Delta\mu \cdot A \qquad (2.1)$$

One can optimise the transformation of the targeted variables attributed to the tasks with kinetic rates by manipulating the rate constants (*k*) and the main driving force (*Δμ*) for generation of a flux (*J*), and the area over which the flux acts (*A*). An example of a task is given in Figure 2.2. **Driving forces** can be created and used to obtain the values for the targeted variables of the tasks, which ultimately aim to reach the desired product quality. The question is how to induce and utilize physical phenomena to obtain the desired rate processes, leading to the targeted values. Tasks are classified according to the involved thermodynamic phases, the range of suitable operating conditions, and possible driving forces. (Lakerveld 2010)

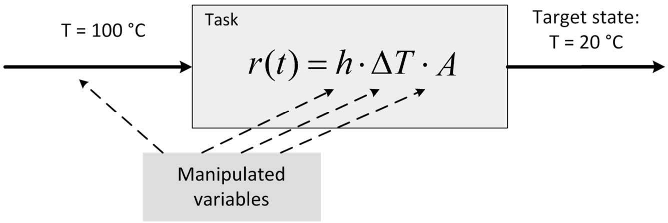

Figure 2.2: Example of the task "Cooling". A stream of 100°C needs to get to the target state of 20°C. To get to this state the following variables can be manipulated: the flowrate, the heat transfer coefficient (which in the design can be manipulated by for instance the surface texture or flow regime), the temperature difference between cooling medium and the stream and the area of heat transfer.

2.4 Novel processing units

For crystallization processes it is difficult to specify physical devices that will execute a single crystallization task as current crystallizers facilitate many of those tasks and the control of individual tasks is not possible. Novel process units are needed to tightly control and possibly enlarge the window of operation for selected crystallization tasks. Those new process units should utilize new methods with alternative driving forces that specifically target a certain task in an attempt to disentangle the physical phenomena, which makes individual optimisation of driving forces possible. Examples are well-defined spaces for primary nucleation (e.g. induced by ultrasound, laser light, magnetic, or electric fields), secondary nucleation (e.g. with stirrer, ultrasound), supersaturation generation (solvent removal using a membrane surface), crystal size manipulation (agglomeration, dissolution, and growth, for example with air-mixed devices).

At the TU Delft, small scale experiments are done with newly built dedicated equipment that makes it possible to isolate and optimise single crystallization tasks. These are isolation of the task crystal growth by using an airlift crystallizer, isolation of supersaturation generation using membranes and the task primary nucleation using ultrasound. These experiments demonstrate the (experimental) feasibility of the TBD approach. (Lakerveld, Kramer and Jansens, et al. 2009)

Although the applications of the novel processing units offer opportunities to improve crystallization processes individually, the real strength is in the combination of the studied experimental setups. The combination creates a crystallization process unit in which production performance is optimised by tailoring the individual tasks. The classification of tasks mentioned earlier can be used to systematically screen for options for combination of tasks in processing compartments. A processing compartment is a spatial region in which a number of tasks are executed in parallel or in a fixed sequence. This aims to exploit synergistic effects and realize process integration for tasks which can be done simultaneously in the same space and/or time and which do not interfere with each other. Unfortunately, in addition to the target rate process, some parasitic rate processes will arise induced by the presence of several driving forces in the compartment. For a good design the parasitic rates must be much lower than the task related rate processes. If small enough, they can be ignored.

2.5 Model based optimisation of a task based crystallization unit

The challenge now is to identify associated physical mechanisms of tasks. The required knowledge can be obtained from small scale experiments in combination with model development. Those models are likely to have improved predictable capabilities compared to models of conventional crystallization equipment in which the effect of simultaneous execution of various coupled tasks is difficult to predict.

State Task Network and Superstructures

The Task Based Design concept shows similarities with the *state task network* (STN, (Kondili, Pantelides and Sargent 1993)) as a representation of multiproduct/multi-purpose batch processes. The main idea is to make a clear distinction between thermodynamic states and tasks accomplishing the changes between those states. The STN represents the physical process itself, but unit operations and their connectivity are not shown explicitly. Equipment that can execute a single crystallization task can be assigned in a STN, which makes optimisation of that particular task as well as optimisation of the interconnections between tasks possible. The aim is to construct the crystallization process from this STN, in such a way so as to achieve the desired product specifications. This allows for the generation of a *superstructure*. A superstructure is a structure in which all process alternative structures of interest are embedded and hence, are candidates for feasible or optimal process flowsheets. (For more information about superstructures, the reader is referred to Biegler, Grossmann and Westerberg (1997).) Such a task-based superstructure for the overall process can be subjected to Mixed Integer Dynamic Optimisation making use of multiple resources (mass, energy, money, etc.) and subject to (Menon 2006):

- *Behavioural models* for each task block with constraints
- *Structural models* for connectivity between task blocks
- *Plant wide controllability* models as physical/operational constraints
- *Performance models* with minimum performance constraints

This work focusses on the first category: models for predicting physical behaviour. Optimisation of the task superstructure can be realized based on product quality, throughput or economic evaluation of the process and can be dependent on design constraints. The superstructure makes use of a Task Library, which contains all rate processes for all tasks.

Requirements for a task based crystallization process modelling tool

A task based process and product model should take into account that industrial crystallization is a spatially distributed and time dependent process involving a product with distributed properties. Therefore ideally the model would contain components such as (Bermingham 2003):

- First principle kinetic models for all tasks
- First principle thermodynamic models to calculate phase equilibria (*S/L/V*), attachment energies (morphology prediction) and periodic bond chain analysis (polymorph prediction).
- First principle hydrodynamic models to calculate liquid motion, particle motion, fluid shear, energy dissipation rates, etc.
- Equations of conservation: component mass balances, energy balances and population balances. The number of distributed properties taken into account (such as size, lattice strain and purity) determines the number of internal coordinates necessary in the population balance.

Current status of task based design modelling

To meet the above requirements, the designer needs to know the detailed geometric parameters of the crystallization equipment, the intrinsic kinetic parameters, etcetera, which are not available at this level yet. Secondly, for certain crystallization phenomena, present computational capabilities are barely sufficient to perform simulations let alone optimisation calculations (as required for design purposes) using a first principle model of that single phenomenon. Regarding the superstructure, solving a superstructure is a difficult optimisation problem involving a mixture of continuous, integer, and logical variables and relationships. Consequently, heuristics, tabulated data, laboratory and pilot plant scale experiments continue to constitute a major part of the domain knowledge necessary for the design and optimisation of crystallization processes. Furthermore, rather than using detailed distributed product composition and quality parameters, simplified modelling including one or two lumped quality parameters can be used. Nobody solved and implemented this more fundamental approach to process synthesis yet. Firstly, a simulation environment needs to be developed for the simulation and optimisation of a task based crystallizer. Therefore this research will be a pre-cursor to more general computational multi-scale model which is just shown.

3 Model Development

This chapter describes how the TBD model is developed. First a general terminology and structure is described. A way to implement tasks in a compartment structure with conservations equations is introduced in a manner which is as general and intuitive as possible. The chapter concludes with how to model various types of crystallization processes and task restrictions.

3.1 Model Terminology & Structure

Compartmental Modelling

The modelling framework needs to support rapid generation of consistent process models for a wide range of crystallization processes. This can be done using *compartmental modelling*. Compartments represent volumes of the crystallizer in which conditions are considered uniform. For modelling flexibility the single compartment model is the general building block for the TBD model. This means that all compartments in the TBD model should be described with the same generic compartment model, with the same equations of conservation, physical and thermodynamic property relations, structures for kinetic rate expressions and parameters. Differences between compartments should be easy to create, using functionalities that can easily be changed per compartment. For setting up a flowsheet for instance, the compartment model should allow an arbitrary number of inlet and outlet streams. (Bermingham 2003)

An important aspect in compartmental modelling if one wants to start optimising, is that the use of compartmental models introduces new model parameters that need to be determined; the number of compartments, the size of the compartments, and the exchange rates between the compartments. The relation between the size or volume and the flowrate of a compartment is the residence time:

$$\tau[s] = \frac{V}{\phi_V} \tag{3.1}$$

One can take these decisions based on residence time; choose a time that is enough to execute a main task but supresses unwanted tasks. One should then keep in mind empirical insights regarding the volume: one large compartment can cause unwanted side effects, whereas a lot of small compartments can be very expensive. Furthermore, the values for these parameters determine whether the influence of crystallizer geometry and operating conditions on the hydrodynamics will be captured correctly. Obtaining correct values for these parameters is thus a key issue.

Terminology & Hierarchy

Before the model can be constructed, it is important to develop a general terminology and hierarchy for all the aspects of the modelling tool. This is largely based on (Menon 2006). The model has several layers, from higher to lower level:

- **Process** - Any operation or series of operations by which a particular (crystallization) objective is accomplished. (Felder en Rousseau 2000)
- **Flowsheet** - Conceptual representation of a process which shows connectivity of units and flows.
- **Operational Unit** – The tasks and compartments must have a real-life embedding or containment. Such containment for a task, task-zone, design compartment or design zone will be called an ‘operational unit’. It is equivalent with an apparatus or equipment, taking into account it can be new apparatus or equipment that does not currently exist. Examples of operational units are vessel, pump, membrane unit and heat exchanger.
- **Compartment** - A spatial region in the operational unit in which a combination of tasks can be carried out. Compartments are connected with **streams**. The state of this stream can be characterized by mass flow, energy, momentum, number of phases, phase ratios, composition per phase, T, p, particle size distribution (for mobile solid particles), etcetera. In this thesis the stream is a combination of phases. One can also construct streams having multiple thermodynamic phases wherein the phases have equal temperature and pressure.
- **Task** - To perform a task, it is necessary to construct a **physical event** to realize its **duty**. In a design context, the task is a conceptual construct to describe an intentional physical/chemical transformation. The **duty** is defined in terms of the desired change in the target variable and the associated amount of resource (mass of a species, energy,….) needed to accomplish that transformation. The duty of a task can only be achieved by means of a **physical event** (which can be visualized as a real-life vehicle). An event is characterized by **rate processes** which are required to change the initial state to the final target state. This is made possible by the use of one or more **driving forces** (thermodynamic, mechanical, electrical, gravitational, …) as is described in chapter 2.
- **Phase Building Block** - Often driving forces emerge from differences between the physical states of two phases that are brought into contact. Hence, one can construct a physical event by combining the relevant thermodynamic phases together. Each phase in a compartment is given here its own **phase building block** (PBB), which facilitates a change in the state variables of the respective material phase stream entering the respective phase building block. A **connection** is made between a task and a PBB. (Note that the location is different from the location in (Menon 2006), because there phase building blocks are in tasks, whereas here PBBs are in the compartment.) In this thesis, the gas phase is not modelled, and solid and liquid phase are taken together in a pseudo slurry phase.

Concerning phases, it is also possible to assign **immobile phases**. When a solute is removed from the liquid phase into the solid phase due to crystallization, this exchange is solely based on thermodynamic considerations. But, there can also be an exchange between the mobile solid phase and the immobile solid phase, which can be purely due to mechanical interactions. Examples are collisions of particles or heat exchange with a foreign body, where the foreign body could be an impeller or just the vessel wall, or mass transport to a membrane solid phase. All these exchanges result in changes to the state variables in the liquid/solid/gas phase, which ultimately provide the realization of a given task. In this thesis all immobile phases are considered inert. All above stated aspects and two examples are illustrated in Figure 3.1.

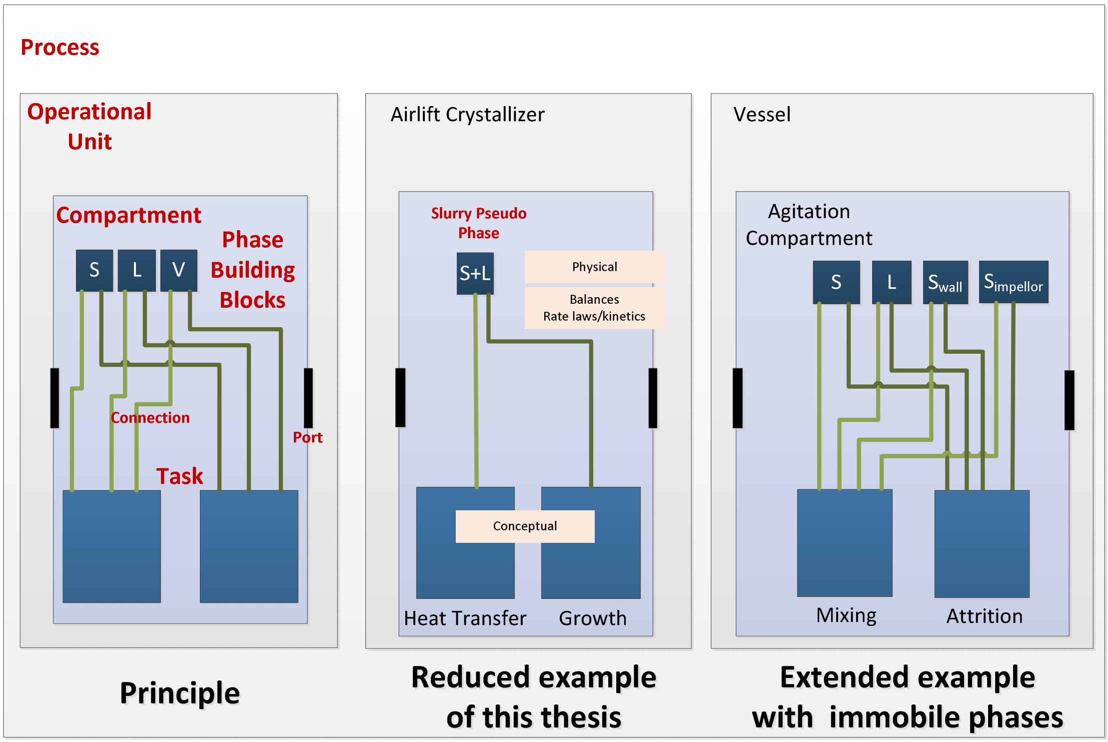

Figure 3.1: Task Based Design model terminology and hierarchy

3.2 Conservation Equations

The combined effect of the kinetics, convective transport and operating conditions on the dynamic process and product behaviour is determined by the equations of conservation. Since the conservation equations are used to describe a compartment, which is considered well-mixed, the equations are written in geometrically lumped form. Multiple thermodynamic phases need to be taken into account: vapour, liquid and solids. In the model described here, only the slurry phase is modelled in which solids and liquids are taken together. In Appendix A these equations are derived in detail, and the results are summarized below. Presented here are the equations of conservation for a single-solute single-solvent system. An overview of all the assumptions is given in Appendix B.

In chapter 1, the general equation for the population balance of a crystallizer having constant volume *V* is introduced:

$$\underbrace{\frac{\partial n(L,t)V(t)}{\partial t}}_{\substack{\text{Number rate of}\\ \text{accumulation [\#/m·s]}}} = \underbrace{-V(t)\frac{\partial(n(L,t)\cdot G(L,\sigma))}{\partial L}}_{\text{Rate of number gain by crystal growth and dissolution}} \underbrace{+\sum_{j}^{Ni}\phi_{V,in,j}\cdot n_{in,j}-\sum_{j}^{No}\phi_{V,out,j}\cdot n_{out,j}}_{\text{Number rate in and out}} + \underbrace{V(t)\cdot B(L)}_{\substack{\text{Number production rate due to}\\ \text{birth of crystals}}} + \underbrace{V(t)\cdot D(L)}_{\substack{\text{Number consumption rate due to}\\ \text{death of crystals}}} \qquad (3.2)$$

The population balance is in fact a distributed mass balance for a solid or dispersed phase, and is linked to the liquid or continuous phase component mass balances via the crystallization kinetics. This can be seen in the formulation of the other conservation relations. The so called moments (m_j) of a distribution can be related to lumped properties of the entire crystal population and are defined as:

$$m_j(t)\left[\frac{m^j}{m^3}\right] = \int_{L_0}^{\infty} n(L,t)L^j dL \tag{3.3}$$

The first five moments are related to measurable physical properties of the distribution such as total surface area A_T and total mass M_T:

$$A_T\left[\frac{m^2}{m^3}\right] = k_A m_2$$

$$M_T\left[\frac{kg}{m^3}\right] = \rho_c k_V m_3 \tag{3.4}$$

The coupling of the PBE with the conservation equations is done via the growth-moment, which represents an interphase mass flux between the liquid and solid phase:

$$gm_2\left[\frac{\#}{s}\right] \equiv 3\int_{L_0}^{\infty} GnL^2 dL \tag{3.5}$$

One can set up a total mass balance for the slurry:

$$\frac{dm^{(s+l)}}{dt} = \phi_{m,in}^{(l)} + \phi_{m,in}^{(s)} - \phi_{m,out}^{(l)} - \phi_{m,out}^{(s)} - \Psi^{(l\rightarrow v)} \tag{3.6}$$

The last term is a so called *transfer term*, describing an interphase flux. Use the following:

$$m^{(s+l)} = \varepsilon\rho_l V + (1-\varepsilon)\rho_c V \tag{3.7}$$

$$\phi_m^{(s+l)} = \phi_V(\varepsilon\rho_l + (1-\varepsilon)\rho_c) \tag{3.8}$$

For implementation in the model this needs to be worked out to prevent index issues (see chapter 5). This leads to the total mass balance, relating the rate of change of the volume of the system to the crystal growth term and the balance of the input and output streams:

$$\underbrace{\rho_l\frac{dV}{dt} - (\rho_l - \rho_c)k_v Vgm_2}_{\text{Accumulation [kg/s]}} = \underbrace{\sum_j^{Ni}\phi_{V,in,j}\rho_l}_{\text{Inflow}} - \underbrace{\sum_j^{No}\phi_{V,out,j}\rho_l}_{\text{Outflow}} - \underbrace{\phi_{V,vap}\rho_v}_{\text{Transfer-term}} \tag{3.9}$$

Initial condition:

$$V(t=0) = V_{init}$$

The mass balance for liquid phase component *i* has the form:

$$\underbrace{\frac{dm}{dt}{}_i^{(l)}}_{\text{Accumulation [kg/s]}} = \underbrace{\phi_{m,i,in}^{(l)}}_{\text{Inflow}} - \underbrace{\phi_{m,i,out}^{(l)}}_{\text{Outflow}} - \underbrace{\Psi_i^{(l\to s)} - \Psi_i^{(l\to v)}}_{\text{Transfer-terms}} + R_i \tag{3.10}$$

Where

$$m_i^{(l)} = \varepsilon \rho_l V w_{l,i} \tag{3.11}$$

Where R_i is the mass production rate due to liquid phase reactions. A similar balance can be set up over the solid phase, and this can again be combined to a slurry phase balance. Now apply this to a single-solute single-solvent system, assuming that the vapour flow only contains solvent. The slurry phase component mass balance for the solute can be rewritten as follows:

$$\underbrace{V\varepsilon\rho_l \frac{dw_l}{dt} + \rho_l w_l \frac{dV}{dt} - \left(\rho_l w_l - \rho_c w_c\right) k_v V g m_2}_{\text{Accumulation [kg/s]}} = \underbrace{\sum_j^{Ni} \phi_{V,in,j} \left(\varepsilon_{in,j}\rho_l w_{l,in,j} + \left(1-\varepsilon_{in,j}\right)\rho_l w_l\right)}_{\text{Inflow}} - \underbrace{\sum_j^{No} \phi_{V,out,j}\rho_l w_l}_{\text{Outflow}} \tag{3.12}$$

Initial condition:

$$w_l(t=0) = w_{l,init}$$

With

$$\begin{aligned} &\varepsilon(t) = 1 - k_V m_3(t) \\ &m_3(t) = \int_{L_0}^{\infty} n(t)\cdot L^3 dL \\ &\sum w_l(t) = 1 \end{aligned} \tag{3.13}$$

The crystal weight fraction in the solute (1) and the solvent (2) are constant. In this thesis, the crystal weight fractions of formula (3.14) are used. Note that in case of hydrates, that contain water molecules as part of the crystal structure, this can be different.

$$\begin{aligned} w_{c,1} &= 1 \\ w_{c,2} &= 0 \end{aligned} \tag{3.14}$$

The sum of all component balances (solutes + solvent) equals the total mass balance. Therefore the solvent mass balance is not used; it is not independent of the total mass balance.

The dynamics of the temperature are given by the energy balance. In this case, the energy balance can be transformed into the enthalpy balance:

$$\frac{dH^{(s+l)}}{dt}=\phi_{H,in}^{(s+l)}-\phi_{H,out}^{(s+l)}-\Psi^{(l\to v)}+Q(t)-W_S \tag{3.15}$$

$$H^{(s+l)}=\varepsilon V\rho_l c_{p,l}T+(1-\varepsilon)\rho_c\left(c_{p,c}T+dH_{crys}\right) \tag{3.16}$$

The enthalpy of crystallization *dH_{crys}* is the amount of heat to be added or removed at a constant temperature during crystallization and is equal to the negative value of the heat of solution that applies when crystals dissolve. An example for a possible immobile phase here would be a transfer term for a solid wall, to incorporate the heating of the walls. Fill in the expression for *H* and obtain:

$$\underbrace{V\left(\varepsilon\rho_l c_{p,l}+(1-\varepsilon)\rho_c c_{p,c}\right)\frac{dT}{dt}-\left(\rho_l c_{p,l}T-\rho_c\left(c_{p,c}T+dH_{crys}\right)\right)k_v Vgm2+\rho_l c_{p,l}T\frac{dV}{dt}}_{\text{Accumulation [J/s]}}$$
$$=\underbrace{\sum_{j}^{Ni}\phi_{V,in,j}\left[\rho_l c_{p,l}T+\left(\varepsilon_{in,j}\rho_l c_{p,l}+\left(1-\varepsilon_{in,j}\right)\rho_c c_{p,c}\right)\left(T_{in,j}-T\right)\right]}_{\text{Enthalpy Inflow}}$$
$$-\underbrace{\sum_{j}^{No}\phi_{V,out,j}\rho_l c_{p,l}T}_{\text{Enthalpy Outflow}}-\underbrace{\phi_{V,vap}\rho_w\left(c_{p,w}T+dH_{evap}\right)}_{\text{Enthalpy out by evaporation}}+\underbrace{Q_{heat}}_{\substack{\text{Net rate of}\\ \text{heat addition}}}-\underbrace{W_s}_{\substack{\text{net rate of}\\ \text{shaft work}}} \tag{3.17}$$

Initial Condition:

$$T(t=0)=\mathrm{T}_{init}$$

A further development of the model would contain fluid-dynamics of the slurry, therefore in addition to matter and energy, the changes in momentum (pumping, compression) should be involved as well in the future.

(Kramer 2011) (Bermingham 2003)

3.3 Transformation to a Task based design compartment model

Task-functions

The next step is to find a way to implement tasks in a compartment structure with balances in a manner which is as general and intuitive as possible. All tasks need to be turned on or off in the same manner. To make a general compartment model with addition of tasks possible, the balances are rewritten with so called *task-functions*, which are used to implement the tasks. The philosophy behind these task-functions is as follows. Tasks are modelled in task sub-models, which contain rate functions. A task rate is denoted by T (Greek capital letter Tau). All tasks that are implemented in the conservation equations in a similar way are summed in one task-function. By default, all tasks are zero, so all task-functions are zero. By turning the tasks on or off in the compartment model, a task rate will be sent to the compartment model, and will be incorporated in the calculation of the conservation equations. The task-functions in this thesis are defined as follows, but after more development this can be changed:

The Growth Task-function contains all tasks that are implemented via the growth term of the population balance. These are tasks Growth and Dissolution:

$$G(t)\left[\frac{m}{s}\right]=\sum \mathrm{T}_G=\mathrm{T}_{G,GROWTH}+\mathrm{T}_{G,DISSOLUTION} \tag{3.18}$$

Classification Task-function is multiplied by the outgoing number density stream of the population balance:

$$C(t)[-]=\sum \mathrm{T}_C=\mathrm{T}_{C,CLASSIFICATION} \tag{3.19}$$

All birth and death terms in the population balance that are distributed over the crystal size *L* are put in one Birth Death Task-function *Y*:

$$Y(t)\left[\frac{\#}{m^3 ms}\right]=\sum \mathrm{T}_Y=\mathrm{T}_{Y,BIRTH}-\mathrm{T}_{Y,DEATH} \tag{3.20}$$

Seeding is implemented via the boundary condition of the population balance and is put in an Initial Distribution Task-function:

$$I(L,t=0)\left[\frac{\#}{m^3 m}\right]=\sum \mathrm{T}_I=\mathrm{T}_{I,SEEDING} \tag{3.21}$$

All tasks modelled at the lower boundary of the crystal size domain, such as the nucleation task, are gathered in the Nucleation Task-function. Here the strength of the tasks functions can be seen. There is more than one option to create nucleation and all these options with their rate laws can be turned on and off individually. Furthermore, if in the future another option is developed, or a more in detailed kinetic rate law is found, this can be easily added in the task-function.

$$N(L_{\min},t)\left[\frac{\#}{m^3 s}\right]=\sum \mathrm{T}_N=\mathrm{T}_{N,PN,ULTRASOUND}+\mathrm{T}_{N,PN,SUPERSAT}+\mathrm{T}_{N,SN,ATTRITION} \tag{3.22}$$

Supersaturation generation can be done in several ways, including cooling and solvent removal. For solvent removal, both membranes and evaporation are considered. Since evaporation also has an influence on the enthalpy balance and membrane has not, these tasks have separated task-functions. If in the future there will be a connection between membrane usage and the energy input, this needs to be modelled using the task-function. The Solvent Removal Task-function and the Solvent Evaporation Task-function are as follows:

$$M(t)\left[\frac{kg}{s}\right] = \sum \mathrm{T}_M = \mathrm{T}_{M,MEMBRANE} \tag{3.23}$$

$$E(t)\left[\frac{kg}{s}\right] = \sum \mathrm{T}_E = \mathrm{T}_{E,EVAPORATION} \tag{3.24}$$

Cooling and Heating are also implemented in the enthalpy balance via the same source/sink term. Therefore these can be added in the Heat Transfer Task-function. It is important to mention that alternative physical events can exist to perform the same task. These tasks will therefore have different rate laws, but will be implemented via the same term in the conservation laws. For example, the task heating can be accomplished both by thermal heat transfer and by for instance microwaves. In this manner, future innovations can be easily added into the model.

$$Q(t)\left[\frac{J}{s}\right] = \sum \mathrm{T}_Q = \mathrm{T}_{Q,COOLING,JACKET} + \mathrm{T}_{Q,HEATING,JACKET} \tag{3.25}$$

All rate laws ‘behind’ these tasks are given in Chapter 4.

The task Mixing is not yet implemented, since it is a special task. It is not an isolated task, but has a direct influence on several other tasks, such as attrition, classification and shaft work. This implementation still needs to be developed.

Furthermore, another task that is not yet implemented is Shaft Work. This work is done by several means: the impellor, the membrane pump etcetera.

The assignment of immobile phases for the wall, impellor and membrane offers a lot of future potential to further develop and generalize the task based design model. Then, extra transfer terms need to be added to the conservation equations.

Rewriting the conservation relations

Up to now the conventional way of writing conservation relations for crystallization processes is explained. To develop a TBD model, it is necessary to make a clear distinction between all the tasks using the task-functions. Below, all conservation relations are rewritten using these task-functions.

The population balance can be described in terms of task-functions as:

$$\frac{\partial nV}{\partial t} = -V\frac{\partial nG}{\partial L} + \sum_{j}^{Ni} \phi_{V,in,j} \cdot n_{in,j} - \sum_{j}^{No} \phi_{V,out,j} \cdot n \cdot C + V \cdot Y \tag{3.26}$$

Also a change in formulation in the boundary conditions occurs:

$$\begin{aligned} n(L=0,t)\left[\frac{\#}{m^3 m}\right] &= \frac{N(t)}{G(L=0,t)} \\ n(L,t=0)\left[\frac{\#}{m^3 m}\right] &= I(L) \end{aligned} \tag{3.27}$$

A new way of writing the total mass balance is:

$$\rho_l \frac{dV}{dt} = \left(\rho_l - \rho_c\right) k_v V g m_2 + \sum_j^{Ni} \phi_{V,in,j}\rho_l - \sum_j^{No} \phi_{V,out,j}\rho_l - E - M \tag{3.28}$$

New is that solvent that is removed via a membrane system was previously modelled via an extra outgoing stream, whereas now it is a separate term so that it is easy to turn the task on or off. A future improvement can be to model *M* as an interphase transfer of mass going from liquid to the immobile solid membrane phase. The definition of *gm₂* stays the same, using the Growth Task-function as growth term.

The solute component mass balance stays the same, as now no specific tasks take place via this balance.

In the enthalpy balance the tasks Heat Transfer, Evaporation and in the future Shaft Work are implemented as follows:

$$\begin{aligned} & V\left(\varepsilon\rho_l c_{p,l} + (1-\varepsilon)\rho_c c_{p,c}\right)\frac{dT}{dt} = \\ & \quad \left(\rho_l c_{p,l} T - \rho_c\left(c_{p,c}T + dH_{crys}\right)\right)k_v V g m_2 - \rho_l c_{p,l} T \frac{dV}{dt} \\ & \quad + \sum_j^{Ni} \phi_{V,in,j}\left[\rho_l c_{p,l} T + \left(\varepsilon_{in,j}\rho_l c_{p,l} + \left(1-\varepsilon_{in,j}\right)\rho_c c_{p,c}\right)\left(T_{in,j} - T\right)\right] \\ & \quad - \sum_j^{No} \phi_{V,out,j}\rho_l c_{p,l} T - E\left(c_{p,w}T + dH_{evap}\right) + Q + \cancel{W_S} \end{aligned} \tag{3.29}$$

An overview of the entire TBD compartment model, visualising all variables, is shown in Figure 3.2.

Differential Equations | **Algebraic Equations** | **Graphical representation of balance**

Population Balance

$$\frac{\partial nV}{\partial t} = -V\frac{\partial nG}{\partial L} + \sum_{j}^{Ni}\phi_{V,in,j}\cdot n_{in,j} - \sum_{j}^{No}\phi_{V,out,j}\cdot n\cdot C + V\cdot Y$$

$$n(L=0,t)\left[\frac{\#}{m^3 m}\right] = \frac{N(t)}{G(L=0,t)}$$

$$n(L,t=0)\left[\frac{\#}{m^3 m}\right] = I(L)$$

$$G(t) = f(\sigma(t))$$

$$\sigma(t) = \frac{w(t) - w_{sat}(t)}{w_{sat}(t)}$$

$$w_{sat} = f(T(t))$$

$$C(t)$$

$$Y(t)$$

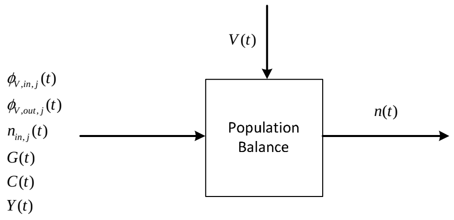

Total Mass Balance

$$\rho_l\frac{dV}{dt} = (\rho_l - \rho_c)k_v V gm_2 + \sum_{j}^{Ni}\phi_{V,in,j}\rho_l - \sum_{j}^{No}\phi_{V,out,j}\rho_l - E - M$$

$$V(t=0) = \mathrm{V}_{init}$$

$$gm_2(t) \equiv 3\int_{L_0}^{\infty} G(t)n(t)L^2 dL$$

$$E(t)$$

$$M(t)$$

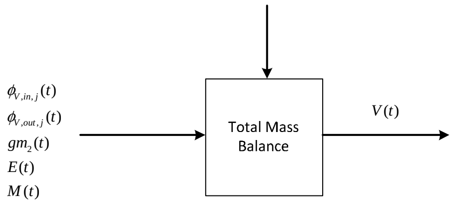

Solute Component Mass Balance

$$\begin{aligned} V\varepsilon\rho_l\frac{dw_{l,i}}{dt} &= -\rho_l w_{l,i}\frac{dV}{dt} + \left(\rho_l w_{l,i} - \rho_c w_{c,i}\right)k_v V gm_2 \\ &+ \sum_{j}^{Ni}\phi_{V,in,j}\left(\varepsilon_{In,j}\rho_l w_{l,i,in,j} + \left(1-\varepsilon_{In,j}\right)\rho_c w_{c,i,in,j}\right) \\ &- \sum_{j}^{No}\phi_{V,out,j}\rho_l w_{l,i} \end{aligned}$$

$$w(t=0) = \mathrm{w}_{init}$$

$$\varepsilon(t) = 1 - k_V m_3(t)$$

$$m_3(t) = \int_{L_0}^{\infty} n(t)\cdot L^3 dL$$

$$\sum w_l(t) = 1$$

$$w_{c,1} = 1$$

$$w_{c,2} = 0$$

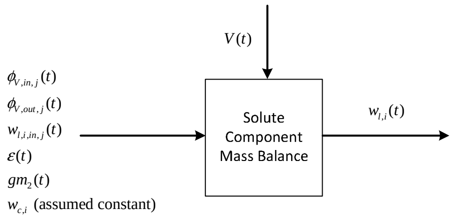

Enthalpy balance

$$\begin{aligned} & V\left(\varepsilon\rho_l c_{p,l} + (1-\varepsilon)\rho_c c_{p,c}\right)\frac{dT}{dt} = \\ & \left(\rho_l c_{p,l}T - \rho_c\left(c_{p,c}T + dH_{crys}\right)\right)k_v V gm_2 - \rho_l c_{p,l}T\frac{dV}{dt} \\ & + \sum_{j}^{Ni}\phi_{V,in,j}\left[\rho_l c_{p,l}T + \left(\varepsilon_{in,j}\rho_l c_{p,l} + \left(1-\varepsilon_{in,j}\right)\rho_c c_{p,c}\right)\left(T_{in,j} - T\right)\right] \\ & - \sum_{j}^{No}\phi_{V,out,j}\rho_l c_{p,l}T - E\left(c_{p,w}T + dH_{evap}\right) + Q + \cancel{W}_S \end{aligned}$$

$$T(t=0) = \mathrm{T}_{init}$$

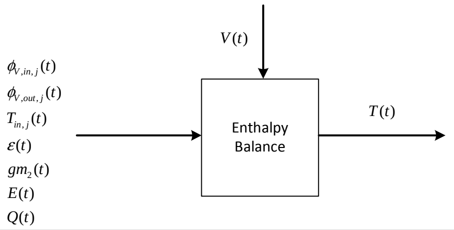

Figure 3.2: Overview of all equations and variables for the TBD model

3.4 Modelling a wide range of processes

As already shown, describing all the regions of a crystallizer with the same compartment model implies that a compartment will have many more functionalities than it actually requires. Next to a variation of tasks, the developed TBD model can be applied to a wide range of crystallization processes:

- **Crystallization method** (cooling, flash-cooling or evaporative). Cooling or Evaporative is modelled using tasks. In case of cooling, the task evaporation can be turned off so that there is no outgoing vapour stream. Furthermore one can choose if for instance the temperature profile is set, the heat input/output term is set, the supersaturation is set or the removed solvent is set.
- **Operation mode** (batch, semi-batch or continuous). Batch and semi-batch processes are dynamic, whereas continuous processes may be either steady-state or dynamic. The user needs to assign the operation mode in the highest model layer, the process

layer. The model is able to cope with fixed and free volumes. This can be assigned per compartment using:

  - Steady state - If the values of all the variables in a process do not change in time:
    - $dV/dt = 0$, $dT/dt = 0$, $\varphi_V(t)$ = constant
  - Dynamic - if any of the process variables change in time:
    - $\varphi_{V,\,in}$ = set, $\varphi_{V,\,out}$ = set ((semi-) batch)
    - $\varphi_{V,\,in}$ = set, $\varphi_{V,\,out}$ is determined by hold-up (continuous dynamic)

  Now, the user needs to be able to identify the number of variables that needs to be free and set. This can be done using the overview of Figure 3.2. Nonetheless, improvement for the user interface is needed.

- **Configuration** (single or multiple stage). This is possible via varying the number of compartments.
- **Crystallizer type** (stirred vessel, DT, DTB, FC or Oslo). Using the concept of compartmental modelling, the same modelling framework can be used to describe different crystallizer types. This is not illustrated though, since for this thesis a new crystallizer unit is tried to be modelled which is not based on existing equipment.

3.5 Task Restrictions

Two types of restrictions concerning the tasks need to be implemented if one wants to use the model in an optimisation environment:

- Physical constraints - Limitations may be set on the task to a physical domain in which the event will effectively work; a range of operating conditions. An example is that Evaporation should be active at the boiling temperature. These constraints can be implemented in the task models.
- Tasks simultaneously - Some tasks cannot occur simultaneously in one compartment (however they can in the process). This should be built in the optimiser. Also tasks evidently occurring simultaneously should be built in. Examples are:
  - Growth and dissolution cannot occur simultaneously
  - Heating is accompanied by dissolution if the solution becomes undersaturated
  - Evaporation has to be accompanied by heat transfer

4 Task Library

In previous chapters, the task concept is explained and the definitions of several physical phenomena occurring during crystallization are given. This chapter gives an overview of all tasks identified and the driving forces/functional dependencies for the rate laws. Unfortunately, for most tasks first principle rate laws are not known yet, so also the used rate laws of all tasks implemented in the developed model are given. The general information on the several tasks below can be used for future improvements of the task models.

4.1 Crystal Growth

Task functional dependency

Crystal growth can be defined as the continuous size enlargement of crystals. Supersaturation is the driving force for both mass transfer and surface integration. The rate of mass transfer has a first order supersaturation dependency. The mass transfer rate is also a function of the diffusion coefficient, crystal size and local hydrodynamics. The supersaturation dependency of the surface integration step is determined by the mechanism: spiral growth, ‘birth and spread’ growth and rough growth, with respectively a second, exponential and first order dependency. These mechanisms only consider the solute species and additional factors such as lattice stress imperfections, crystal size and hydrodynamics have not been taken into account although these have a pronounced influence on the growth rate of individual crystals. Two theories can then be of importance:

- Growth Rate Dispersion (GRD): GRD is the phenomenon wherein crystals of the same size and material exhibit a stochastic variation in crystal growth rates, under identical global conditions of supersaturation, temperature and hydrodynamics. The chemical potential of two neighbouring crystals may differ due to differences in lattice structure and/or lattice strain. As a result, similarly sized crystals exposed to identical growth conditions can exhibit different growth rates.
- Size Dependent Growth (SDG): SDG is defined as a phenomenon whereby crystals of different sizes grow at different rates, under identical conditions of supersaturation, temperature and the overall hydrodynamics. This can happen due to the influence of the crystal size on the local hydrodynamics thereby, altering the diffusion rate, which in turn affects the growth rate.

Task implementation in the model

In the model it is assumed that all crystals grow at the same rate. The crystal growth task is given as (Lakerveld 2010):

$$\mathrm{T}_{G,GROWTH}\left[\frac{m}{s}\right]=k_G\cdot\sigma^{\delta}\qquad \text{for } \sigma>0 \tag{4.1}$$

The kinetic parameters k_G and δ and the operating conditions under which these are valid are stated in literature and depend on the system.

4.2 Dissolution

Task functional dependency

The opposite task of crystal growth is the task Dissolution. The mechanism of crystal dissolution is not the exact opposite of growth. This is because dissolution does not require surface diffusion and orientation of atoms, ions or molecules and is generally limited by mass transfer. Crystal dissolution thus has a first order dependency on the supersaturation, its driving force. The rate coefficient for dissolution is a function of the diffusion coefficient, crystal size and the local hydrodynamics.

Task implementation in the model

The rate equation implemented in the model is:

$$\mathrm{T}_{G,DISSOLUTION}\left[\frac{m}{s}\right]=-k_{DIS}\sigma^{\zeta} \qquad \text{for}\,\sigma<0 \tag{4.2}$$

This is only implemented to illustrate the influence of the dissolution task. Therefore, the same formula as for growth is used.

4.3 Primary Nucleation

Task functional dependency

Primary nucleation is the formation of crystals from a crystal-free solution. The driving force for primary nucleation is the supersaturation of the crystallizing substance. Creating new surface costs energy. An energy barrier, corresponding to a critical nucleus size, has to be passed after which further growth of the cluster of molecules leads to a decrease in free energy and a stable nucleus. As the supersaturation increases, both the height of the energy barrier and the value of the critical size decreases. The rate of nucleation is defined as the rate at which clusters grow through this critical size and so become crystals. This rate is a function of supersaturation, temperature and cluster-liquid interfacial tension. Also transport processes such as diffusion and viscous flow can have an influence.

Task implementation in the model

Primary nucleation may be represented by the following kinetic law (David, et al. 1991):

$$\mathrm{T}_{N,PN,SUPERSAT}\left[\frac{\#}{m^3 s}\right]=A_{PN}\exp\left(-\frac{B_{PN}}{\ln^2(1+\sigma)}\right) \qquad \text{for}\,\sigma>0 \tag{4.3}$$

The nucleation rate constants A_{PN} and B_{PN} are temperature dependent.

4.4 Primary Nucleation using Ultrasound

Task functional dependency

Ultrasound is an interesting tool for task-based design as it can manipulate individual crystallization phenomena. For many components in different solvents it has been shown that ultrasound can reduce induction time and decrease the mean crystal size compared to batch crystallization using conventional primary nucleation. Furthermore, experimental studies showed that ultrasound can be effective in preventing agglomeration. For some systems it has been shown that ultrasound can induce attrition of existing crystals. Besides influencing the crystal size distribution, ultrasound can also be used to manipulate the type of polymorph of the crystals as is shown by several experimental studies. The mechanism explaining the influence of ultrasound on crystallization phenomena is still not clear. Ultrasonic waves can create cavities in the solution (causing possibly pressure gradients), improve mixing (due to presence of bubbles) and transfer heat (also possibly the formation of hot spots), which all can be potential sources of the experimentally observed effects. The translation to an industrial process is not trivial. This is caused by a lack of fundamental understanding of key physical phenomena but also by the inherent dependency of the scale of the ultrasonic equipment used in the experimental studies. In case of a small lab-scale setup it is possible to insonate most of the working volume and therefore observe a significant effect of ultrasound on crystallization for the studied cases. However, on a larger scale it is difficult to insonate a large part of the working volume, which requires different methods and thus a different product quality compared to the lab-scale experiments can be expected. (Lakerveld 2010)

In this work, Ultrasound will be used for the task Primary Nucleation.

Task implementation in the model

In general, a nucleation rate induced by ultrasound is reported to be dependent on supersaturation (Kordylla, et al. 2009). In this work the primary nucleation rate is assumed to be as follows (Lakerveld 2010):

$$\mathrm{T}_{N,PN,ULTRASOUND}\left[\frac{\#}{m^3 s}\right] = k_{PN} \cdot \kappa_{US} \cdot \sigma^{\alpha} \qquad \text{for } \sigma > 0 \tag{4.4}$$

where κ_{US} represents the fraction of the time that ultrasound is active within a time interval.

4.5 Secondary nucleation

Task functional dependency

Secondary nucleation results from the presence of crystals in the supersaturated solution and can occur by different mechanisms such as:

- Contact nucleation/attrition - Contacts between a growing crystal and walls of the container, a stirrer or pump impeller, or other crystals result in contact nucleation.
- Shear nucleation - Shear forces imposed on a crystal face by the solution flowing past it can be sufficient to produce secondary nuclei from the surface.

- Initial breeding/dust breeding - Tiny crystallites are formed on the crystal surface during the growth of seed crystals or due to fragmentation during storage.

The mechanism modelled in the TBD model is Attrition.

The rate of attrition is difficult to describe and various correlations can be found in literature. The driving force for attrition is determined by the concentration of the various sized crystals and their relative motion with respect to the pump blades, vessel walls or other crystals. The relative kinetic energy of a collision is determined by the size and relative velocity of the particle, which in its turn is a function of the slurry motion, viscosity and particle inertia (thus particle size). The rate coefficient or resistance for attrition is a function of the shape, surface roughness and mechanical properties of the colliding crystal. The rate is also indirectly influenced by the supersaturation, since that determines factors such as surface roughness and healing of corners and surfaces damaged due to previous collisions and it determines the fraction of attrition fragments that actually grow out and thus 'survive'.

Task implementation in the model

A typical form of a power law for description of attrition, which is also used in the model, is (Lakerveld 2010):

$$\mathrm{T}_{N,SN,ATTRITION}\left[\frac{\#}{m^3 s}\right]=k_{SN}\cdot\frac{\omega}{\omega_{\max}}\cdot\sigma\cdot(1-\varepsilon) \qquad \text{for } \sigma>0 \tag{4.5}$$

Attrition is induced by a stirrer with power duty ω [J] in a well-defined geometry and is assumed to be dependent on supersaturation σ and liquid fraction ε.

4.6 Seeding

Task functional dependency

Seeding can be considered as an alternative task for primary nucleation. Adding seeds is an appropriate way of starting the crystallization process under reproducible operating conditions and of avoiding primary nucleation, which is difficult to control. Seeding offers more flexibility for design as seed properties can be optimised for a given design objective. The application of seeding is not straightforward however, and requires careful optimisation for each application. The mass and its size distribution, on the one hand, and the time of addition at a certain supersaturation in the crystallizer, on the other hand, must be chosen in such a way that spontaneous nucleation, but also dissolution are avoided. The origin, the purity, the temperature, and the morphology of the seeds are important material parameters.

The task Seeding cannot be implemented as a rate law, but is introduced as an initial distribution as initial condition in the population balance. This requires values for the crystal number density at each node of the discretised crystal size domain. However, the CSD measurements typically encompass fewer points on the crystal size domain than the number of nodes. Furthermore, the nodes of the size domain used by the crystallization model do usually not coincide with the points on the size domain used by the CSD measurement technique. This discrepancy is overcome by using CSD measurements to estimate the parameters of a continuous distribution function approximating the initial CSD. Several one-dimensional two-parameter unimodal distribution functions are known that can be used to empirically represent the CSD. Any number of parameters might be used in the distribution function, but a minimum of two is necessary to describe both the mean and variance of the distribution. The form of the distributions functions is flexible enough that most unimodal experimental distributions can be represented by one of the functions with an appropriate choice of parameters. Commonly used empirical distribution functions are the normal distribution, the log-normal distribution, the gamma distribution the Rosin-Rammler Distribution and the Gaudin-Melloy Distribution (Randolph and Larson 1988). The properties of the seed crystals have a large influence on the final product of a crystallization process. Therefore it is very important to have an accurate measure of amount of seeds and the size distribution of the seed crystals.

Task implementation in the model

In the TBD model a mathematical expression for the initial distribution is obtained by fitting two additive log normal distributions to the volume density distribution (Bermingham 2003). The five parameters in this equation (L_{g1}, L_{g2}, σ_1, σ_2, and F_1) are used as fitting parameters. $L_{g,i}$ is the geometric mean (location parameter), σ_i the geometric standard deviation (spread parameter) and F_1 gives the relative weighting of the two log-normal distributions.

$$\tilde{v}_0(L) = \frac{F_1}{L}\frac{1}{\ln\sigma_1\sqrt{2\pi}}\exp\left(-\frac{\ln^2(L/L_{g1})}{2\ln^2\sigma_1}\right) + \frac{(1-F_1)}{L}\frac{1}{\ln\sigma_2\sqrt{2\pi}}\exp\left(-\frac{\ln^2(L/L_{g2})}{2\ln^2\sigma_2}\right) \quad (4.6)$$

Transformation to an initial number density is done via:

$$\mathrm{T}_{I,SEEDING}\left[\frac{\#}{m^3 m}\right] = \frac{\tilde{v}_0(L)}{k_V L^3}\frac{c_{SEEDS}}{\rho_c} \quad (4.7)$$

In this formula, c_{SEEDS} denotes the initial concentration of seeds in [kg/m^3].

4.7 Heat Transfer: Cooling & Heating

Task functional dependency

The tasks Cooling and Heating can be considered as one task: Heat Transfer. Heat Transfer is used to change solubility by changing the temperature and thus manipulate the supersaturation. Furthermore, heating can be used to create supersaturation via evaporation of solvent. The heat transfer rate is defined by the equation:

$$\mathrm{T}_{Q,HEATTRANSFER}\left[\frac{J}{s}\right] = h\cdot A\cdot(T_{jacket} - T) \quad (4.8)$$

Traditionally, heat transfer is done using a jacket in cooling crystallization and external heat exchangers in evaporative crystallization, but also other forms of heat transfer may exist which can be implemented to support the task based design. Examples of other driving forces for heat transfer are microwaves and solar energy.

Task implementation in the model

For now, the task Heat Transfer is modelled using a setpoint for the addition or removal of heat in the system:

$$\mathrm{T}_{Q,HEATTRANSFER}\left[\frac{J}{s}\right]=\mathrm{Setpoint} \tag{4.9}$$

This setpoint is either set or used as free variable in the model to implement a cooling curve for instance.

4.8 Solvent Removal using Evaporation

Task functional dependency

Evaporative crystallization is useful when the solubility increases only slightly, remains almost constant, or even decreases with temperature. Unfortunately, an evaporative crystallization process suffers from several drawbacks, which can be divided into aspects related to a lack in flexibility for design and operation, and energy consumption.

The solvent evaporation rate depends on the saturation of the outlet gas flow, the vapour pressure of the solution and the evaporation surface area. Solvent evaporation should be modelled with a thermodynamic model, relating pressure p, saturation vapour pressure p_{sat} and the boiling surface in the vessel to the amount of solvent evaporating. This model should only be active at the boiling temperature.

Task implementation in the model

The evaporation task-function is modelled as a mass flow, occurring in both the enthalpy balance and the total mass balance. Then:

$$\mathrm{T}_{E,EVAPORATION}\left[\frac{kg}{s}\right]=\phi_{V,vap}\rho_{v} \tag{4.10}$$

Evaporation is not used in any of the cases, so although the task-function is present, no task model is implemented.

4.9 Solvent Removal using membranes

Task functional dependency

Membrane-assisted crystallization (MaC) offers an interesting opportunity to generate supersaturation by removing the solvent from a crystallizer. It is an alternative to conventional evaporative crystallization processes, which have high energy demands. By using membranes instead of a boiling zone for solvent removal, the surface area available for solvent removal per unit crystallizer volume can be increased. Since membranes can, in principle, be placed at any location in a crystallizer vessel, areas of low supersaturation can be chosen as membrane location to reduce the gradients in supersaturation within the crystallizer. This can lead to smaller and more efficient equipment. In terms of operational flexibility, it has been shown that application of membranes within a task-based design framework for crystallization processes showed an increase in operational flexibility. Finally, from an energetic point of view, membranes in which no phase change from liquid to vapour occurs (reverse osmosis), have a high potential to significantly reduce energy consumption as a replacement of conventional evaporative crystallizers.

The concept of MaC-RO offers additional process actuators and design variables compared to conventional evaporative or cooling crystallization. In reverse osmosis processes, both the retentate side and the permeate side are in the liquid phase. A pressure difference is applied over the membrane, resulting in a chemical potential difference, which is the driving force for mass transport. the pressure difference, Δp, can be related to the water flux across the membrane, J_w, by the solution diffusion model, using the membrane thickness, the solubility and diffusivity of the permeating component in the membrane. The last two are temperature dependent parameters. Concentration polarization also needs to be taken into account. Concentration polarization is the increase of the concentration of the retained components at the membrane surface, reducing the driving force for the selectively permeating species. Minimizing this effect is one of the main challenges in the MaC concept. Since the MaC process is operated close to saturation, an increase in concentration can lead to scale formation on the membrane surface. This should always be avoided. (Kuhn, et al. 2009)

Task implementation in the model

For now, the task Membranes is modelled using a setpoint for the addition or removal of solvent in the system:

$$\mathrm{T}_{M,MEMBRANE}\left[\frac{kg}{s}\right]=\phi_m \tag{4.11}$$

This setpoint is either set or used as free variable in the model to set a certain supersaturation for instance.

4.10 Classification

Task functional dependency

Fines destruction and classified product removal are used to change the crystal size distribution and the median crystal size. Reducing the number of fine particles is very efficient provided that particles which grow to a product-relevant size during the batch or retention time are substantially removed. It should be noted that the operation of all of the equipment can be troublesome and cause attrition and breakage. (Mersmann 2001)

Unfortunately, classification can also occur unwanted. Whenever there is a material density difference between the solid and liquid phase, crystals will not always follow the stream lines of the liquid phase. As a result, the flow pattern and distribution of solids in the crystallizer will differ from the liquid phase. This phenomenon increases with increasing particle size and increasing density difference. The slip of a particle is defined as its relative motion with regard to the liquid. As slip is a result of inertia, the slip velocity of a particle depends on its size. Besides particle size, the slip velocity also depends on the density difference between the solid and liquid phase, particle shape and the dynamic viscosity of the liquid phase. Furthermore, if multiple particles are present, the volume fraction of solids and the particle size distribution also influence the particle slip velocity.

Correctly accounting for this effect, requires two-phase computational fluid dynamics, i.e. simultaneous solution of the equations of motion for the liquid phase and for the various particle sizes in the solid phase, while taking into account particle-particle and particle-liquid interactions as well as equipment related boundary conditions. However also a simplified approach can be implemented in the compartmental modelling framework. The approach comprises the calculation of classification functions, to account for the difference in flow pattern of the liquid and solid phase due to particle slip.

The ratio of the crystal number density in a certain outlet stream and in the compartment is defined as the classification function of that stream:

$$h_{out}(L)[-] = \frac{n_{out}(L)}{n(L)} \tag{4.12}$$

The classification function actually determines a size dependent residence time of crystals in a compartment, and therefore account for the difference in flow pattern of the liquid and solid phase. A lower classification function value implies a higher residence time, i.e. a lower tendency to leave the compartment. Classification functions thus provide a simple but effective way to describe a non-uniform crystal size distribution throughout a crystallizer. The introduction of a classification function allows one to have compartments that are perfectly mixed internally but not necessarily with respect to the outlet streams. The latter only refers to the crystal size distribution; the temperature and liquid phase composition of the outlet stream are always assumed to be equal to the temperature and composition within the compartment. (Bermingham 2003)

Task implementation in the model

Classification is a special task. It works on all outgoing streams, so on the boundary of the compartment, not in the compartment itself. In the model, classification is implemented as a perfect size independent solid/liquid separation defined for all the outgoing steams. This means:

$$\mathrm{T}_{C,CLASSIFICATION}[-] = h_j \tag{4.13}$$

with:

If *h* = 0, there are no crystals in the outgoing stream.

If *h* = 1, there are crystals in the outgoing stream.

4.11 Mixing/suspension

The task mixing is intended to compensate for local differences in for instance temperature, concentration (thus supersaturation) and suspension density. Furthermore mixing should minimize the variation in the residence time experienced by crystals flowing through the system. The impeller in a stirred vessel has the task not only of mixing, but also of suspending the crystals that have a difference in density compared to the solution. The task mixing depends on the geometry of the crystallizer, properties of the compounds in the crystallizer (such as viscosity), the type and size of the impellor, and properties related to suspension such as the density and size of the crystals. This functional relationship can be transformed into a minimum tip speed necessary. From this a power input can be deduced. In case of thorough mixing, heat can be released so an additional term in the enthalpy balance is necessary. Besides transport processes, mixing on a smaller scale also influences the shear rates acting on a crystal surface, which can induce secondary nucleation. A higher velocity of the impellor also increases the rate of attrition. In the model perfect mixing is assumed, and the task mixing is not implemented.

4.12 Agglomeration/Breakage

Agglomeration of particles is a reversible process which involves transport and collision of the particles, interaction of the particles, rupture of aggregates and cementation of aggregates into stable agglomerates. The modelling of these four steps separately is difficult, especially while they occur simultaneously. The aggregation kinetics is difficult to describe, mainly because it depends on many different parameters such as the hydrodynamic conditions, the properties (size, shape, density) of the particles, kinetic processes, most importantly crystal growth (so also the supersaturation) and the interactions between two particles or a particle with the solvent. The agglomeration rate is therefore mostly described with one size dependent function, the so called agglomeration kernel (β). Agglomeration is an important mechanism in the smaller size range (smaller than 50 µm) and in particular for sparingly soluble systems. When enough surface area is present in the system, the agglomeration process can be neglected for all practical purposes (for moderately and easily soluble compounds). High fluid shear can not only increase the number of collisions, but it can also break down agglomerates. It creates a competition between collisions and destruction of agglomerates as a function of mixing intensity.

Regarding the modelling, agglomeration and breakage are implemented as birth and death terms in the population balance as is described in chapter 1. Attractive and repulsive forces of the primary particles decide on the progress and the rates of aggregation. The population balances can only be solved when the total interplay of attractive and repulsive forces of small primary particles, the tensile strength of aggregates, and the forces acting on aggregates are known.

Since agglomeration highly increases the model complexity, it is not modelled in this work.

4.13 Ostwald ripening

The solubility of a crystal depends on its size, small crystals being more soluble than large. This effect becomes significant as crystal sizes approach critical size. This dependence of solubility on size gives rise to Ostwald Ripening. A solution that is in equilibrium with large crystals is undersaturated with respect to small ones. This in a slurry of crystals having a wide range of sizes it is possible for the small crystals to dissolve and for their mass to subsequently to be deposited on the large crystals which grow. In this way , the mean crystal size in the sample increases. This means Ostwald ripening and can be used as a size-enlargement task. Ostwald ripening is only relevant for systems containing small crystals. The rate of Ostwald ripening depends on supersaturation, crystal sizes and parameters like the diffusion coefficient and the specific surface energy.

Note that if the growth rate is negative for certain crystal size intervals and positive for others, the PBE requires more than one boundary condition with respect to crystal size. For such systems, one could define a separate PBE for each size interval within which the growth rate of all crystals have the same sign.

Ostwald ripening is not modelled in this work.

5 Model implementation using numerical methods

This chapter covers aspects of implementation of the developed TBD model using gPROMS. First some definitions concerning process models are given. In order to solve the population balance equation and moment equations numerically, a transformation into ordinary differential equations or algebraic equations is needed, for which the finite volume method is used. The facilities of the selected software tool gPROMS are given. Finally, the TBD model structure in gPROMS is explained.

5.1 Important definitions concerning process models

Simulation versus optimisation

In general, the use of a model can take various forms depending upon what is assumed to be known and what is to be computed, among which:

- Dynamic simulation – With the process model developed to represent changes in time, it is possible to predict the outputs given all inputs, the model structure and parameters.
- Design problem/optimisation – Here, the values of certain parameters are calculated from the set of parameters, given known inputs and desired outputs and a fixed structure. This type of problem is usually solved using an optimisation technique which finds the parameter values that generate the desired outputs.

In this thesis the model is solely used for dynamic simulation. However, it is possible to transform the model into an optimisation problem. The three essential categories for an optimisation problem are (Edgar, Himmelblau and Lasdon 2001):

1. At least one objective function to be optimised (cost function)
2. Equality constraints (equations)
3. Inequality constraints (inequalities)

Types of dynamic models

In terms of dynamic models two classes can be identified:

- Distributed parameter dynamic models – These contain various forms of partial differential equations (PDEs)
- Lumped parameter dynamic models – These are systems of ordinary differential equations (ODEs) coupled with many (non-)linear algebraic constraints. The total system is referred to as a differential-algebraic equation set (DAE).

Despite the fact that in chapter 3 the conservation equations are written in a lumped parameter form, the crystallization model presented also comprises a PDE, namely the population balance equation (PBE), and a number of integral equations (IEs) for the calculation of among others the moments. In order to solve these equations in gPROMS they must be reduced to a set of DAEs.

The index of a DAE set

After this transformation, which will be explained in the next paragraph, the model is a DAE set. The equations need to have a specified set of consistent initial conditions for all states. This can be a challenging problem due to the effects of the nonlinear constraints which can impose extra conditions on the choice of initial values. To understand this, the term index is introduced (Hangos and Cameron 2001):

The index is the minimum number of differentiations with respect to time that the algebraic system of equations has to undergo to convert the system into a set of ODEs.

The index of a pure ODE system is zero by definition. If the index of a DAE is one, the initial values of the differential variables can be selected arbitrarily, and easily solved. If, however, the index is higher than one, special care should be taken in assigning the initial values of the variables, since some hidden constraints lie behind the problem specifications. In other words, the initial estimate of the differential variable cannot be an arbitrary variable, but should be exactly consistent with the algebraic equations. This requirement of index-one for a DAE set is equivalent to the requirement that the algebraic equation set should have Jacobian (matrix of partial derivatives) of full rank with respect to the algebraic variables. The rank of a matrix is the number of the linearly independent rows or columns of the matrix. Therefore a non-singular Z x Z matrix must be of rank Z, and is said to be of full rank (Beers 2007). This is a problem because numerical techniques which are used to solve higher index problems fail to control the solution error and can fail completely. Therefore, modelling in such way to obtain an index-one problem is preferred. Guidelines to prevent index issues in modelling flowsheets with the TBD model are given in Appendix C.

5.2 Numerical solution of the population balance using finite volume method

The PBE is a PDE dominated by convection (due to the convection term $\partial(G(L,t)n(L,t))/\partial L)$ and can thus be classified as a hyperbolic partial differential equation. Common problems associated with the numerical solution of hyperbolic PDEs include numerical diffusion and instability.

The oldest and most widely used method to solve the PBE is the method of moments. In this technique, the PBE is transformed into a set of ordinary differential equations that describe the evolution of the moments of the crystal size distribution; see chapter 3. However, the moment equations cannot reconstruct the full crystal size distribution. In order to solve the full PBE, a finite volume scheme is used, which subdivides the internal variable crystal size, L in equidistant intervals. Finite volume methods do not suffer from numerical instabilities when used correctly, but they do exhibit numerical diffusion. As a result, acceptable solutions require relatively fine grids. There are more efficient methods, which are numerically more stable and exhibit less numerical diffusion, but these methods cannot be directly implemented in a DAE solver such as gPROMS because they involve a changing number of equations during the simulation. For a comprehensive overview of various population balance solution methods, the reader is referred to (Mesbah 2010).

For the discretisation of the crystal size domain at least three aspects need to be chosen:

- The lower bound of the domain, L_{min}
- The upper bound of the domain, L_{max}
- The discretisation resolution (number and distribution of gridpoints)

The lower bound should be equal to or smaller than the critical nucleus size and equal to or larger than zero. The upper bound should be chosen such that the concentration of crystals at this point can assumed to be zero.

An equidistant linear scheme is used in this research. The transformation to this scheme with N_g gridpoints is done is by writing as crystal size corresponding to gridpoint *i* (see Figure 5.1):

$$L_i = L_{\min} + (i - 0{,}5)\Delta L \tag{5.1}$$

with

$$\Delta L = \frac{L_{\max} - L_{\min}}{N_g} \tag{5.2}$$

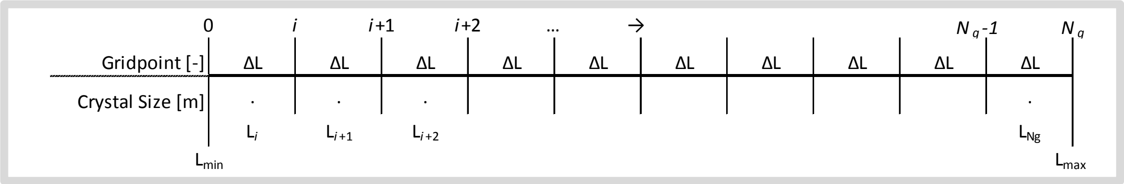

Figure 5.1: Discretization of the crystal size domain

The population balance can now be rewritten as stated below (recall that growth is assumed size independent here):

For task-function $G \geq 0$, at L_i:

$$\frac{dn_i}{dt} = -\frac{G_i n_i - G_{i-1} n_{i-1}}{\Delta L} - \frac{n_i}{V}\frac{dV}{dt} + Y_i + \sum_j \frac{\phi_{V,in,j} n_{i,in,j}}{V} - \sum_j \frac{\phi_{V,out,j} n_{i,out,j}}{V} \qquad i = 2, \ldots, N_g \tag{5.3}$$

Now, n_0 is taken to be equal to the number density at the lower boundary, which follows from the boundary condition of the population balance that nuclei only appear at the lower boundary:

$$n_0 = \frac{N}{G_0} \tag{5.4}$$

So for task-function $G \geq 0$, at L_1:

$$\frac{dn_1}{dt} = -\frac{G_1 n_1 - N}{\Delta L} - \frac{n_1}{V}\frac{dV}{dt} + Y_1 + \sum_j \frac{\phi_{V,in,j} n_{1,in,j}}{V} - \sum_j \frac{\phi_{V,out,j} n_{1,out,j}}{V} \qquad i = 1 \tag{5.5}$$

Note that in this way, also zero growth can be modelled.

If task-function *G* < 0, so for dissolution, at L_i:

$$\frac{dn_i}{dt} = -\frac{G_{i+1}n_{i+1} - G_i n_i}{\Delta L} - \frac{n_i}{V}\frac{dV}{dt} + Y_i + \sum_j \frac{\phi_{V,in,j} n_{i,in,j}}{V} - \sum_j \frac{\phi_{V,out,j} n_{i,out,j}}{V} \qquad i = 1, \ldots, N_g\text{-}1 \quad (5.6)$$

Assuming that the location of the domain's upper boundary, L_{max}, has been chosen correctly, then the boundary number density is zero:

$$n_{N_g+1} = 0 \qquad (5.7)$$

So for task-function *G* < 0, at L_{Ng}:

$$\frac{dn_{N_g}}{dt} = -\frac{0 - G_{N_g} n_{N_g}}{\Delta L} - \frac{n_{N_g}}{V}\frac{dV}{dt} + Y_{N_g} + \sum_j \frac{\phi_{V,in,j} n_{N_g,in,j}}{V} - \sum_j \frac{\phi_{V,out,j} n_{N_g,out,j}}{V} \qquad i = N_g \quad (5.8)$$

Integrals with respect to the crystal size can be calculated using a Riemann summation. For instance the third moment can be written as:

$$m_3(t) = \int_{L_0}^{\infty} n(L,t)L^3 dL = \sum_{i=1}^{N_g} n_i(t) L_i^{\,3} \Delta L \qquad (5.9)$$

5.3 gPROMS Model Builder Facilities

The TBD model does not use the traditional process unit operation as the key building block for process synthesis. It goes one level deeper and will be able to find innovative operational units. Software is needed which supports this and is able to solve adequately the numerous equations set up in the previous chapters. The dynamic flowsheeting program gPROMS Model Builder is used in this work.

gPROMS is a modelling tool that has a powerful modelling language and can simultaneously solve mixed systems of algebraic equations and ordinary differential equations with respect to time (DAEs). Equations can be written implicitly, which means that per simulation variables can either be used as input or as an output using the same formulation of the problem. Because gPROMS represents processes as sets of equations that can be solved in a number of modes (steady state simulation, dynamic simulation, steady-state optimisation, dynamic optimisation, steady-state parameter estimation, dynamic parameter estimation) it allows a single underlying model of a process to be suitable from concept to engineering design and operation. It has a track record on solving optimisation and parameter estimation problems using its built-in mathematical algorithms for automatically optimising large-scale, dynamic processes (both lumped and distributed). One can design own process units, using hierarchical modelling structures. In this way, a model of complex flowsheets and procedures can be easily constructed by decomposing them into sub-models that call on other sub-models. Furthermore gPROMS has a topology option, so that flowsheets can be made visual, and values of variables can be easily changed in the overview of the flowsheet.

gPROMS has several checks built in, which make the performed calculations more reliable. At the start of each simulation, gPROMS analyses the mathematical model so as to assist the user in identifying structural problems and errors in the modelling and/or the problem specification. Hereto gPROMS determines if the model is well-posed in terms of degrees-of-freedom, if the underlying set of differential and algebraic equations is not of index exceeding 1 and if the initial conditions are consistent. It does not continue if these requirements are not satisfied and gives suggestions what to change to improve the problem. The user can assign each variable a variable type. In a separate variable type list, all variable types are given a lower bound, higher bound and default value. If a bound is hit, gPROMS notifies this, and if a bound needs to be violated for the solution, gPROMS will not solve the problem. In this way one can make sure that a sensible solution is obtained. The default values are also used as initial guesses in order to provide the solution algorithm with a starting point in the initialisation.

As can be seen, the variable type section provides a way to put inequality constraints to the problem; the model can only run if variables are in certain ranges of values. Furthermore, it is possible to formulate CASE constructs to impose discontinuous equations, the form of which depends on the current variable values. This has significant consequences for solution robustness. This feature is for instance used in the task models to turn kinetics on if the supersaturation is positive, and off if the supersaturation is negative. In the TBD model, this can also be of interest for the construction of State-Task-Networks as the CASE constructs provide a direct description of general STNs in the gPROMS language. In this way tasks can be turned on and off if one wants to start optimising. A big disadvantage in the use of CASE constructs is that the number of equations in each section of a CASE construct must be the same.

It is also possible to schedule certain actions in time, which is necessary to implement for instance discontinuous cooling curves. Representation of data can be done using the gRMS (gPROMS Results Management Service) application and it can be done using the Palette option to present certain values or graphs directly on the output channel of the flowsheet.

There are two standard mathematical solvers for the solution of mixed sets of differential and algebraic equations in gPROMS, namely DASOLV (based on variable time step/variable order Backward Differentiation Formulae (BDF)) and SRADAU (a variable time step, fully-implicit Runge-Kutta method). DASOLV is used in all simulations. The solvers make use of a default absolute error tolerance of 10^{-5}.

(Process Systems Enterprise Ltd. June 2004)

5.4 Robustness

Regarding the robustness of the model, a few comments. The check that gPROMS automatically performs on the problem before solving it, enhances greatly the robustness of the model. The assignment of ranges for variables prevents the solution to converge to a trivial solution, as often happens in optimisation, and causes the outcome to make sense. In this model, a linear grid is used, which is accurate for a kinetic model with size independent crystal growth rates and crystal birth at one crystal size only. However, if in the future the model is extended with agglomeration and size dependent growth, the accuracy of the numerical solution obtained on a logarithmic grid might be better than obtained on a linear grid according to (Bermingham 2003). Regarding the solution of the PBE, the finite volume method is known to be robust for highly convective PDEs, even when the sign of the convective term changes (so from growth to dissolution). It is good to realize that the need for short computational times and robustness are significantly more important for control than off-line design purposes.

5.5 Model structure & Flowsheet creation in gPROMS

There are different ways of structuring the model equations and the tasks in gPROMS. An overview of the options is given in Appendix D. Below a guide through the chosen structure in gPROMS is given, also see Figure 5.2.

- The flowsheet, compartment model, task models and other attributes are gPROMS MODELs, consisting of parameter, variable and equation declarations.
- The coupling of MODELs with the settings of a dynamic simulation is done in a PROCESS. Here for instance the grid parameters, initial conditions and operation modes are set.
- Ideally, the user should be able to construct a flowsheet using the topology option of gPROMS, without writing any code in the flowsheet MODEL. Now, this is approximately the case, but a considerable amount of information should still be assigned in the PROCESS. This can still be improved.
- In gPROMS, MODELs can be used as sub-models of other MODELs. The sub-model is then called a UNIT. The UNIT connections are also depicted in Figure 5.2. For instance, the flowsheet MODEL contains several Compartment MODELs.
- In the TBD model, there are three CONNECTION TYPEs: Slurry, System Properties and Product CONNECTIONs. In mathematical terms, connections between models can be seen as equality constraints between subsets of their variables. The slurry connection for instance is used to equate outgoing variables ($n(L)$, φ_V, T, ε, w_l) of one compartment to incoming variables of another compartment. Furthermore, all system properties are listed in a separate MODEL, and these values are sent to the different models using a CONNECTION.
- For the activation and deactivation of tasks the user can double-click on a compartment MODEL in the flowsheet MODEL and assign in the appearing dialogue box which tasks are on and off and how many input and output streams there are.
- There is a separate Product Calculations MODEL, since calculations of for instance quantiles require a lot of computational effort. This model can be connected to only those compartments of which these values need to be known.

The gPROMS code of the compartment model and examples of a flowsheet and a task model can be found in Appendix J.

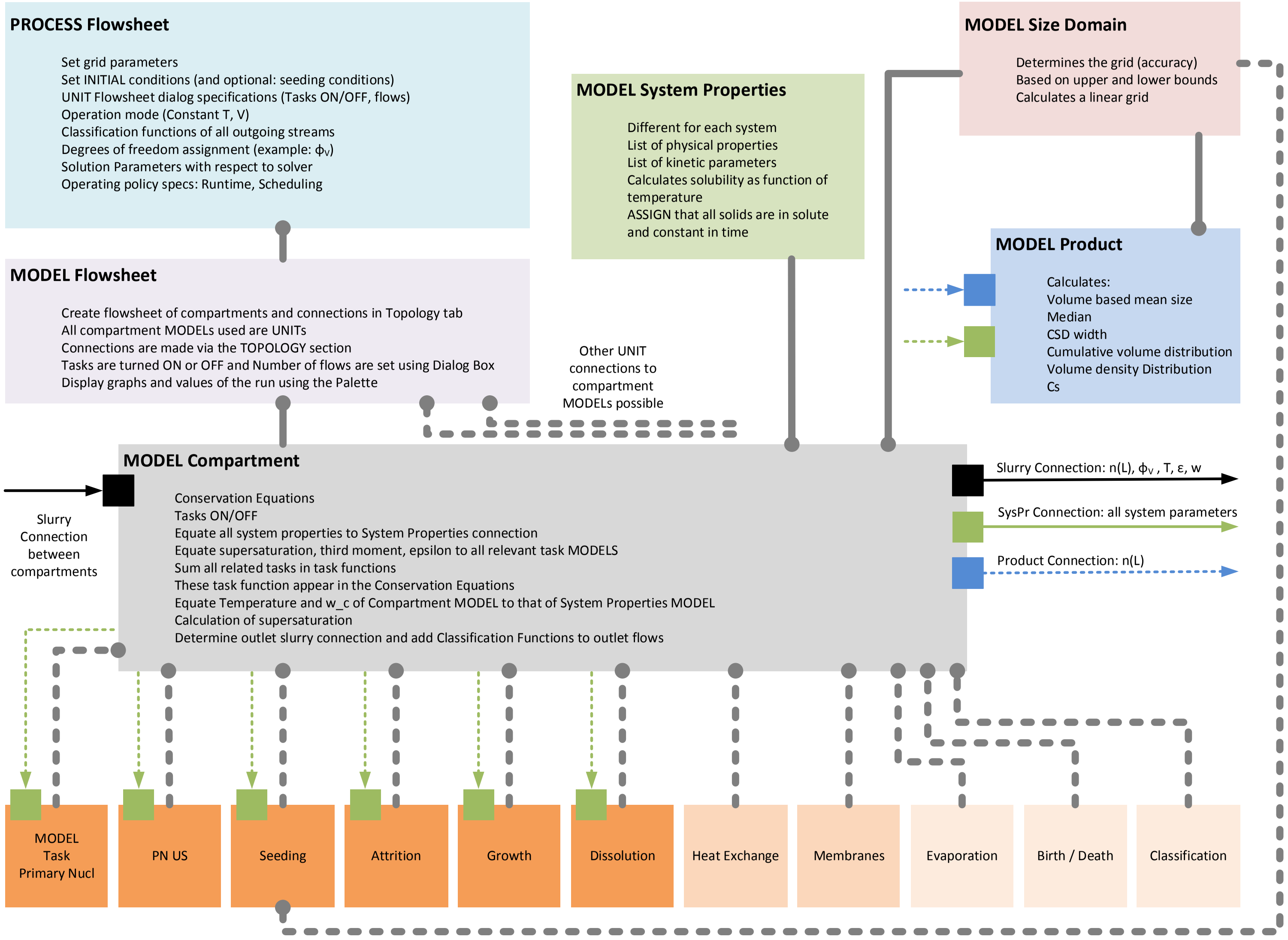

Figure 5.2: Task Based Design model structure in gPROMS

6 Pilot task-based synthesis cases

In this chapter model verification and validation are covered. Three task-based synthesis problem cases are worked out and discussed, which show the facilities of the TBD model.

6.1 Model verification and validation

Implementation of the model is just the start. Now the model needs to be verified and validated. Verification is determining whether the model is behaving correctly; is it giving the answers expected? The TBD model can be verified well using a structured approach, since the model is built in modules which can be tested individually. First one can simulate only solvent going in and out of the system. Then also solute can be added. After that crystallization can be included using the different task models. In this way mass preservation can be checked, but also the numerical solution of the population balance needs to be checked. This is verified using an MSMPR analytical solution, see Appendix E. After the verification, model validation is performed, where the model is checked against reality. There are various possibilities to validate a process model. The possibilities include but are not limited to (Hangos and Cameron 2001):

- Verify experimentally the simplifying assumptions
- Compare with other models using a common problem
- Develop analytical models for simplified cases and compare the behaviour
- Compare the model directly with process data

6.2 Objectives of the cases

Validation of the TBD model is challenging, due to the lack of experimental data and an uncertainty with respect to the predictive quality of the (heuristic) kinetic task models. This validation is performed by simulating three different crystallization processes and evaluating the resulting numerical solutions with literature to see if the trends observed in literature are recognised. Furthermore, the design of the cases is done such that all facilities of the TBD model are shown. In the cases also different aspects of the process and product are of importance. In Figure 6.1 an overview of the cases is depicted.

The aim of case 1 is to simulate experiments of batch solution crystallization of ammonium sulphate in an airlift crystallizer. A cooling curve is implemented and results checked are median sizes and CSD shapes. Case 2 is designed to validate trends found in batch crystallization of adipic acid. This case includes the modelling of a membrane unit. Aspects that are covered are supersaturation and crystal mass trends and the ease of turning tasks on and off. In the third case continuous crystallization of adipic acid in a cascade of airlift crystallizers is modelled. Influence of the crystallizers in series on the CSD width is investigated. Other aspects are the use of supersaturation control, modelling with a higher number of compartments and production of nuclei using an ultrasound vessel.

Parameter settings for all cases and their argumentation can be found in Appendix F.

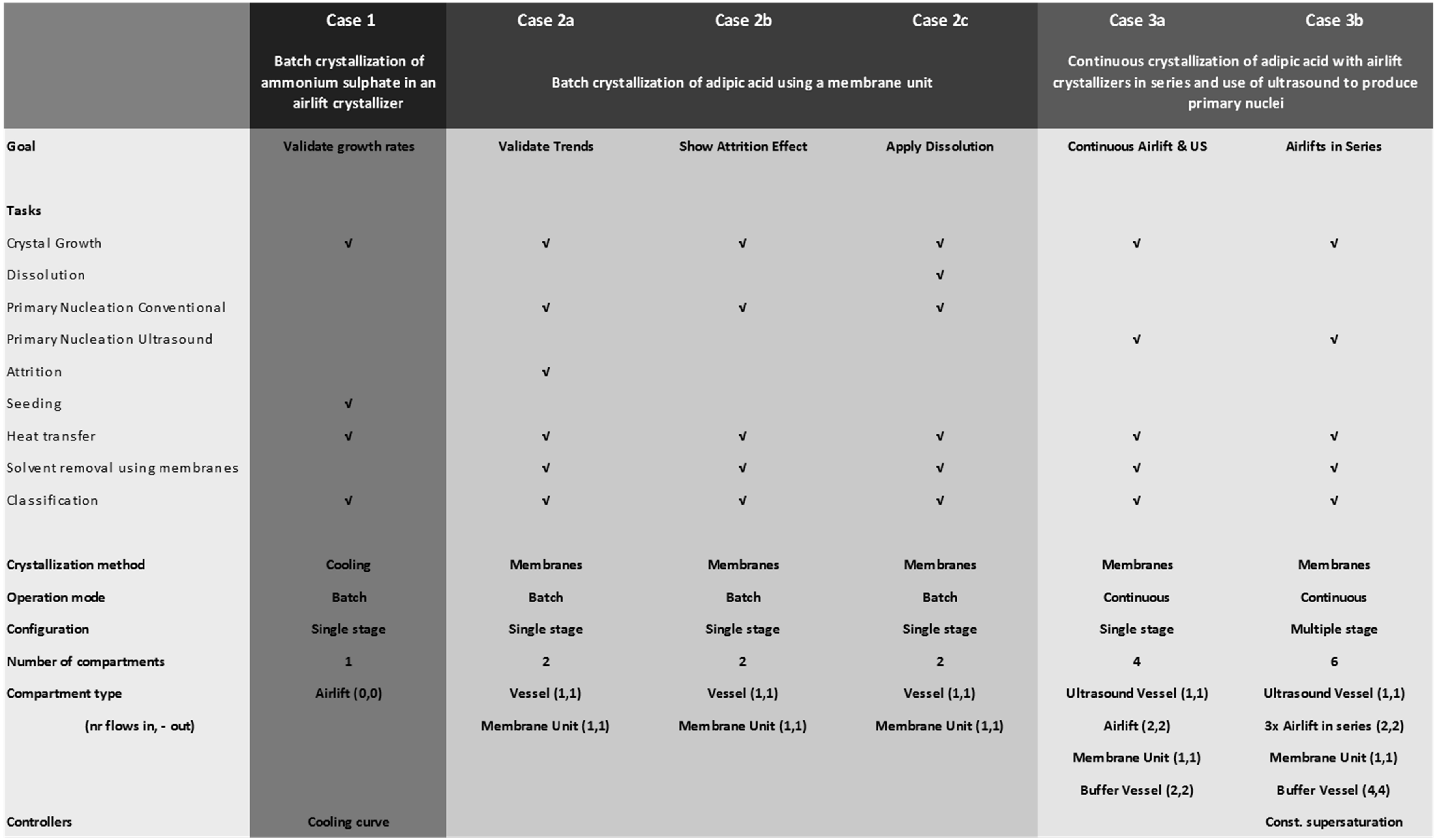

	Case 1	Case 2a	Case 2b	Case 2c	Case 3a	Case 3b
	Batch crystallization of ammonium sulphate in an airlift crystallizer	Batch crystallization of adipic acid using a membrane unit			Continuous crystallization of adipic acid with airlift crystallizers in series and use of ultrasound to produce primary nuclei	
Goal	Validate growth rates	Validate Trends	Show Attrition Effect	Apply Dissolution	Continuous Airlift & US	Airlifts in Series
Tasks						
Crystal Growth	√	√	√	√	√	√
Dissolution				√		
Primary Nucleation Conventional		√	√	√		
Primary Nucleation Ultrasound					√	√
Attrition		√				
Seeding	√					
Heat transfer	√	√	√	√	√	√
Solvent removal using membranes		√	√	√	√	√
Classification	√	√	√	√	√	√
Crystallization method	Cooling	Membranes	Membranes	Membranes	Membranes	Membranes
Operation mode	Batch	Batch	Batch	Batch	Continuous	Continuous
Configuration	Single stage	Single stage	Single stage	Single stage	Single stage	Multiple stage
Number of compartments	1	2	2	2	4	6
Compartment type (nr flows in, - out)	Airlift (0,0)	Vessel (1,1) Membrane Unit (1,1)	Vessel (1,1) Membrane Unit (1,1)	Vessel (1,1) Membrane Unit (1,1)	Ultrasound Vessel (1,1) Airlift (2,2) Membrane Unit (1,1) Buffer Vessel (2,2)	Ultrasound Vessel (1,1) 3x Airlift in series (2,2) Membrane Unit (1,1) Buffer Vessel (4,4)
Controllers	Cooling curve					Const. supersaturation

Figure 6.1: Overview of pilot task based synthesis problem cases

6.3 Case 1: Batch crystallization of ammonium sulphate in an airlift crystallizer

Set-up of case

The aim of case 1 is to reproduce results of experiments done with ammonium sulphate in an airlift crystallizer by (Soare, et al. 2012). An airlift system is an interesting alternative for conventional suspension crystallizers to produce large crystals of high quality due to the minimization of the shear forces acting on particles. The airlift crystallizer can be seen as a piece of equipment used for isolation of the task Growth.

A flowsheet of this case is shown in Figure 6.2. The task growth is isolated, so it is assumed that no primary nucleation occurs. Furthermore, no evaporation is assumed. The initial solution in the crystallizer is saturated and seeded, after which a cooling curve is applied. In the experiment, seeds had a healing period after which the solution is cooled down. In the model, the seed distribution of the original seeds is determined by fitting the measured distribution to two lognormal distributions as is described in chapter 4. After this, the fit is extrapolated to simulate the healed seeds. The initial temperature is 334,65 K (61,5 °C) after which the solution is cooled down to 298,15 K (25 °C) in two steps. First a cooling rate of 0,125K/min is applied followed by a cooling rate of 0,25 K/min. This means that the total batch time is 96 minutes. The model is ran for four different seed loads: 7, 20, 30 and 40g per total volume of the crystallizer.

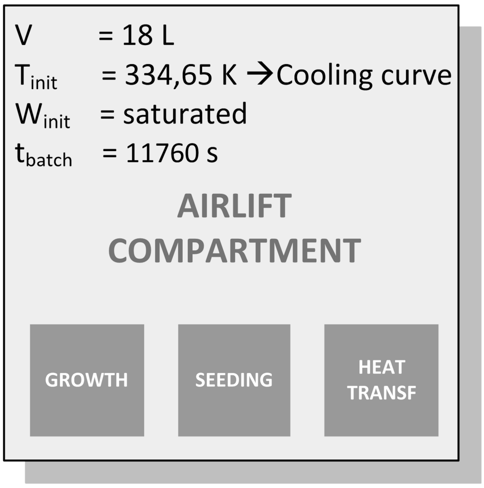

Figure 6.2: Flowsheet of batch airlift crystallizer model

Growth rates are compared to ideal growth rates and experimental values. Furthermore the volume density distributions are compared. The normalized volume density distribution is given by:

$$\tilde{v}(L) = \frac{n(L)k_V L^3}{\int_{L_{\min}}^{L_{\max}} n k_V L^3 dL} \tag{6.1}$$

The CSD width and median size of the crystal population at different seed loads simulated by the model are compared with the experimental values. For the median size and the CSD width, the so called quantiles need to be calculated. Therefore an expression for the normalized cumulative volume density distribution is needed:

$$\tilde{V}(L)=\frac{\int_{L_{\min}}^{L} n(L)k_V L^3 dL}{\int_{L_{\min}}^{L_{\max}} nk_V L^3 dL} \quad (6.2)$$

The quantiles, symbolically denoted as L_q, are defined as the crystal size for which q% of the observed volume density distribution has a size smaller than or equal to this value:

$$\frac{q}{100}=\tilde{V}(L_q) \quad (6.3)$$

The CSD width is L_{90}/L_{10} and the median size is L_{50}, which can be seen in Figure 6.3. Parameter settings for ammonium sulphate are given in Appendix G.

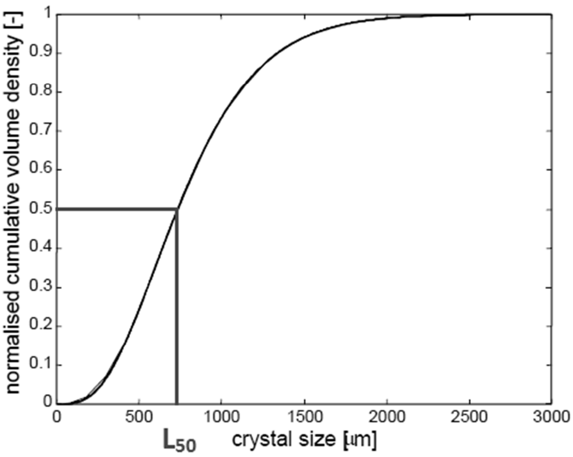

Figure 6.3: Normalized cumulative volume density distribution and the location of quantile q_{50}, which represents the median crystal size

Results and Discussion

Median sizes are compared for ideal growth, experiments and the model. In the ideal growth situation, the number of crystals remains constant during the batch, which means that there is only growth and no nucleation. Then the following equation can be used to calculate the crystal size (Jagadesh, et al. 1999):

$$L_{MAX}=L_{SEED}\left(\frac{C_{SEED}+1}{C_{SEED}}\right)^{1/3} \quad (6.4)$$

Here L_{SEED} is the seed volume based mean size and C_{SEED} is the seed load defined as the seed mass divided by the theoretical yield of crystals:

$$C_{SEED}=\frac{w_{SEED}}{w_{th}} \quad (6.5)$$

This equation assumes that the number of crystals remains constant, the crystal shape does not change, and all supersaturation deposits on equally sized seeds. Furthermore, the width of the CSD should be sufficiently small as the method uses the volume based mean size to estimate the total number of crystals, and not the median. Note that this approach does not take into account changes in supersaturation. The levels of supersaturation are in general low for an ammonium sulphate water system, which justifies this assumption.

In Figure 6.4, the results are depicted. It can be seen that for higher seed loads the ideal growth, experimental and model values are closer together than for lower seed loads. This is due to other mechanisms occurring such as nucleation. The line obtained by the model is closer to ideal growth then to the experiments. In the model, the task attrition is turned off which means that the number of crystals stay the same during the batch. The only thing that is different in the ideal growth, is that there all seed crystals are assumed to have the same size, which is not the case in the modelled seeds. Furthermore, the supersaturation is not constant in the model.

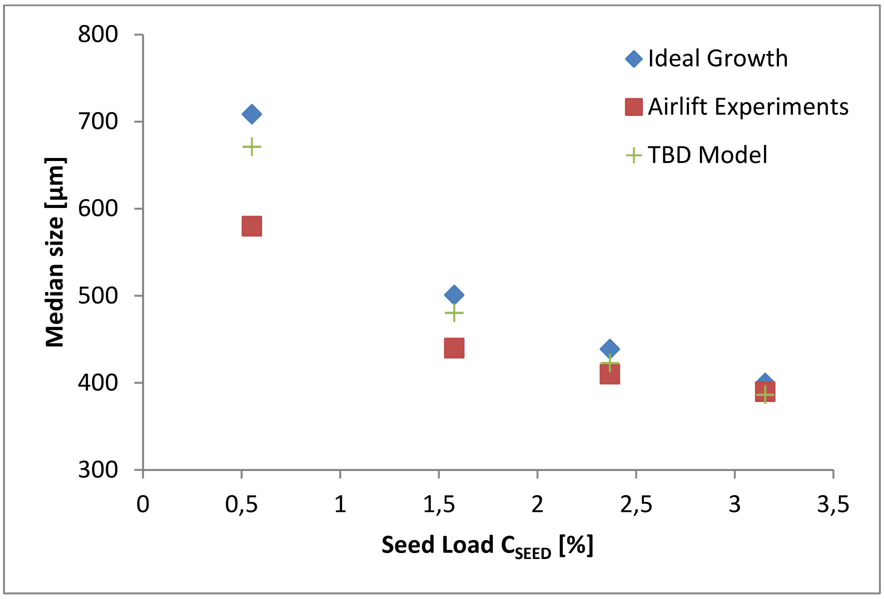

Figure 6.4: Comparison of median sizes in an airlift crystallizer, calculated for ideal growth, from experiments and by the TBD model

The differences between the model and the experiments are better visible in the crystal size distributions. These are shown in Figure 6.5, Figure 6.6 and Figure 6.7. The results from the experiment show that different sizes of product may effectively be reached by varying the amount of seeds inserted into the crystallizer. The more seeds, the less all the seeds can grow with the same amount of supersaturation. The supersaturation values are also higher the less seeds are inserted. The experimental CSD obtained with 7 g is broader than the ones obtained with 20, 30 and 40 g of seeds, which can be explained by nucleation. The total surface area of the seeds crystals is not high enough in this case to consume all the supersaturation by growth, which results in a burst of nucleation. Nucleation is seen at the lower crystal sizes, but broadening of the CSD due to a long tail at the higher crystal sizes could be due to agglomeration.

In Figure 6.6, the trends of the modelled CSDs are shown for the several seed loads. Also here, with higher seed load lower crystal sizes are obtained. This trend can also be seen in the experimentally obtained CSDs. The broadening of the peak in the model is explained by the fact that a certain value at a low size corresponds to more crystals than to a large size. In other words: a large crystal has more volume, so will individually account for more volume density in the graph. Therefore, as the CSD moves to the right due to growth, it also broadens and the maximum becomes lower. This means the m_3 (total crystal mass) of the product is still the same for all seed loads.

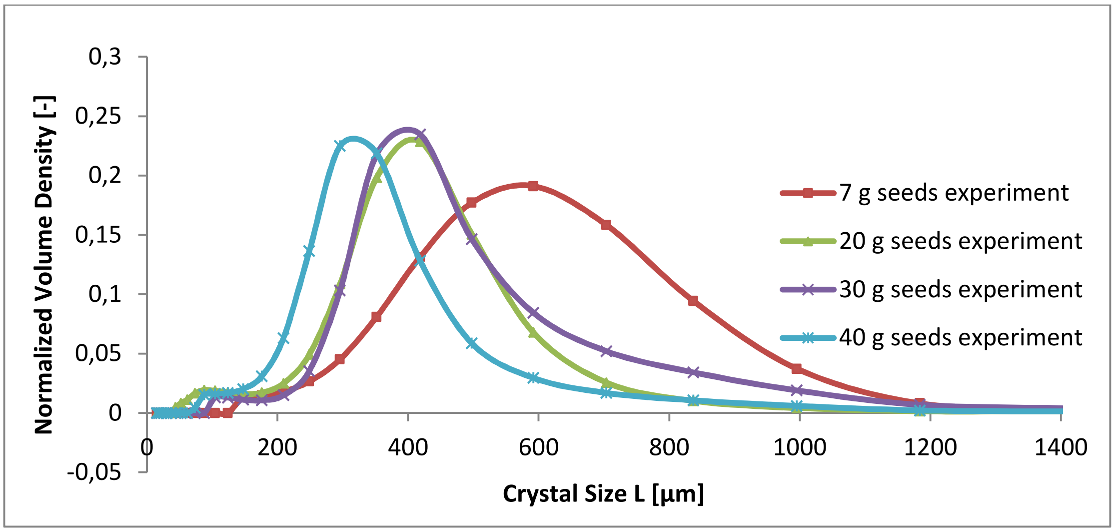

Figure 6.5: Experimental normalised volume density distributions for several seed loads

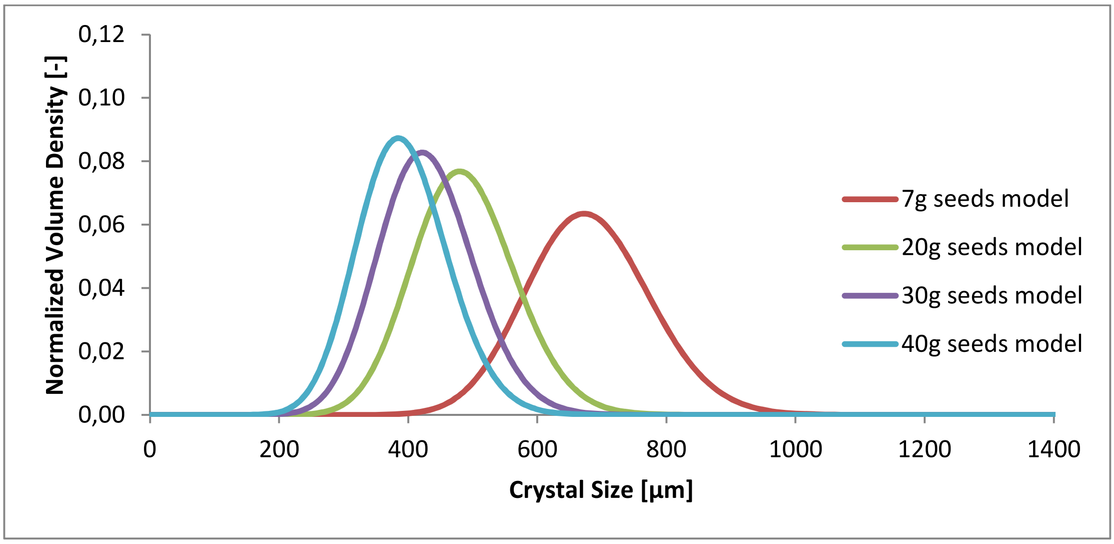

Figure 6.6: Normalized volume density distributions of several seed loads obtained by the TBD model

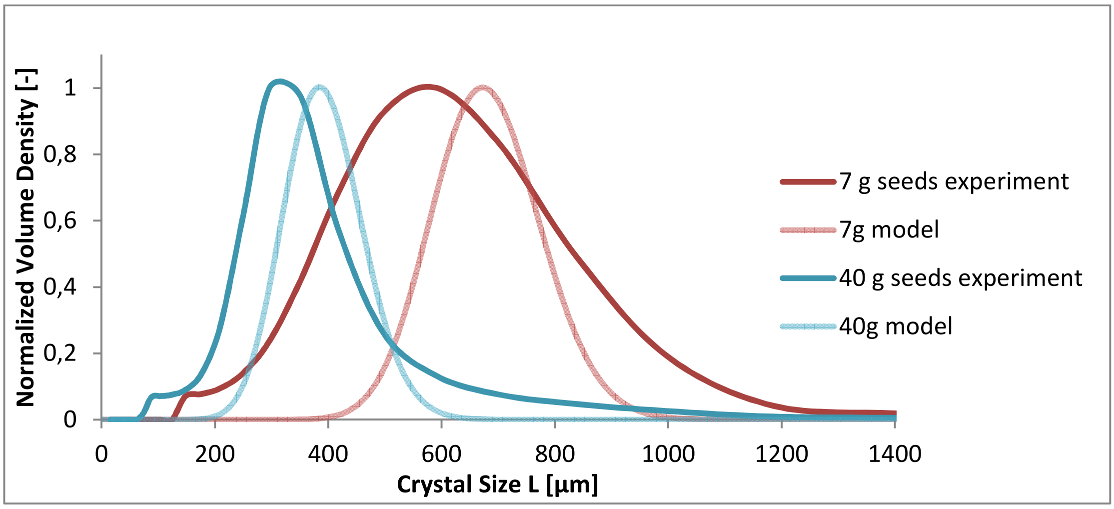

Figure 6.7: Volume density distributions, with maxima at 1 to compare the location and shapes of experimental and modelled distributions

In Figure 6.7 the graphs of experiments and models are scaled such that the location of the maximum and the shape of the curves are well visible. Note that the value on the *y*-axis has no physical meaning now. Here it can be seen that the model resembles the experimental values better with higher seed loads than with lower. This is due to the mechanisms described above, which occur less with higher seed load.

The CSD widths calculated by the model and of the experiments are listed in Table 6.1. There is no trend in the experimental results and the CSD width of experimental results is generally higher due to the reasons explained. Furthermore, the ratio of L_{90} and L_{10} and thus the value of the CSD width decreases as both quantiles increase with the same amount. As the median sizes obtained by the model are larger than the experimental values, this can be a second reason of the smaller values in the CSD width. If tasks such as agglomeration are added in the model, presumably the CSD widths would be closer together. Or, the other way around, the model values show the potential of the airlift crystallizer as growth compartment if in the future mechanisms such as attrition and agglomeration can be suppressed.

Note that even more phenomena could have occurred during the experiments. Mechanisms such as nonuniform distribution of supersaturation, mass transfer limitations and growth rate dispersion are not encountered in the model. It is also good to realise that seed distributions have large influence on the simulated product. With slightly other fits, significantly different median sizes are obtained.

Table 6.1: CSD widths obtained with several seed loads, experimental values and modelled values

Seed Load [kg]	***CSD Width Model [-]***	***CSD Width Experiments [-]***
0,007	1,44	2,37
0,02	1,52	2,17
0,03	1,57	2,66
0,04	1,58	2,62

6.4 Case 2: Batch solution crystallization of adipic acid

Set-up of case

This case is designed to validate trends found in batch crystallization of adipic acid. The flowsheet of the case is depicted in Figure 6.8. The left compartment is a crystallizer, the right compartment is a membrane unit. Initially, there is an undersaturated solution of adipic acid in water in the crystallizer. At *t* = 0 a constant liquid flow goes to the membrane unit, which removes solvent at a constant rate. The remaining liquid is flown back into the crystallizer. Note that there is classification of the flow to the membrane unit. The values of the parameters of the membrane unit are equal to experimental results from (Kuhn, et al. 2009). Parameter settings for adipic acid are given in Appendix H.

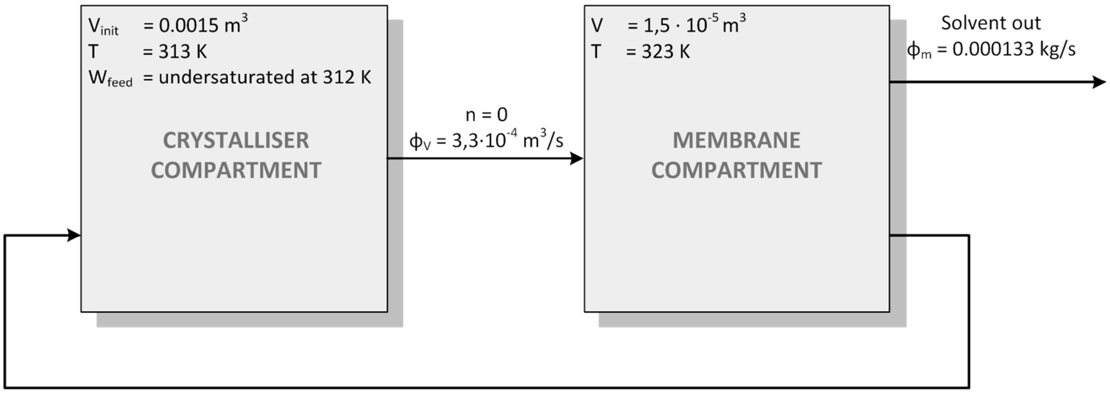

Figure 6.8: Flowsheet of Case 2

The case is split in three parts, showing the influence of tasks in the crystallizer on the system:

a) Growth, Primary Nucleation, Attrition and Heat Transfer; showing the trends found in literature.
b) Growth, Primary Nucleation and Heat Transfer; showing the effect of removal of attrition.
c) Growth, Primary Nucleation, Attrition, Dissolution and Heat Transfer; showing the effect of a sudden temperature increase of a certain period and that the growth term in the model becomes negative as the supersaturation becomes negative.

Different mechanisms occur after each other during the crystallization process. Figure 6.9 indicates the zones where each mechanism prevails. In the experiment of these curves, a hot solution of adipic acid is gradually fed into a crystallizer, which initially contained pure water at constant temperature.

First, supersaturation is established and no crystallization takes place during this period. When supersaturation becomes positive and sufficiently high, primary nucleation begins. As the mass and size of crystals increase, secondary nucleation, diffusion growth and agglomeration appear whereas primary nucleation rapidly drops.

The solid concentration in the crystallizer is given by (Marchal, et al. 1988):

$$c_S\left[\frac{mol}{m^3}\right] = k_V m_3 \frac{\rho_c}{M} \tag{6.6}$$

In this case primary nucleation, secondary nucleation and growth is modelled, so no agglomeration. Furthermore, no distinction between chemical and diffusional growth is modelled.

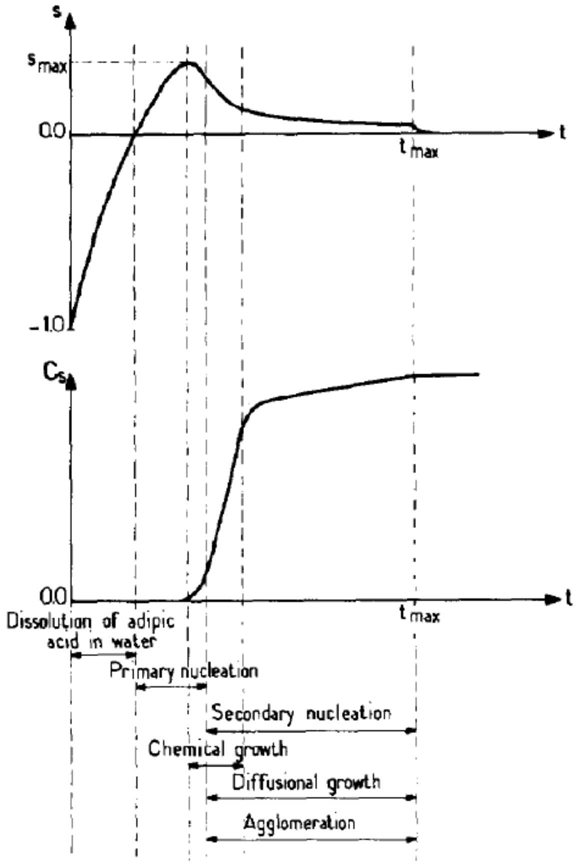

Figure 6.9: Typical curves of supersaturation and crystal concentration vs. time. (David, et al. 1991)

Results and Discussion

Figure 6.10, Figure 6.11 and Figure 6.12 present the relative supersaturation, the solid concentration (both for original and lower dependency of growth on supersaturation) and the occurrence of tasks in time of Case 2a.

In the supersaturation plot, one can see a similar trend as in literature. The main difference is the first part of the graph; the model result shows a straight line from negative to positive supersaturation values, whereas in literature the rate is decreasing in time to the maximum value. This is because in the model supersaturation is only created by solvent removal, which is done at a constant rate. In the experiment, the concentration is increased by addition of pure solute, but this is also a hot solution, so there is also a temperature influence on the supersaturation. By addition of the hot liquid, the temperature of the solution increases, so the rate of supersaturation generation decreases in time.

Also the trend of the solid concentration in time is clearly visible. The concentration of solid increases and the supersaturation decreases as the acid in solution turns into crystal. In the original model, the growth rate exponential factor, δ, is 0,85. In that graph, there is a smoother transition from the first part (nucleation) to the second part (growth) of the graph. This can be due to the fact that in the model no difference is made between chemical and diffusional growth. In literature, the differences in growth types are modelled with a so called 'growth effectiveness factor' (Garside 1971), which is in turn a function of the supersaturation. The effectiveness factor is defined as the measured overall growth rate divided by the growth rate obtained when crystal surface is exposed to conditions in the bulk solution. So it will become unity as the surface integration step increasingly dominates the growth process and the diffusion step becomes less important. At low supersaturations the factor is higher than at high supersaturations and pure surface integration growth has a higher dependency on supersaturation than pure diffusion growth. Therefore to compare, the model is ran with a arbitrarily chosen lower dependency on supersaturation (δ = 0,25). This result resembles the graph found in literature better, but the last part of the graph is less flat. This can be explained by the absence of agglomeration in the model. Agglomerates are not smooth; there are defects on the surface. This causes more difficult surface integration and diffusion, so a lower growth rate. Hence the solid concentration increases slower.

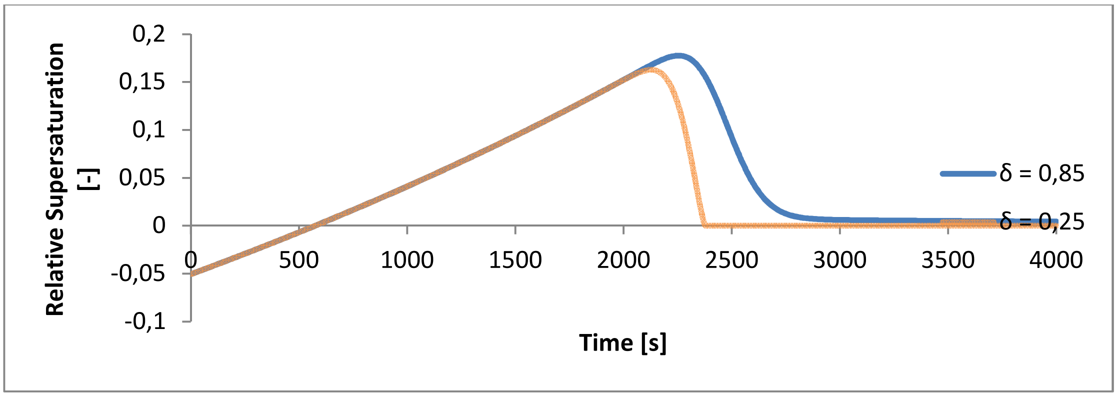

Figure 6.10: Case 2a - Relative supersaturation for different growth rate exponential factors δ

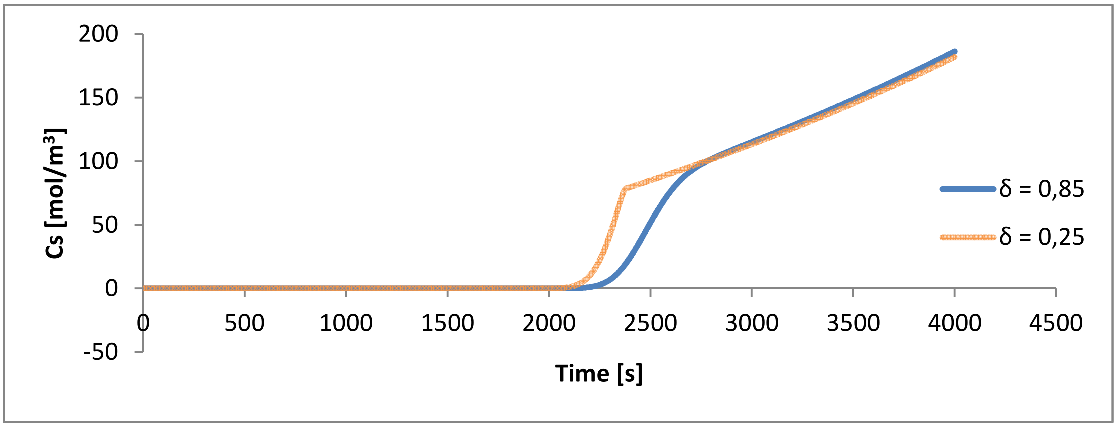

Figure 6.11: Case 2a - Solid concentration for different growth rate exponential factors δ

The differences between literature and model occur due to differences in kinetic models of the tasks, and do not undermine the effectiveness of the separation of tasks; these trends are approximately correct as can be seen in Figure 6.12. If the supersaturation is positive, the growth term is there. Clearly there is no growth until the first crystals appear, around *t* = 2000 seconds. Short after that, attrition occurs and as the supersaturation lowers, the terms decrease and stay constant to the end of the batch.

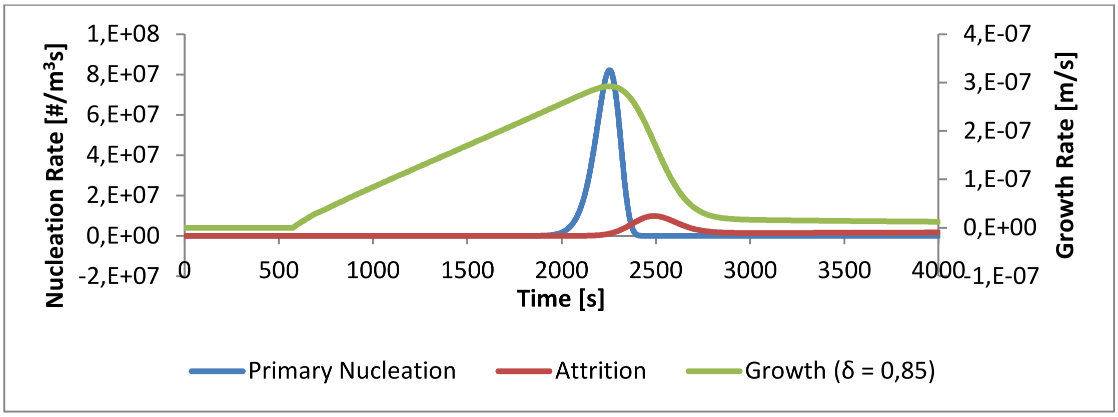

Figure 6.12: Case 2a – Occurrence of various tasks in time

In case 2b, the effect of attrition is shown. In Figure 6.13 it is clearly visible that with attrition there is a 'tail' of small crystals in the number density distribution, whereas without attrition all created primary nuclei only grow.

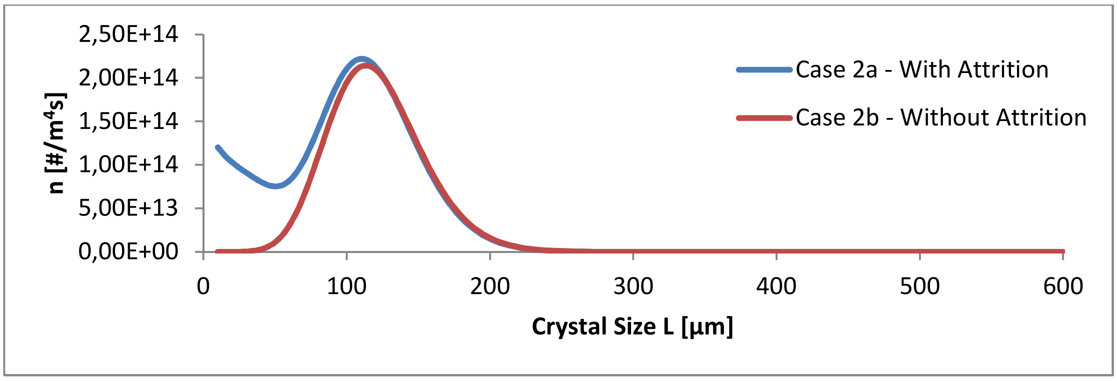

Figure 6.13: Case 2a and 2b – Number Density Distributions with and without attrition

In case 3c, a sudden temperature increase is imposed, to show the effect of the task Dissolution on the system. In Figure 6.14, the imposed temperature profile is shown, together with the corresponding supersaturation profile. It can be seen here that the supersaturation drops below zero when the temperature is increased.

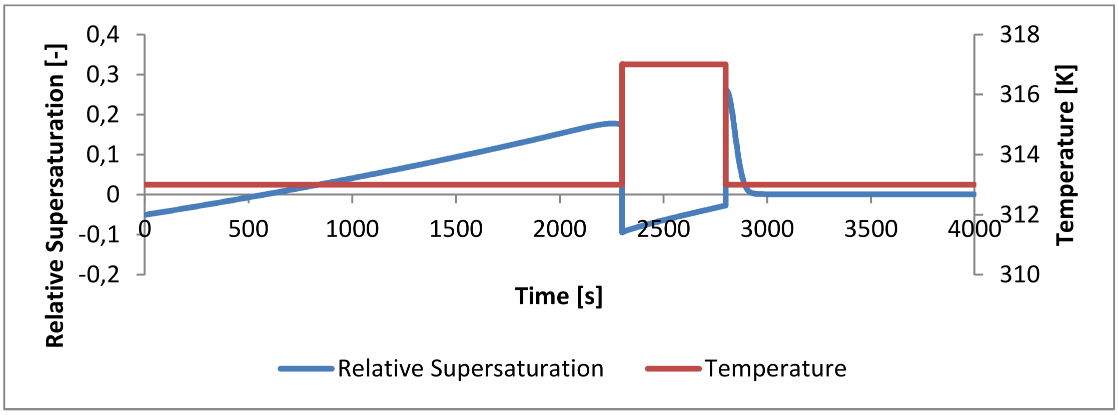

Figure 6.14: Case 2c – Influence of temperature on relative supersaturation

The influence of dissolution on the tasks is shown in Figure 6.15. As supersaturation becomes negative, the tasks Primary Nucleation and Attrition are zero, and the growth task-function becomes negative. Recall that the growth task-function equals the task growth plus the task Dissolution.

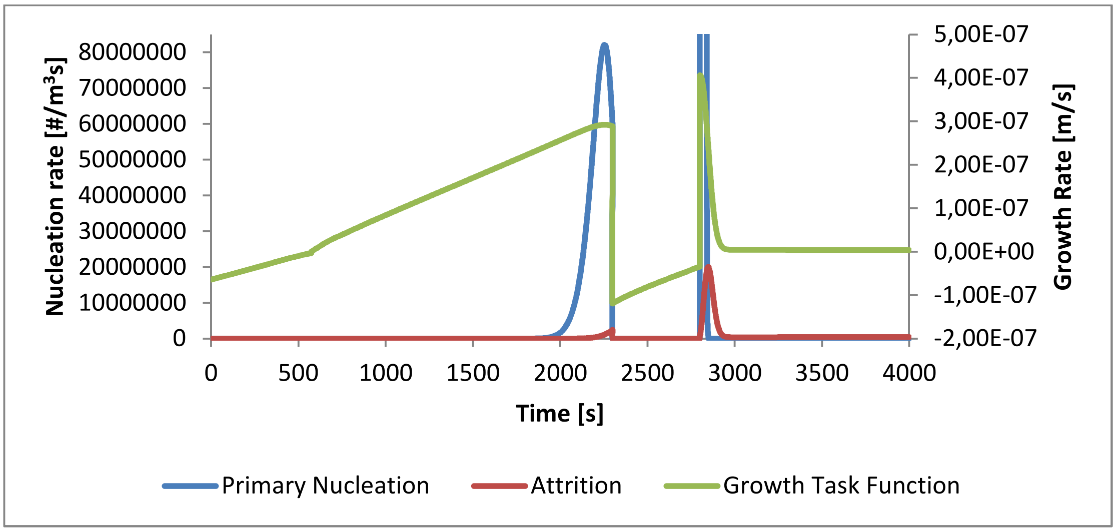

Figure 6.15: Case 2c – Occurrence of various tasks in time

In Figure 6.16 the volume based mean size[1] is shown in time. When the supersaturation becomes positive, the first crystals appear and start to grow immediately. When the temperature is increased, crystals start to dissolve so the mean size decreases. When supersaturation is increased again by the temperature decrease, secondary nucleation appears. There is a sharp discontinuity as small crystals are produced again. In the last part of the process the crystals grow a bit. This result is in agreement with the trends expected.

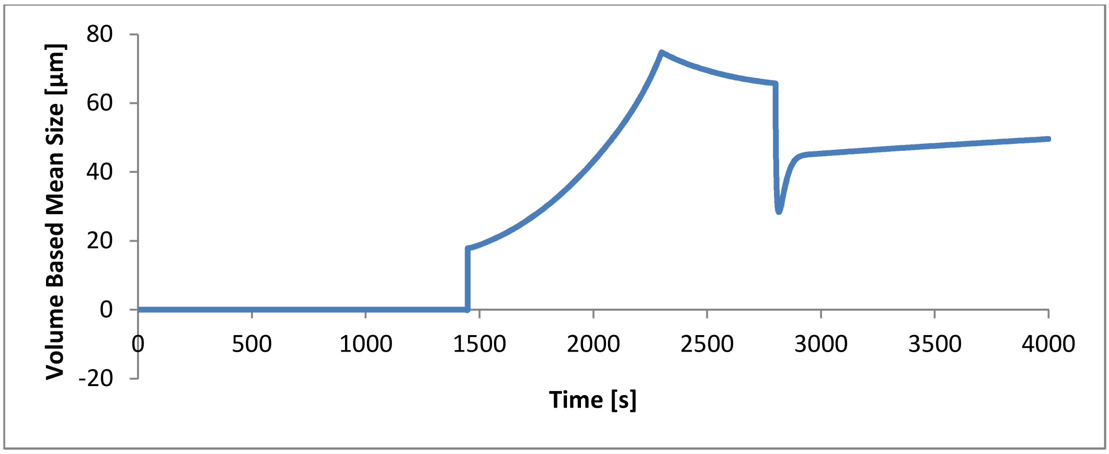

Figure 6.16: Case 2c – Volume Based Mean Size in time with the task Dissolution turned on and off during the batch

---

[1] The volume based mean size is defined as the fourth moment over the third moment:

$$\bar{L}_{vb} = \frac{m_4}{m_3} \tag{6.7}$$

6.5 Case 3: Airlift crystallizers in series

Set-up of case

In this case the airlift system of case 1 is put in a continuous mode and is used for adipic acid instead of ammonium sulphate. A continuous crystallization process can be employed in a single or multiple stage configuration. A possible reason for a multiple stage configuration is the requirement to produce a narrow CSD. By operating a multiple stage process in series, the residence time distribution and hence the crystal size distribution will be narrower than the CSD produced in a single crystallizer of the same volume.

To investigate if this effect is also visible using the TBD model, two different set-ups are modelled: in case 3a there is one continuous airlift crystallizer, and in case 3b there are three airlift crystallizers in series. Note that this system is never experimentally tested; it is a case to show the potential of task based design.

The flowsheet of case 3a is shown in Figure 6.17. Nuclei are created using a small ultrasound vessel in front of the airlift crystallizer. The nucleation tasks are off in the airlift crystallizer. This means that the number of crystals stay the same throughout the crystallization step; supersaturation is only consumed by growth. Supersaturation is controlled by a membrane unit, coupled to a buffer vessel. This buffer vessel is important to assure that the membrane will not run dry and because in case 3b more airlift compartments are added to one membrane system, as can be seen in Figure 6.18. All parameter settings can be found in Appendix F. The supersaturation controller is implemented as a PI controller, of which the algorithm is given in Appendix I.

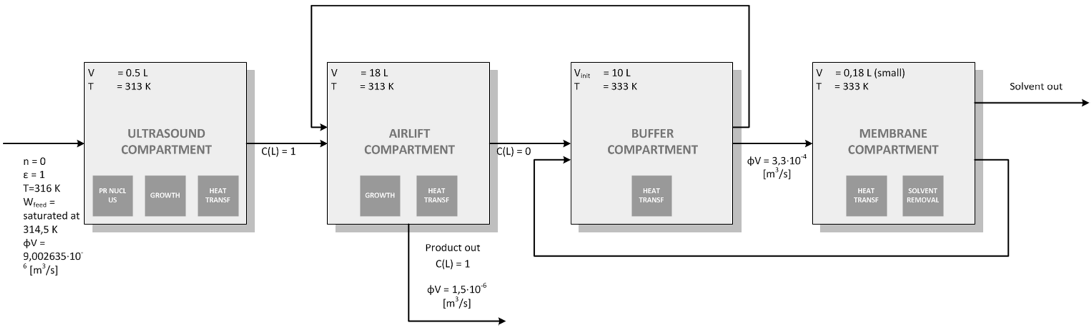

Figure 6.17: Flowsheet of Case 3a

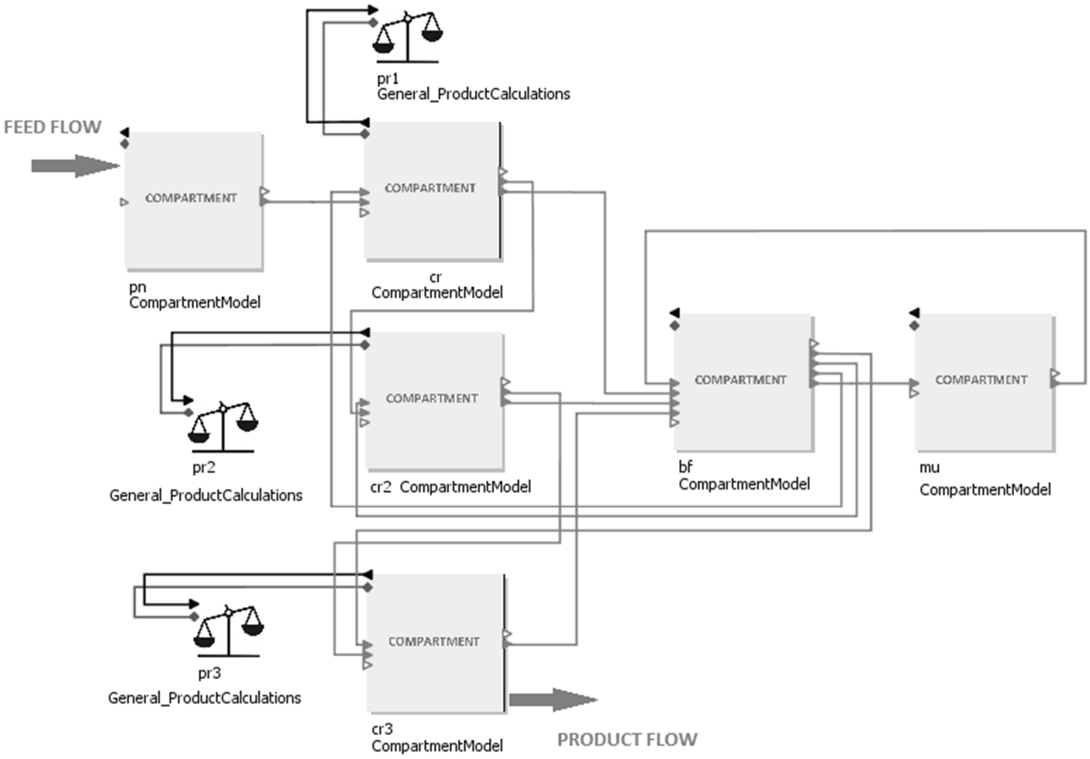

Figure 6.18: gPROMS flowsheet of Case 3b

Results and Discussion

In Table 6.2 simulation values of case 3a and case 3b are given.

In simulating, there is an aim on getting exactly the same parameters in the cases, except for the volumes of the airlift crystallizers. Unfortunately, this is hard to achieve. Therefore, a decision is made on what are the most important values to have the same. Since the product rate determines the residence time in the system, this needs to be equal. Furthermore, the feed rate gives the residence time in the ultrasound vessel, which in turn determines the initial distribution in the (first) airlift crystallizer. This is also important since the initial distribution has a large influence on the product quality. In case 3b, the supersaturation values in the three crystallizers are equal, to ensure constant growth rates for a comparison with literature which is given later in this paragraph. Note that this is a choice; the designer can also decide to use a different supersaturation for each crystallizer. The solvent removal rate is also a parameter which needs to be approximately constant, since this says something about the total mass of crystals that can be produced. As can be seen, the most important aspects are equated, but unfortunately supersaturation in the crystallizers and buffers, thus final crystal contents are not exactly the same at the steady states. This has an influence on the trends seen.

Table 6.2: Comparison of case 3a and case 3b

Variable	***Case 3a*** *Overall*	***Case 3b*** *Overall*	*Airlift 1*	*Airlift 2*	*Airlift 3*
Solvent Removal Rate [kg/s]	0,0079	0,0079			
Ultrasound Supersaturation [-]	0,0806	0,0806			
Ultrasound Volume [L]	0,5	0,5			
Buffer Supersaturation [-]	-0,6377	-0,6071			
Total Crystallizer volume [L]	18L	18L	6L	6L	6L
Supersaturation [-]	0,007	0,010	0,010	0,010	0,010
Growth Rate [m/s]	1,79E-08	2,53E-08	2,53E-08	2,53E-08	2,53E-08
Feed Flowrate [m^3/s]	9,55E-06	9,55E-06	9,55E-06	1,61E-06	1,57E-06
Product Flowrate [m^3/s]	1,50E-06	1,50E-06	1,61E-06	1,57E-06	1,50E-06
Crystal content C_s [mol/m^3]	2287	2326	253	918	2326
m_3 [-]	0,475	0,483	0,052	0,191	0,483
Median [µm]	826	616	385	500	616
Volume Based Mean Size [µm]	915	668	435	551	668
CSD Width [-]	3,93	3,06	4,06	3,41	3,06

In Figure 6.19, the volume density distributions are depicted of the two cases. Residence time in case 3a is three times higher than in case 3b. Therefore there is a bigger difference in residence times of individual crystals. This means that some crystals will grow bigger than in the case of crystallizers in series and some will stay smaller. The narrowing of the distribution in the case with three crystallizers in series is clearly visible and is also seen in the CSD width values. The volume based mean size and median is larger in the single stage process. The crystals that stay smaller have far less volume so have a small influence on the distribution, whereas bigger crystals have much more volume so cause a higher volume density fraction at the right side of the graph. To make this more clear, also number densities are plotted in Figure 6.20.

Case 3a resembles a MSMPR crystallizer, but since there is no nucleation in the crystallizer, the logarithmic plot is not exactly a straight line (as is visible in the analytical solution of an MSMPR in Appendix E). It can be seen that in case 3b the number density distribution narrows more down to a certain value. The peak in the number density distribution of case 3b is at a higher value than of case 3a, as expected. The number of crystals is the same in case 3a and 3b, which means, counted in numbers, more larger crystals are produced in the cascade of airlifts. Since the supersaturation of case 3a is lower, also the final crystal content is lower. Even though the growth rate in case 3a is lower than in case 3b, the volume based mean size is larger.

It is very difficult to get all the parameters exactly the same for the two cases using only simulation. These results are obtained by manual optimisation. In the future this can be done using optimisation methods.

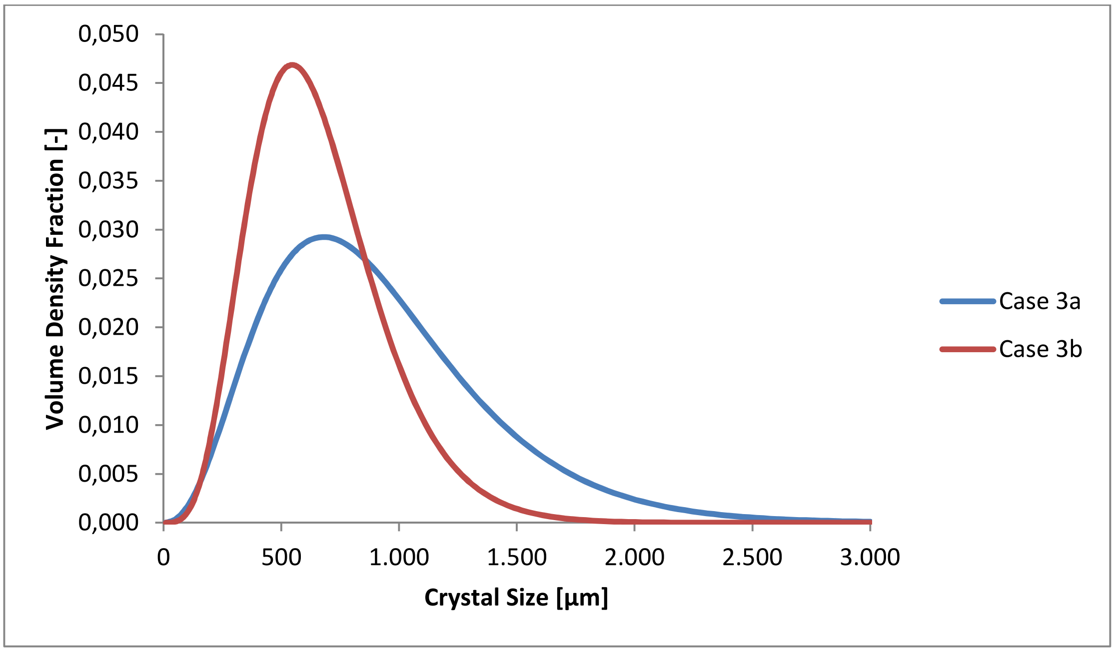

Figure 6.19: Volume density distribution comparison between case 3a and case 3b

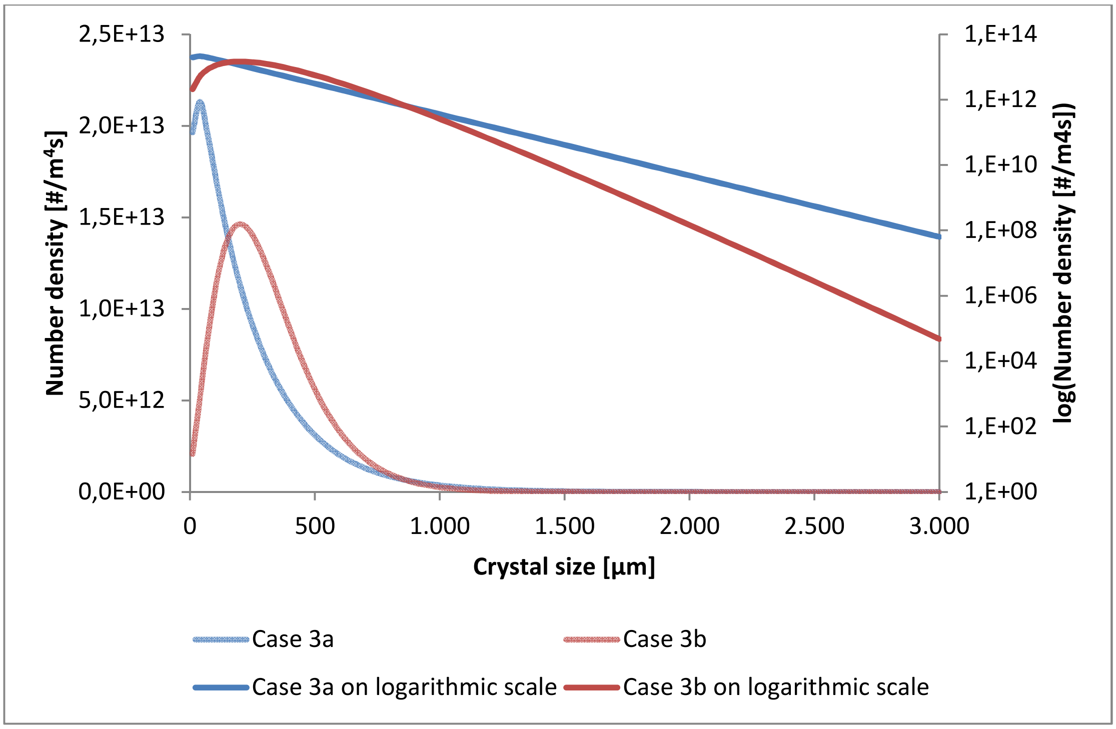

Figure 6.20: Number density distribution comparison between case 3a and case 3 plotted on linear and logarithmic scales

In literature, analytical solutions can be found for MSMPR crystallizers in series. To conclude, results of case 3b are compared with literature trends. In the analytical solutions, the following is assumed:

- Equal volumes in all stages
- The residence time is the same in each stage
- Equal constant growth rate in all stages and growth rate is size independent
- Primary nucleation in the first stage only (in the model, an ultrasound vessel is used for nucleation)
- No secondary nucleation
- No agglomeration

The analytical solutions and results of the model are depicted in Figure 6.21, Figure 6.22 and Figure 6.23. For the third graph, the following dimensionless quantities are introduced for the crystal size and the number density:

$$x = \frac{L}{G\tau}$$

$$f(x) = \frac{Gn(L)}{N} \tag{6.8}$$

In which *N* is the nucleation task-function.

As can be seen in the graphs, the median crystal size increases with the number of crystallizers operating in series. The same trends as in literature are clearly visible in the modelled results. The heights are not the same due to different conditions. In the analytical solutions, nucleation takes place in the first crystallizer but in the model, the first has no nucleation. This is also visible in Figure 6.23, since the graph of the first crystallizer is not entirely straight. Actually the first crystallizer would be the ultrasound vessel, but since the residence time is much smaller there, it would be incorrect to compare that CSD with the airlift crystallizers.

Since this set-up is not experimentally tested yet, the question remains if this is a realistic result. In reality the crystallization kinetics may alter from stage to stage due to differing operating conditions such as supersaturation. Consequently, other mechanisms that are not modelled will occur in the crystallizer. The increase in the median crystal size with extended residence time in the cascade competes with an increase in the secondary nucleation rate caused by impeller-crystal and crystal-crystal collisions for an optimum supersaturation and growth rate. Furthermore, agglomeration can occur and has a large influence on the CSD. Finally, growth rate dispersion limits the ultimate narrowness of the CSD. Also tasks that have a positive influence on the CSD can be included, such as Classification of the slurry that is withdrawn from one crystallizer going into the next to further narrow the CSD. Controllability is also a challenging topic. For example, since the amount and the size of nuclei have a big influence on the product, the primary nucleation vessel should be operated tightly. Nevertheless, this case shows the ease of flowsheet creation, the possibility to model staged operation and get the expected trends with reasonable results using the TBD model.

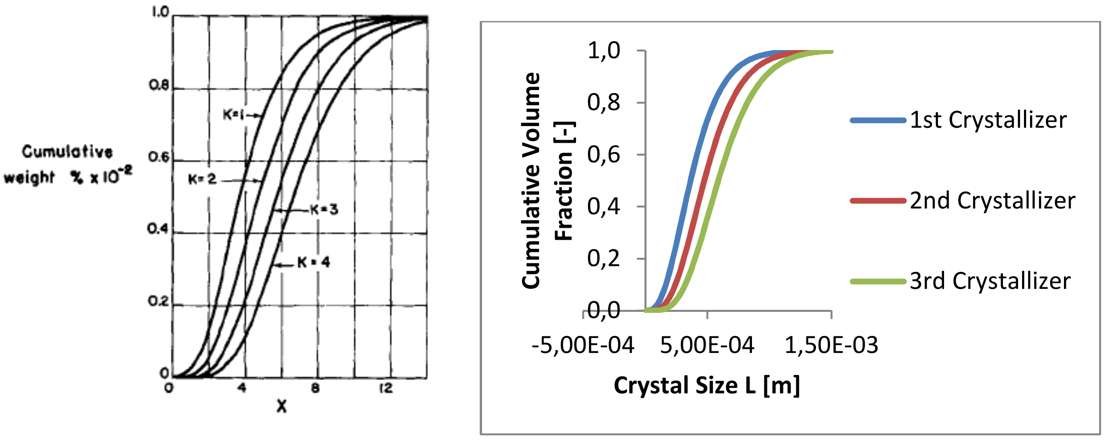

Figure 6.21: Left: Literature plot of cumulative weight per cent vs. dimensionless size for k agitator-crystallizers operating in series and nucleation only in first tank (Randolph and Larson 1962). Right: Cumulative volume density distribution obtained by the model.

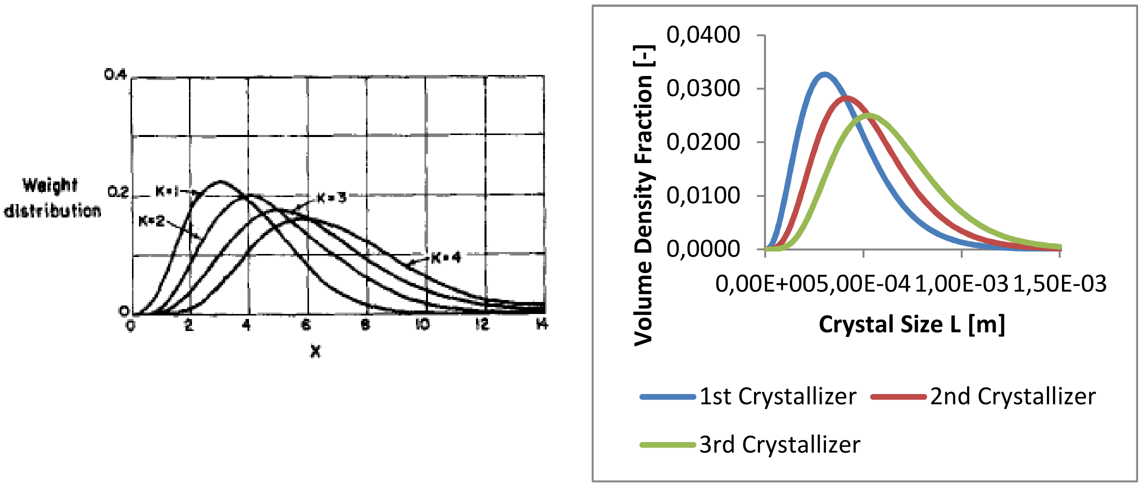

Figure 6.22: Left: Literature plot of weight distribution vs. dimensionless size for multi-tank operation and nucleation only in first tank (Randolph and Larson 1962). Right: Volume density distribution obtained by the model.

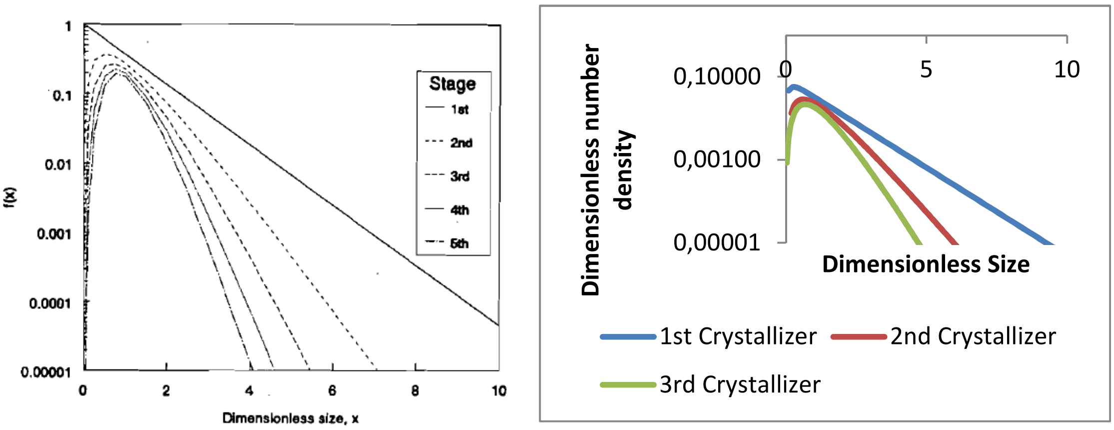

Figure 6.23: Left: Literature plot of number density distribution for a five stages cascade with nucleation in the first stage and no agglomeration (Chung, Lee and Saleeby 1998). Right: Number density distribution obtained by the model.

Conclusions and Recommendations

6.6 Conclusions

In this research, a modelling tool for dynamic simulation of task based solution crystallization processes is developed. Crystallization tasks, representing fundamental changes needed to arrive at desired product quality, are used as building blocks rather than existing equipment. This TBD model can be applied to a wide range of crystallization processes: various crystallization methods, operation modes, configurations and a variety in number of streams, compartments and crystallization tasks. The framework supports rapid generation of consistent process models and facilitates analysis of the influence of individual tasks. The model is implemented in gPROMS.

The general terminology and hierarchy for all the aspects of the TBD modelling tool are revised. The modelling structure is developed based on compartmental modelling. A new way to connect tasks to a compartment model is developed. Hereto, traditional spatially lumped conservation equations are rewritten using so called task-functions which each can contain several tasks. Rate laws for those tasks are written in separate sub-models listed in a task library. The following tasks are tested: Growth, Dissolution, Primary nucleation (conventional and using ultrasound), Attrition, Seeding, Heat Transfer, Solvent removal using membranes and Classification.

To show the ability to quickly construct networks of units representing all kinds of crystallization processes, three different cases are simulated. Already existing innovative task based equipment from the TU Delft is also implemented. Case 1 simulates batch cooling crystallization experiments of ammonium sulphate in an airlift crystallizer with tasks Growth and Seeding and a cooling curve. Comparison of median sizes with ideal growth and experimental values gives good results. Trends in crystal size distributions are also clearly visible, but at higher seed loads results are more promising than at lower seed loads due to extra occurring phenomena which are not modelled.

Case 2 shows the effect of tasks on a batch adipic acid crystallization system using a membrane unit for solvent removal. Supersaturation and solid concentration profiles are similar as in literature and a clear distinction in rate processes of tasks is visualised. The product differences when the task Attrition is turned on and off and a nice transition from growth to dissolution, which influenced product related values such as mean size, are seen.

To show the future potential of TBD, in the third case a crystallization process is modelled which is never experimentally tested: continuous crystallization of adipic acid in a cascade of airlift crystallizers. Here a comparison in CSDs is made between a single airlift and three airlifts in series. Other aspects are the use of supersaturation control, modelling a higher number of compartments and production of nuclei using an ultrasound vessel. As expected, more larger crystals with a narrower CSD are produced in the cascade of airlifts. The CSDs obtained by the crystallizers in series are compared with analytical solutions for a MSMPR, and showed similar trends.

In constructing the flowsheets of the three cases, it is concluded that the developed structure works well. Using the task-function framework, newly developed tasks can be easily added, such that innovative Process Intensifications can be included in the model. Based on above findings it can be concluded that the developed model forms a good basis for further research.

6.7 Recommendations for future work

On conservation equations and the general structure

In this work compartmental modelling is used. The compartment is considered well-mixed, such that spatially lumped conservation equations can be used. A prerequisite for this approach is that the network of compartments approximates the main hydrodynamic characteristics of the crystalliser. One should keep this in mind in the development of models for (novel) crystallization equipment. Throughout this thesis, it is assumed that transport through the surfaces of a compartment does not cost energy. It might be possible to create a task to account for this convective transport. For a more in depth description of tasks such as Mixing, Heat Transfer and Membranes, modelling of interaction with immobile phases is advisable. Then extra transfer terms need to be added to the conservation equations. In addition to matter and energy, changes in momentum (pumping, compression) should be involved to be able to describe the membrane unit adequately. For a better description of airlift crystallizers, the vapour phase can be added to the model in addition to the slurry phase. Also note that this slurry phase does not account for differences in flow pattern of the liquid and solid phase due to particle slip.

Modelling of tasks

In general, to increase the predictive capability of the TBD model, more detailed rate laws for the tasks are needed, since description of complex kinetics is not an aim of this work. An idea of the functional dependencies of these rates is given in chapter 4 of this report.

Since mixing has a significant influence on process conditions and the validity of lumped process models, the task Mixing should be implemented in the model. It can be modelled for instance using a relation for minimum tip speed necessary for well mixed conditions, and connecting that to mechanisms such as attrition, power input and temperature. To get a better insight in the energy usages, tasks Shaft Work and Heat Transfer and the membrane unit need to be worked out. For Heat Transfer and the membrane unit, the used equipment can be modelled in detail, relating task rates to driving forces and energy usages. Shaft work can then be added to the enthalpy balance to account for its influence on the temperature of the system by for instance the impeller (in case of viscous slurry). Evaporation can be used as task for solvent removal, and is not implemented yet. It can be modelled with a thermodynamic model relating pressure, saturation vapour pressure and the boiling surface to the amount of solvent evaporating. The task Classification is a task occurring on the compartment boundary and not in the bulk; different classification functions can be assigned for different outgoing streams. Therefore it is not yet modelled in the form of a task-function. A study can be done on how to generalize this task, so that one is able to list several different size dependent classification functions in the task library and turn these functions on and off for individual outgoing streams.

Regarding the population balance equation, also improvements can be made. The PBE needs to be adjusted for simulation of mechanisms such as size dependent growth, growth rate dispersion, agglomeration and breakage, Ostwald ripening, strain in the crystal lattice and use of Dissolution for size manipulation. Possibilities for improvement include solving two-population balances and PBEs with more internal coordinates than just the crystal length. As one changes the population balance and the purposes of the model in general, one should reconsider the numerical solution of the PBE; the distribution of the grid and the solution method. Currently the finite volume method is used.

gPROMS

As software tools develop quickly, the solvers that are best at that time need to be used. The TBD model is now implemented in gPROMS. Modelling is intuitive in gPROMS; it is possible to design new units and use hierarchical modelling structures. Tasks are worked out in sub-models and can be easily added, adjusted and individually tested, which simplifies debugging. The build in check that gPROMS automatically performs on the problem before solving it, enhances greatly the robustness of the model. Also options for user interfaces are promising for task based design, since ideally no code should be written by the user during the construction of a flowsheet. Tasks can now be intuitively turned on and off using the topology option of gPROMS. Using the separate system properties model for each species system, it is easy for the user to change to another system. Currently, the user still needs to have great knowledge of the model to be able to assign the right variables to prevent index issues. Therefore, a solution strategy needs to be developed and built in the model.

Further recommendations

During the simulation cases perfect control of all variables is assumed, but in reality this is not the case. This topic should be addressed in future studies since the design of the crystallization process and control structure is strongly connected. One should keep in mind that an alternative task structure directly results in a different set of feasible control structures (Lakerveld 2010).

Validation of the TBD model is challenging, due to the lack of experimental data and an uncertainty with respect to the predictive quality of the (heuristic) kinetic task models. Exact physical mechanisms of tasks using different driving forces have to be identified. Furthermore no uncertainty-analysis is done on the used parameters and differences in measurement tools are not encountered. This can be of importance for the accuracy and predictive capability of the TBD model. The required knowledge can be obtained from experiments combined with further model development.

In the introduction it is mentioned that this work is essential for a long term goal of model-based optimisation driven process synthesis. This means that the next step after dynamic simulation is optimisation. Two types of restrictions concerning the tasks need to be implemented if the model is used in an optimisation environment: physical constraints (limitations set on the task to a physical domain in which the event will effectively work) and a restriction on tasks that cannot or will always occur in the same compartment. Timescales of tasks can be used to determine residence times such that main tasks can be executed, but unwanted tasks are suppressed or small enough to ignore. The costfunction of the optimisation problem may include process economics, sustainability aspects such as minimizing energy usage and waste losses, and product requirements such as maximizing crystal size or minimizing the CSD width. If these objective functions can be optimised using the TBD model, there is great potential for model based process design of innovative task based solution crystallizers.

References

Beers, K.J. *Numerical Methods for Chemical Engineering.* Cambridge: University Press, 2007.

Bermingham, S.K. *A design procedure and predictive models for solution crystallisation processes.* Delft, The Netherlands: DUP science, 2003.

Biegler, L.T., I.E. Grossmann, and A.W. Westerberg. *Systematic Methods of Chemical Process Design.* New Jersey: Prentice Hall, 1997.

Chung, S.H., H.W. Lee, and E.G. Saleeby. "Modelling a cascade of continuous MSMPR crystallizers with agglomeration." *Chem. Eng. Comm.* 163 (1998): 177-200.

Daudey, P.J. *Crystallisation of ammonium sulphate.* Delft University of Technology, 1987.

Davey, R.J., and J. Garside. *From Molecules to Crystallizers.* Oxford University Press, 2000.

David, R., J. Villermaux, P. Marchal, and J. Klein. "Crystallization and precipitation engineering - IV. Kinetic model of adipic acid crystallization." *Chem. Eng. Sci.* 46 (1991): 1129–1136.

Edgar, T.F., D.M. Himmelblau, and L.S. Lasdon. *Optimization of chemical processes.* 2nd. New York: McGraw-Hill, 2001.

Felder, R.M., and R.W. Rousseau. *Elementary Principles of Chemical Processes.* 3rd. John Wiley & Sons, 2000.

Garside, J. "The concept of effectiveness factors in crystal growth." *Chem. Eng. Sci.* 26 (1971): 1425-1431.

Grievink, J. "Model Development Steps - Power Point slide." 2012.

Hangos, K.M., and I.T. Cameron. *Process Modelling and Model Analysis.* London: Academic Press, 2001.

Invista. *Adi-pure High Purity Adipic Acid.* n.d. http://adi-pure.invista.com/e-trolley/page_11546/index.html (accessed July 27, 2012).

Jagadesh, D., N. Kubota, M. Yokota, N. Doki, and A. Sato. "Seeding Effect on Batch Crystallization of Potassium Sulfate under Natural Cooling Mode and a Simple Design Method of Crystallizer." *Journal of Chemical Engineering of Japan* 32, no. 4 (1999): 514-520.

Janssen, L.P.B.M., and M.M.C.G. Warmoeskerken. *Transport phenomena data companion.* 3rd. Delft, The Netherlands: VSSD, 1987.

Kondili, E., C.C. Pantelides, and R.W.H. Sargent. "A general algorithm for short-term scheduling of batch operations – I. MILP formulation." *Comp. chem. Eng.* 17 (1993): 211-227.

Kordylla, A., T. Krawczyk, F. Tumakaka, and G. Schembecker. "Modeling ultrasound-induced nucleation during cooling crystallization." *Chem. Eng. Sci.* 64 (2009): 1635-1642.

Kramer, H.J.M. "Generalised material balances v3 Version August 2011." 2011.

—. *PowerPoint slides of course WB4403 crystallization - Process Design & Operation.* Delft University of Technology, 2011.

Kramer, H.J.M., and G.M. van Rosmalen. *Crystallization.* Vol. 1, in *Encyclopedia of Separation Science*, by I.D. Wilson, 64-84. 2000.

Kuhn, J., R. Lakerveld, H.J.M. Kramer, J. Grievink, and P.J. Jansens. "Characterization and Dynamic Optimization of Membrane-Assisted Crystallization of Adipic Acid." *Ind. Eng. Chem. Res.* 48 (2009): 5360-5369.

Lakerveld, R. *Development of a Task-Based Design Approach for Solution Crystallization Processes.* Delft, The Netherlands, 2010.

Lakerveld, R., H.J.M. Kramer, A.I. Stankiewicz, and J. Grievink. "Application of generic principles of process intensification to solution crystallization enabled by a task-based design approach." *Chem. Eng. Process.* 49 (2010): 979-991.

Lakerveld, R., H.J.M. Kramer, P.J. Jansens, and J. Grievink. "The application of a task-based concept for the design of innovative industrial crystallizers." *Comp.Chem. Engng.* 33 (2009): 1692-1700.

Marchal, P., R. David, J.P. Klein, and J. Villermaux. "Crystallization and precipitation Engineering - I. An efficient method for solving population balance in crystallization with agglomeration." *Chem. Eng. Sci.* 43 (1988): 59-67.

Menon, A.M. *A task based design procedure and modelling approaches for industrial crystallization processes.* Delft, The Netherlands: Delft University press, 2006.

Mersmann, A. *Crystallization Technology Handbook.* 2nd. New York: Marcel Dekker, Inc., 2001.

Mesbah, A. *Optimal Operation of Industrial Crystallizers.* Delft, The Netherlands: CPI Wohrmann, 2010.

Mohan, R., K.A. Boateng, and A.S. Myerson. "Estimation of crystal growth kinetics using differential scanning calorimetry." *J. Cryst. Growth* 212 (2000): 489-499.

Process Systems Enterprise Ltd. *gPROMS Introductory User Guide.* Release 2.3.1. London, UK, June 2004.

Randolph, A.D., and M.A. Larson. *Theory of Particulate Processes.* 2nd. San Diego, USA: Academic Press, Inc., 1988.

Randolph, A.D., and M.A. Larson. "Transient and Steady State Size Distributions in Continuous Mixed Suspension Crystallizers." *A.I.Ch.E. Journal* 8, no. 5 (1962): 639-645.

Rosmalen van, G.M., P.J. Jansens, H.J.M. Kramer, and M.M. Seckler. *Industrial crystallisation and precipitation - Handbook of PAON course.* Delft University of Technology, The Netherlands, 2003.

Seborg, D.E., T.F. Edgar, and D.A. Mellichamp. *Process Dynamics and Control.* 2nd. John Wiley & Sons, 2004.

Soare, A., R. Lakerveld, J. van Royen, G. Zocchi, A.I. Stankiewicz, and H.J.M. Kramer. "Minimization of attrition and breakage in an airlift crystallizer." *Ind. Eng. Chem. Res.*, 2012: Submitted for publication June 19 2012.

Westhoff, G.M. *Design and analysis of suspension crystallisers - Aspects of crystallisation kinetics and product quality.* Delft, 2002.

List of Symbols

A	surface area	[m^2]
A_{PN}	primary nucleation rate constant	[#/m^{3}s]
A_T	total crystal surface area	[m^2/m^3]
B	crystal birth rate	[#/m^{4}s]
B_0	birth rate of crystals at L_0	[#/m^{3}s]
B_{PN}	primary nucleation rate constant	[-]
C	classification task-function	[-]
$C_{p,c}$	heat capacity solid phase	[J/kgK]
$C_{p,l}$	heat capacity liquid phase	[J/kgK]
$C_{p,w}$	heat capacity solvent	[J/kgK]
c_S	solid concentration in suspension	[mole/m^3]
C_{SEED}	seed load	[-]
c_{SEEDS}	concentration of seeds	[kg/m^3]
D	crystal death rate	[#/m^{4}s]
dH_{evap}	heat of evaporation	[J/kg]
dH_{crys}	enthalpy of crystallization	[J/kg]
E	solvent evaporation task-function	[kg/s]
E	energy	[J]
E_k	kinetic energy	[J]
E_p	potential energy	[J]
f	dimensionless number density	[-]
F_1	fraction of first lognormal distribution	[-]
G	crystal growth rate	[m/s]
G	growth task-function	[m/s]
gm_2	growth moment	[#/s]
H	enthalpy	[J]
h	classification function	[-]
h	heat transfer coefficient	[J/m^{2}Ks]
I	initial distribution task-function	[#/m^4]
J	flux	task dependent
k	rate constant	task dependent
k_{DIS}	dissolution rate constant	[m/s]
k_G	growth rate constant	[m/s]
k_{PN}	ultrasound primary nucleation rate constant	[#/m^{3}s]
k_S	surface shape factor	[-]
k_{SN}	secondary nucleation rate constant	[#/m^{3}s]
k_V	volumetric shape factor	[-]

L	crystal length	[m]
L_0	lower bound of crystal size domain	[m]
L_{g1}	geometric mean of log normal distribution	[-]
L_i	crystal size at gridpoint *i*	[m]
L_{max}	higher bound of crystal size domain	[m]
L_{min}	lower bound of crystal size domain	[m]
L_q	quantile	[m]
L_{SEED}	crystal size of seeds	[m]
M	molecular weight	[kg/mole]
M	solvent removal task-function	[kg/s]
m	mass	[kg]
m_j	*j*-th statistical moment of crystal size distribution	[m^i/m^3]
M_T	total mass	[-]
N	nucleation task-function	[$\#/m^3s$]
N	number of particles per unit volume	[$\#/m^3$]
n	crystal number density	[$\#/m^4$]
N_g	number of gridpoints	[-]
p	pressure	[Pa]
Q	net rate of heat addition	[J/s]
Q	heat transfer task-function	[J/s]
q	quantile number	[-]
R	reaction rate	[mole/s]
T	temperature	[K]
t	time	[s]
T_{jacket}	temperature of jacket	[K]
U	internal energy	[J]
V	volume	[m^3]
$\boldsymbol{v}$	particle velocity vector	[m/s]
$\boldsymbol{v_e}$	external particle velocity vector	[m/s]
$\boldsymbol{v_i}$	internal particle velocity vector	[m/s]
w	weight fraction	[-]
W_S	shaft work	[J/s]
w_{sat}	solubility weight fraction	[-]
w_{SEEDS}	seed mass	[kg]
w_{th}	theoretical yield of crystals	[kg]
W_{vc}	work due to volume change	[J/s]
x	mole fraction	[-]
x	dimensionless crystal size	[-]
Y	birth death task-function	[$\#/m^4s$]

Greek

α	ultrasound primary nucleation rate exponential factor	[-]
δ	growth rate exponential factor	[-]
ε	liquid fraction	[-]
ζ	dissolussion rate exponential factor	[-]
κ_{US}	ultrasound activity fraction	[-]
μ	driving force	task dependent
ν	stoichiometric coefficient matrix	[-]
ρ_c	material density of the solid phase	[kg/m^3]
ρ_l	material density of the liquid phase	[kg/m^3]
ρ_v	material density of the vapour phase	[kg/m^3]
σ	relative Supersaturation	[-]
σ_i	geometric standard deviation lognormal distribution	[-]
τ	residence time	[s]
T	task rate	task dependent
φ_E	energy flowrate	[J/s]
φ_H	enthalpy flowrate	[J/s]
φ_m	mass flowrate	[kg/s]
φ_V	volumetric flowrate	[m^3/s]
Ψ	interphase transfer term	balance dependent
ω	energy dissipation stirrer	[J/s]
ω_{MAX}	maximum power duty	[J/s]

Subscripts

0	initial
c	crystal
in	inlet
init	initial
l	liquid
out	outlet
vap	vapour

Superscripts

l	liquid phase
s	solid phase
v	vapour phase

Appendices

Appendix A - Conservation Equations

Coupling Population Balance & Mass Balance

In chapter 1 the following expression for the spatially lumped population balance is introduced:

$$\frac{\partial nV}{\partial t} = -V\frac{\partial nG}{\partial L} + \sum_{j}^{Ni} \phi_{V,in,j} \cdot n_{in,j} - \sum_{j}^{No} \phi_{V,out,j} \cdot n_{out,j} + VB(L) - VD(L)$$

$$n(L=0,t)\left[\frac{\#}{m^3 m}\right] = \frac{B_0(t)}{G(L=0,t)}$$

$$n(L,t=0) = \text{ Initial distribution}$$

By multiplying all the terms of the PBE with L^3 and integrating over the size domain one obtains the crystal volume balance:

$$\int_{L_0}^{\infty} \frac{\partial nVL^k}{\partial t} dL = -V\int_{L_0}^{\infty} \frac{\partial Gn}{\partial L} L^k dL + \int_{L_0}^{\infty} \sum_{j}^{Ni} \phi_{V,in,j} n_{in,j} L^k dL - \int_{L_0}^{\infty} \sum_{j}^{No} \phi_{V,out,j} n_{out,j} L^k dL +$$

$$V\int_{L_0}^{\infty} B(L) L^k dL - V\int_{L_0}^{\infty} D(L) L^k dL$$

Use the third moment of the crystals:

$$m_3(t) = \int_{L_0}^{\infty} n(L,t) L^3 dL$$

Now the partial differential equation can be transformed into an ordinary differential equation:

$$\frac{dm_3V}{dt} = \underbrace{-V\left[GnL^3\right]_{L_0}^{\infty} + 3V\int_{L_0}^{\infty} GnL^2 dL}_{\text{Chain rule}} + \sum_{j}^{Ni} \phi_{V,in,j} m_{3,in,j} - \sum_{j}^{No} \phi_{V,out,j} m_{3,out,j} +$$

$$V\int_{L_0}^{\infty} B(L) L^3 dL - V\int_{L_0}^{\infty} D(L) L^3 dL$$

The first RHS term vanishes if the lower limit of the domain or the nucleation size of the crystals, *L_0*, is very small. When *B* and *D* only represent agglomeration and breakage, the sum of the two last RHS terms is also equal to zero:

$$\frac{dm_3V}{dt} = V\frac{dm_3}{dt} + m_3\frac{dV}{dt} = 3V\int_{L_0}^{\infty} GnL^2 dL + \sum_{j}^{Ni} \phi_{V,in,j} m_{3,in,j} - \sum_{j}^{No} \phi_{V,out,j} m_{3,out,j}$$

The population balance is in fact a distributed mass balance for a solid or dispersed phase, and is linked to the liquid or continuous phase mass balances via the crystallization kinetics.

This is represented by a simplified notation for the growth term, which represents an interphase mass flux between the liquid and solid phase:

$$gm_2\left[\frac{1}{s}\right] \equiv 3\int_{L_0}^{\infty} GnL^2 dL$$

Now the PBE can be expressed in terms of the liquid fractions and this can be used in the other balances. Substituting the expression for ε and rearrange:

$$\varepsilon(t) = 1 - k_V m_3(t)$$

$$\frac{d\varepsilon}{dt} = \frac{1-\varepsilon}{V}\frac{dV}{dt} - k_v gm2 - \frac{1}{V}\sum_{j}^{Ni}\phi_{V,in,j}\left(1-\varepsilon_{in,j}\right) + \frac{1}{V}\sum_{j}^{No}\phi_{V,out,j}\left(1-\varepsilon_{out,j}\right)$$

Total Mass Balance

The total mass balance for liquid phase has the form:

$$\underbrace{\frac{dm^{(l)}}{dt}}_{\text{Accumulation [kg/s]}} = \underbrace{\phi_{m,in}^{(l)}}_{\text{Inflow}} - \underbrace{\phi_{m,out}^{(l)}}_{\text{Outflow}} - \underbrace{\Psi^{(l\to s)} - \Psi^{(l\to v)}}_{\text{Transfer-terms}}$$

With

$$m_l = \varepsilon V \rho_l$$

Gives:

$$\frac{d}{dt}\{\varepsilon V \rho_l\} = \phi_{V,in}\{\varepsilon_{in}\rho_l\} - \phi_{V,out}\{\varepsilon\rho_l\} - \Psi^{(l\to s)} - \Psi^{(l\to v)}$$

The total mass balance for solid phase has the form:

$$\frac{dm^{(s)}}{dt} = \phi_{m,in}^{(s)} - \phi_{m,out}^{(s)} + \Psi^{(l\to s)}$$

With

$$m_s = (1-\varepsilon)V\rho_c$$

Gives:

$$\frac{d}{dt}\{(1-\varepsilon)V\rho_c\} = \phi_{V,in}\{(1-\varepsilon_{in})\rho_c\} - \phi_{V,out}\{(1-\varepsilon)\rho_c\} + \Psi^{(l\to s)}$$

Add above balances to obtain the mass balance for the slurry *(s+l)*:

$$\frac{dm^{(s+l)}}{dt} = \phi_{m,in}^{(l)} + \phi_{m,in}^{(s)} - \phi_{m,out}^{(l)} - \phi_{m,out}^{(s)} - \Psi^{(l\rightarrow v)}$$

$$\frac{d}{dt}\underbrace{\left\{\varepsilon V\rho_l + (1-\varepsilon)V\rho_c\right\}}_{\text{Total mass in crystallizer}} = \sum_j^{Ni}\phi_{V,in}\left\{\varepsilon_{in}\rho_l + (1-\varepsilon_{in})\rho_c\right\} - \sum_j^{Ni}\phi_{V,out}\left\{\varepsilon\rho_l + (1-\varepsilon)\rho_c\right\} - \phi_{V,vap}\rho_v$$

The accumulation term of the equation can be rewritten as (assuming constant densities):

$$\frac{d}{dt}\left\{\varepsilon V\rho_l + (1-\varepsilon)V\rho_c\right\} = \left(\varepsilon\rho_l + (1-\varepsilon)\rho_c\right)\frac{dV}{dt} + V\left(\rho_l - \rho_c\right)\frac{d\varepsilon}{dt}$$

Substitute the expression for the derivative of the liquid fraction from the population balance:

$$\frac{d}{dt}\left\{\varepsilon V\rho_l + (1-\varepsilon)V\rho_c\right\} = \left(\varepsilon\rho_l + (1-\varepsilon)\rho_c\right)\frac{dV}{dt} +$$
$$\left(\rho_l - \rho_c\right)\left[(1-\varepsilon)\frac{dV}{dt} - k_v V g m_2 - \sum_j^{Ni}\phi_{V,in,j}\left(1-\varepsilon_{in,j}\right) + \sum_j^{No}\phi_{V,out,j}\left(1-\varepsilon_{out,j}\right)\right]$$

Rearranging the terms of *dV/dt* and substitution of the RHS equation in the total mass balance gives:

$$\rho_l\frac{dV}{dt} + \left(\rho_l - \rho_c\right)\left[-k_v V g m_2 - \sum_j^{Ni}\phi_{V,in,j}\left(1-\varepsilon_{in,j}\right) + \sum_j^{No}\phi_{V,out,j}\left(1-\varepsilon_{out,j}\right)\right]$$
$$= \sum_j^{Ni}\phi_{V,in,j}\left(\varepsilon_{in,j}\rho_l + \left(1-\varepsilon_{in,j}\right)\rho_c\right) - \sum_j^{No}\phi_{V,out,j}\left(\varepsilon_{out,j}\rho_l + \left(1-\varepsilon_{out,j}\right)\rho_c\right) - \phi_{V,vap}\rho_v$$

Rearranging of all the inlet and outlet streams leads to the total mass balance over the slurry which can also be seen as an equation relating the rate of change of the volume of the system to the crystal growth term and the balance of the input and output streams:

$$\underbrace{\rho_l\frac{dV}{dt} - \left(\rho_l - \rho_c\right)k_v V g m_2}_{\text{Accumulation [kg/s]}} = \underbrace{\sum_j^{Ni}\phi_{V,in,j}\rho_l}_{\text{Inflow}} - \underbrace{\sum_j^{No}\phi_{V,out,j}\rho_l}_{\text{Outflow}} - \underbrace{\phi_{V,vap}\rho_v}_{\text{Transfer-term}}$$

Initial condition:

$$V(t=0) = V_{init}$$

Solute Component Mass Balance

The mass balance for liquid phase component *i* has the form:

$$\underbrace{\frac{dm}{dt}{}_i^{(l)}}_{\text{Accumulation [kg/s]}} = \underbrace{\phi^{(l)}_{m,i,in}}_{\text{Inflow}} - \underbrace{\phi^{(l)}_{m,i,out}}_{\text{Outflow}} - \underbrace{\Psi_i^{(l\to s)} - \Psi_i^{(l\to v)}}_{\text{Transfer-terms}} + R_i$$

This can be filled in as follows: (Bermingham 2003)

$$\underbrace{\frac{dm(t)}{dt}{}_i^{(l)}}_{\substack{\text{Mass rate of}\\ \text{accumulation [kg/s]}}} = \underbrace{\sum_{k=1}^{N\_in} \phi^{(l)}_{m,i,in,k} - \sum_{n=1}^{N\_out} \phi^{(l)}_{m,i,out,n} - \phi^{(l\to v)}_{m,i,out}}_{\text{Mass rates in and out via convective transport}} + \underbrace{M_i \cdot \sum_{p=1}^{N\_react^{(l)}} \nu^{(l)}_{i,p} \cdot r_p}_{\text{Mass production rate due to liquid phase reactions}} +$$

$$\underbrace{M_i \cdot \sum_{q=1}^{N\_phases^{(s)}} \nu^{(s)}_{i,q} \cdot \left[\phi_{mol,nucl,q}{}^{(l\to s)} + \phi_{mol,grow,q}{}^{(l\to s)} - \phi_{mol,dis,q}{}^{(s\to l)}\right]}_{\substack{\text{Interphase mass flux due to crystal growth and primary nucleation}\\ \text{and dissolution at the critical nucleus size}}}$$

Now apply this to a single-solute single-solvent system, such as ammonium sulphate from water or adipic acid. Take:

- Liquid phase component 1 = solute
- Liquid phase component 2 = solvent
- There is one solid phase
- No liquid phase reactions

Using these definitions, the crystallization reaction in the above-mentioned system can be written as follows:

$$\underbrace{\nu_1^{(s)}}_{=-1} A + \underbrace{\nu_2^{(s)}}_{=0} B + C = 0$$

With these definitions and by assuming that the vapour flow only contains solvent the **liquid phase** component mass balance for the **solute** can be rewritten as follows:

$$\underbrace{\frac{dm}{dt}{}_1^{(l)}}_{\substack{\text{Mass rate of}\\ \text{accumulation [kg/s]}}} = \underbrace{\sum_{k=1}^{N\_in} \phi^{(l)}_{m,1,in,k} - \sum_{n=1}^{N\_out} \phi^{(l)}_{m,1,out,n} \cancel{- \phi^{(l\to v)}_{m,i,out}}}_{\text{Mass rates in and out via convective transport}} \underbrace{- M_1 \cdot \left[\phi_{mol,nucl,q}{}^{(l\to s)} + \phi_{mol,grow,q}{}^{(l\to s)} - \phi_{mol,dis,q}{}^{(s\to l)}\right]}_{\substack{\text{Interphase mass flux due to crystal growth and primary nucleation}\\ \text{and dissolution at the critical nucleus size}}}$$

The following equation for the mass accumulation rate of **solvent** in the liquid phase is obtained:

$$\underbrace{\frac{dm}{dt}{}_2^{(l)}}_{\substack{\text{Mass rate of}\\ \text{accumulation [kg/s]}}} = \underbrace{\sum_{k=1}^{N\_in} \phi^{(l)}_{m,2,in,k} - \sum_{n=1}^{N\_out} \phi^{(l)}_{m,2,out,n} - \phi^{(l\to v)}_{m,2,out}}_{\text{Mass rates in and out via convective transport}}$$

The solvent mass balance is not used because it is not independent of the total mass balance. Removal of solvent is incorporated via the total mass balance. For the model, the equation for the solute needs to be for the slurry phase instead of the liquid phase. First use for the mass of the solute:

$$m_1^{(s+l)} = V\left\{\varepsilon\rho_l w_l + (1-\varepsilon)\rho_c w_c\right\}$$

With ε is volumetric fraction of liquid phase, and w is liquid and crystal weight fraction of the solute. When constant crystal weight fraction is assumed, which is valid when impurities are negligible, rewriting the LHS of the solute mass balance gives:

$$\frac{dm^{(s+l)}}{dt}_1 = \frac{d\left[V\left\{\varepsilon\rho_l w_l + (1-\varepsilon)\rho_c w_c\right\}\right]}{dt} = \left(\varepsilon\rho_l w_l + (1-\varepsilon)\rho_c w_c\right)\frac{dV}{dt} + V\left(\rho_l w_l - \rho_c w_c\right)\frac{d\varepsilon}{dt} + V\varepsilon\rho_l\frac{dw_l}{dt}$$

Substitute again the expression for the derivative of the liquid fraction from the population balance:

$$\frac{dm^{(s+l)}}{dt}_1 = \left(\varepsilon\rho_l w_l + (1-\varepsilon)\rho_c w_c\right)\frac{dV}{dt} + V\varepsilon\rho_l\frac{dw_l}{dt} + \left(\rho_l w_l - \rho_c w_c\right)\left[(1-\varepsilon)\frac{dV}{dt} - \underbrace{k_v V g m2}_{\substack{\text{Interphase mass flux}\\ \text{between liquid and solid}}} - \sum_j^{Ni}\phi_{V,in,j}\left(1-\varepsilon_{in,j}\right) + \sum_j^{No}\phi_{V,out,j}\left(1-\varepsilon_{out,j}\right)\right]$$

The interphase mass flux has appeared here. Since this is a slurry phase balance, the term appears as accumulation and not as sink. Rearranging the terms of *dV/dt*, the solute component mass balance becomes:

$$\begin{aligned}\frac{dm^{(s+l)}}{dt}_1 &= \rho_l w_l\frac{dV}{dt} + V\varepsilon\rho_l\frac{dw_l}{dt} - \left(\rho_l w_l - \rho_c w_c\right)k_v V g m2 + \\ &\quad \rho_l w_l\left[-\sum_j^{Ni}\phi_{V,in,j}\left(1-\varepsilon_{in,j}\right) + \sum_j^{No}\phi_{V,out,j}\left(1-\varepsilon_{out,j}\right)\right] \\ &\quad -\rho_c w_c\left[-\sum_j^{Ni}\phi_{V,in,j}\left(1-\varepsilon_{in,j}\right) + \sum_j^{No}\phi_{V,out,j}\left(1-\varepsilon_{out,j}\right)\right] \\ &= \sum_j^{Ni}\phi_{V,in,j}\left(\varepsilon_{in,j}\rho_l w_{l,in,j} + \left(1-\varepsilon_{in,j}\right)\rho_c w_{c,in,j}\right) - \sum_j^{No}\phi_{V,out,j}\left(\varepsilon_{out,j}\rho_l w_l + \left(1-\varepsilon_{out,j}\right)\rho_c w_c\right)\end{aligned}$$

Now assuming that the solid composition for all streams is the same, ($w_{c,in,j} = w_c$) and that the liquid mass fraction of component i is the same for each output stream, the equation reduces to:

$$\underbrace{V\varepsilon\rho_l \frac{dw_l}{dt} + \rho_l w_l \frac{dV}{dt} - \left(\rho_l w_l - \rho_c w_c\right) k_v V g m_2}_{\text{Accumulation [kg/s]}} = \underbrace{\sum_j^{Ni} \phi_{V,in,j}\left(\varepsilon_{in,j}\rho_l w_{l,in,j} + \left(1-\varepsilon_{in,j}\right)\rho_l w_l\right)}_{\text{Inflow}} \underbrace{-\sum_j^{No}\phi_{V,out,j}\rho_l w_l}_{\text{Outflow}}$$

Initial condition:

$$w_l(t=0) = w_{l,init}$$

From Energy balance to Enthalpy Balance

In general, the dynamics of the temperature are given by the energy balance (Bermingham 2003):

$$\underbrace{\frac{dE}{dt}}_{\substack{\text{Rate of accumulation}\\ \text{of total energy [J/s]}}} = \underbrace{\sum_{k=1}^{N\_in}\phi_{E,in,k} - \sum_{l=1}^{N\_out}\phi_{E,out,l} - \phi_{E,vapour,out}}_{\text{Rate of total energy in and out by convection}} + \underbrace{Q}_{\substack{\text{net rate of}\\ \text{heat addition}}} - \underbrace{W_s}_{\substack{\text{net rate of}\\ \text{shaft work}}} -$$

$$\underbrace{W_{vc}}_{\substack{\text{net rate of}\\ \text{work due to}\\ \text{volume change}}} + \underbrace{\sum_{k=1}^{N\_in}\phi_{m,in,k}\cdot\frac{p_{in,k}}{\rho_{in,k}}}_{\substack{\text{Work needed to}\\ \text{introduce inlet streams}}} - \underbrace{\sum_{l=1}^{N\_out}\phi_{m,out,l}\cdot\frac{p_{out,l}}{\rho_{out,l}}}_{\substack{\text{Work needed to}\\ \text{remove outlet streams}}} - \underbrace{\phi_{m,vapour,out}\cdot\frac{p_{vapour,out}}{\rho_{vapour,out}}}_{\substack{\text{Work needed to}\\ \text{remove vapour stream}}}$$

With

$$E = U + E_k + E_p$$

$$\phi_E = \phi_m\left(\hat{U} + \hat{E}_k + \hat{E}_p\right)$$

Initial condition:

$$E(t=0) = E_{init}$$

For crystallization processes, kinetic energy and potential energy can usually be neglected:

$$\frac{dU}{dt} = \sum_{k=1}^{N\_in}\phi_{m,in,k}\cdot\left(\hat{U}_{in,k} + \frac{p_{in,k}}{\rho_{in,k}}\right) - \sum_{l=1}^{N\_out}\phi_{m,out,l}\cdot\left(\hat{U}_{out,l} + \frac{p_{out,l}}{\rho_{out,l}}\right) -$$

$$\phi_{m,vapour,out}\cdot\left(\hat{U}_{vapour,out} + \frac{p_{vapour,out}}{\rho_{vapour,out}}\right) + Q - W_{vc} - W_s$$

Nevertheless, sometimes shaft work does need to be taken into account, for instance if the work of an agitator is significant. Then there needs to be an expression relating rpm to shaft work. The energy balance can be transformed into the enthalpy balance. The sum of internal energy and work due to the entrance and exit of mass is the enthalpy:

$$\hat{H} = \hat{U} + P\hat{V} = \hat{U} + \frac{p}{\rho}$$

$$\phi_H = \phi_m \cdot \hat{H}$$

$$\frac{dU}{dt} = \sum_{k=1}^{N\_in} \phi_{H,k} - \sum_{l=1}^{N\_out} \phi_{H,l} - \phi_{H,vapour,out} + Q - W_{vc} - W_s = \frac{d(H-pV)}{dt} = \frac{dH}{dt} - \frac{d(pV)}{dt}$$

And

$$W_{vc} = \frac{d(pV)}{dt}$$

The resulting balance is the enthalpy balance as is frequently used in process engineering problems:

$$\frac{dH(t)}{dt} = \sum_{k=1}^{N\_in} \phi_{H,in,k}(t) - \sum_{l=1}^{N\_out} \phi_{H,out,l}(t) - \phi_{H,vapour,out}(t) + Q(t) - W_s(t)$$

Initial condition:

$$H(t=0) = H_{init}$$

Now use this result to set-up an enthalpy balance over the slurry phase. Use for enthalpy:

$$H^{(s+l)} = \varepsilon V \rho_l c_{p,l} T + (1-\varepsilon)\rho_c \left(c_{p,c} T + dH_{crys}\right)$$

The heat of crystallization *dH_{crys}* is the amount of heat to be added or removed at a constant temperature during crystallization and is equal to the negative value of the heat of solution that applies when crystals dissolve. Fill in the expression for *H* and obtain:

$$\begin{aligned}\frac{dH^{(s+l)}}{dt} &= \sum_{j}^{Ni} \phi_{V,in,j} \left(\varepsilon_{in,j}\rho_l c_{p,l} T_{in,j} + \left(1-\varepsilon_{in,j}\right)\rho_c \left(c_{p,c} T_{in,j} + dH_{crys}\right)\right) \\ &-\sum_{j}^{No} \phi_{V,out,j} \left(\varepsilon_{out,j}\rho_l c_{p,l} T + \left(1-\varepsilon_{out,j}\right)\rho_c \left(c_{p,c} T + dH_{crys}\right)\right) \\ &-\phi_{V,vap}\rho_w \left(c_{p,w} T + dH_{evap}\right) + Q_{heat} - W_s\end{aligned}$$

Assuming the density, specific heat and crystallization heat are constant, the LHS can be written as:

$$\begin{aligned}\frac{dH^{(s+l)}}{dt} &= \left(\varepsilon\rho_l c_{p,l} T + (1-\varepsilon)\rho_c \left(c_{p,c} T + dH_{crys}\right)\right)\frac{dV}{dt} + V\left(\varepsilon\rho_l c_{p,l} + (1-\varepsilon)\rho_c c_{p,c}\right)\frac{dT}{dt} \\ &+V\left(\rho_l c_{p,l} T - \rho_c \left(c_{p,c} T + dH_{crys}\right)\right)\frac{d\varepsilon}{dt}\end{aligned}$$

Substitute again the expression for the derivative of the liquid fraction from the population balance:

$$\begin{aligned}\frac{dH^{(s+l)}}{dt} &= \left(\varepsilon\rho_l c_{p,l}T + (1-\varepsilon)\rho_c\left(c_{p,c}T + dH_{crys}\right) + (1-\varepsilon)\rho_l c_{p,l}T - (1-\varepsilon)\rho_c\left(c_{p,c}T + dH_{crys}\right)\right)\frac{dV}{dt}\\
&+V\left(\varepsilon\rho_l c_{p,l} + (1-\varepsilon)\rho_c c_{p,c}\right)\frac{dT}{dt}\\
&+\left(\rho_l c_{p,l}T - \rho_c\left(c_{p,c}T + dH_{crys}\right)\right)\left[-k_v Vgm2 - \sum_j^{Ni}\phi_{V,in,j}\left(1-\varepsilon_{in,j}\right) + \sum_j^{No}\phi_{V,out,j}\left(1-\varepsilon_{out,j}\right)\right]\end{aligned}$$

The enthalpy balance now becomes:

$$\begin{aligned}&\frac{dH^{(s+l)}}{dt} = \left(\rho_l c_{p,l}T\right)\frac{dV}{dt} + V\left(\varepsilon\rho_l c_{p,l} + (1-\varepsilon)\rho_c c_{p,c}\right)\frac{dT}{dt} - \left(\rho_l c_{p,l}T - \rho_c\left(c_{p,c}T + dH_{crys}\right)\right)k_v Vgm2\\
&-\sum_j^{Ni}\phi_{V,in,j}\left(1-\varepsilon_{in,j}\right)\left(\rho_l c_{p,l}T - \rho_c\left(c_{p,c}T + dH_{crys}\right)\right)\\
&+\sum_j^{No}\phi_{V,out,j}\left(1-\varepsilon_{out,j}\right)\left(\rho_l c_{p,l}T - \rho_c\left(c_{p,c}T + dH_{crys}\right)\right)\\
&=\sum_j^{Ni}\phi_{V,in,j}\left(\varepsilon_{in,j}\rho_l c_{p,l}T_{in,j} + \left(1-\varepsilon_{in,j}\right)\rho_c\left(c_{p,c}T_{in,j} + dH_{crys}\right)\right)\\
&-\sum_j^{No}\phi_{V,out,j}\left(\varepsilon_{out,j}\rho_l c_{p,l}T + \left(1-\varepsilon_{out,j}\right)\rho_c\left(c_{p,c}T + dH_{crys}\right)\right) - \phi_{V,vap}\rho_v\left(c_{p,v}T + dH_{evap}\right) + Q_{heat} - W_s\end{aligned}$$

After rearranging, this results in the following enthalpy balance over the slurry phase:

$$\begin{aligned}&\underbrace{V\left(\varepsilon\rho_l c_{p,l} + (1-\varepsilon)\rho_c c_{p,c}\right)\frac{dT}{dt} - \left(\rho_l c_{p,l}T - \rho_c\left(c_{p,c}T + dH_{crys}\right)\right)k_v Vgm2 + \rho_l c_{p,l}T\frac{dV}{dt}}_{\text{Accumulation [J/s]}}\\
&=\underbrace{\sum_j^{Ni}\phi_{V,in,j}\left[\rho_l c_{p,l}T + \left(\varepsilon_{in,j}\rho_l c_{p,l} + \left(1-\varepsilon_{in,j}\right)\rho_c c_{p,c}\right)\left(T_{in,j} - T\right)\right]}_{\text{Enthalpy Inflow}}\\
&\underbrace{-\sum_j^{No}\phi_{V,out,j}\rho_l c_{p,l}T}_{\text{Enthalpy Outflow}} - \underbrace{\phi_{V,vap}\rho_w\left(c_{p,w}T + dH_{evap}\right)}_{\text{Enthalpy out by evaporation}} + \underbrace{Q_{heat}}_{\substack{\text{Net rate of}\\ \text{heat addition}}} - \underbrace{W_s}_{\substack{\text{net rate of}\\ \text{shaft work}}}\end{aligned}$$

Initial condition:

$$T(t=0) = T_{init}$$

Appendix B - Assumptions for conservation equations

The following conservation equations are used in the TBD model:

- Population balance for solid phase particles
- Total mass balance over the slurry phase
- Component mass balance for the solute over the slurry phase
- Enthalpy balance over the slurry phase

Momentum conservation equations are not used

Assumptions

- The compartment is considered well-mixed, so spatially lumped conservation equations can be used
- Gas phase is not modelled
- Immobile phases are not modelled
- The liquid and solid phases are modelled together in a spatially homogeneous slurry phase. There is no difference in flow pattern of the liquid and solid phase due to particle slip
- Rate phenomena occurring in the balances are modelled as separate tasks, and have their own assumptions (see task library in chapter 4).
- Single-solute single-solvent system
- Nucleation occurs at the size boundary and the mass of the nuclei is neglected
- Constant physical properties: ρ_l, ρ_c, ρ_v, $c_{p,l}$, $c_{p,c}$, $c_{p,w}$, dH_{crys}, dH_{evap}
- The solid composition for all streams is the same, i.e. $w_{c,in,j} = w_c$
- The liquid mass fraction of all components is the same for each output stream
- Negligible impurities, such that $w_{c,i}$ is constant
- The model assumes atmospheric pressure.
- The compartment is an open system, capable of exchanging mass and energy with its environment by means of fluxes through one or more of its surfaces (Bermingham 2003). It is assumed that this exchange does not cost energy.
- The particle distribution has one distributed property: the crystal size L
- Solid phase only contains a single pure component
- No agglomeration & breakage
- No growth rate dispersion
- The vapour flow only contains solvent and no solute or crystals
- No liquid phase reactions
- It is assumed that all outlet streams have the same liquid and crystal mass fraction of solute.
- The solid composition for all streams is the same, ($w_{c,in,j} = w_c$)
- The liquid mass fraction of all components is the same for each output stream
- Neglect kinetic and potential energy, such that the energy balance is transformed in an enthalpy balance
- No heat loss to the environment
- No energy input via the mechanical action of the impeller
- In this work, shaft work is omitted

Appendix C - Guidelines to prevent index issues

As described in chapter 5, the model of a flowsheet should be of index-1. Obtaining an index-1 model can be a challenging assignment, therefore below instructions are given for assigning the right variables to prevent index issues.

- First draw the desired flowsheet structure; all compartment blocks with their tasks and all connectivity's.
- Figure 3.2 gives an overview of all differential equations and algebraic equations in one compartment model and also contains a graphical representation of each differential equation. With this representation it is easy to identify all inputs and outputs of one compartment. Essentially the compartment model is described by overlapping those blocks.
- There are several states of the system: $V(t)$, $n(t)$, $w_{l,i}(t)$ and $T(t)$. First determine what happens with these states in time for each compartment. Do these states vary in time or are they constant (steady state)?
- Specify the initial conditions in each compartment. These need to be provided for gPROMS.
- Now the other variables need to be assigned using the balances. As an example the total mass balance for a membrane unit is illustrated. The general total mass balance is:

  $$\rho_l \frac{dV}{dt} = (\rho_l - \rho_c) k_v V g m_2 + \sum_j^{Ni} \phi_{V,in,j} \rho_l - \sum_j^{No} \phi_{V,out,j} \rho_l - E - M \tag{3.28}$$

  In case of a membrane unit, the graphical representation of this balance changes to:

  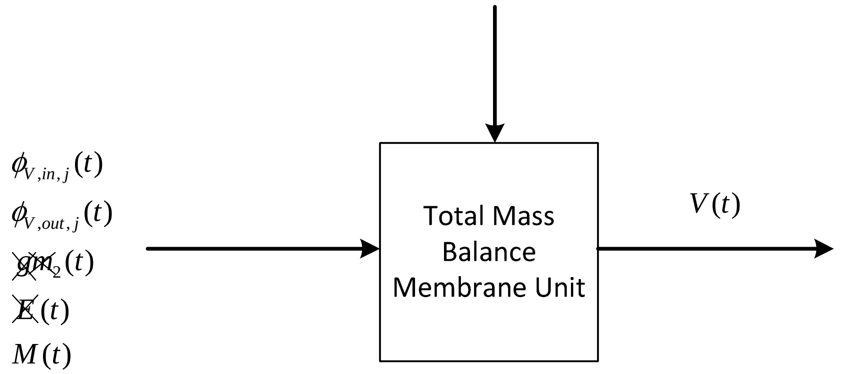

  It can be easily seen that the following options are available:
  - If the volume varies in time, all streams ($\varphi_{V,in,j}(t)$, $\varphi_{V,out,j}(t)$ and $M(t)$) should be specified
  - If the volume is constant all streams *except one* should be specified.
- The same principle holds for all other balances. For instance if the temperature should be constant, the task Heat Transfer can be free to adjust the temperature to the initial value. (Pay attention that this task is then turned on in the model)
- Now specify all the variables in the system using this principle. Use the drawing of the flowsheet to do this, because the output of one compartment can be the input of another compartment. Such a stream can only be assigned once. Recall that a stream contains the following variables: φ_V, $n(L)$, T, ε, w_l.
- Now all inputs for the model are determined, without index issues.

Appendix D - Options for structuring TBD model in gPROMS

Below identified options to structure the TBD model in gPROMS are listed. Note that the final model of this work has the structure of Option 1.

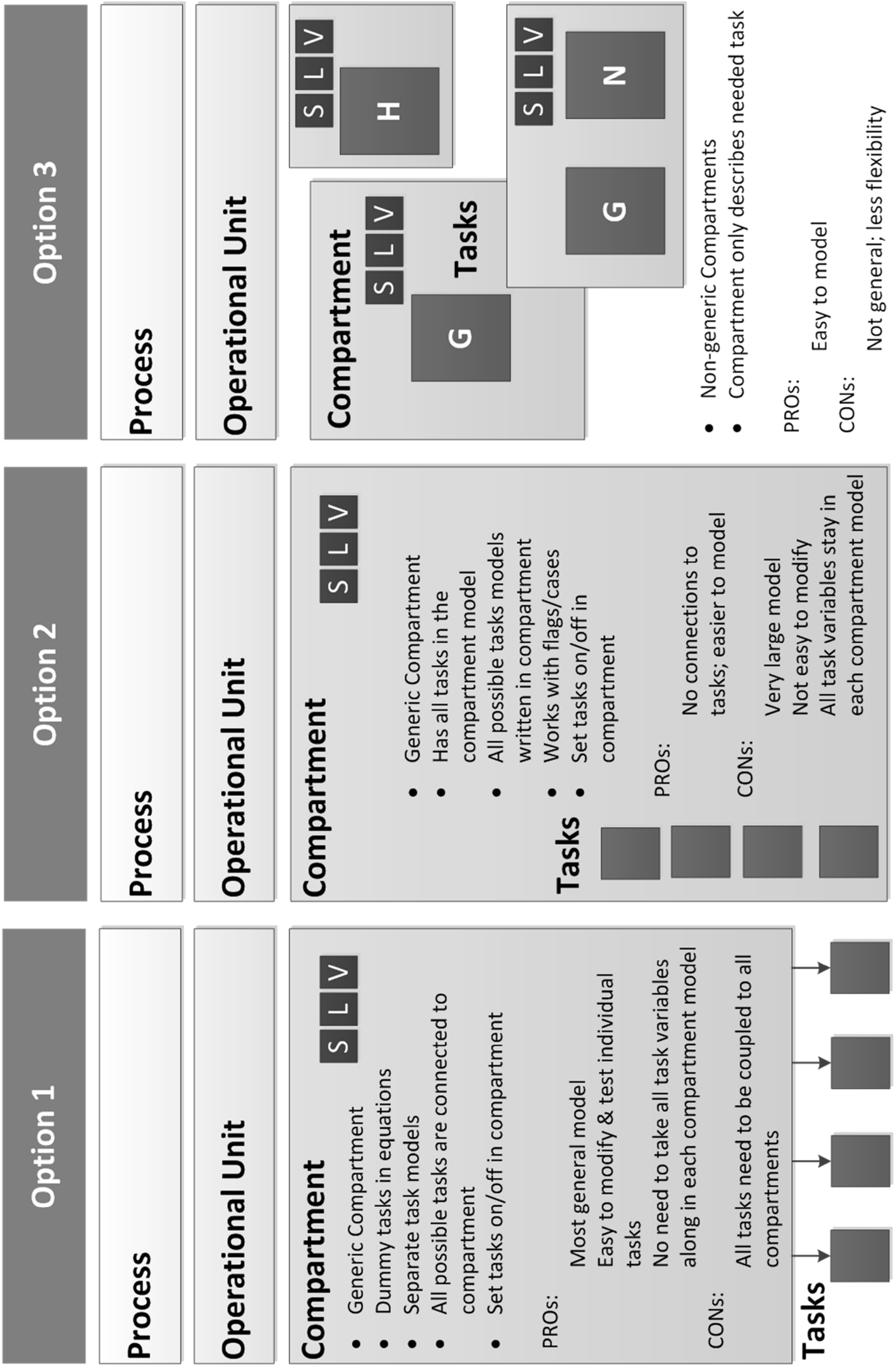

Option 1

- Generic Compartment
- Dummy tasks in equations
- Separate task models
- All possible tasks are connected to compartment
- Set tasks on/off in compartment

PROs:
Most general model
Easy to modify & test individual tasks
No need to take all task variables along in each compartment model

CONs:
All tasks need to be coupled to all compartments

Option 2

- Generic Compartment
- Has all tasks in the compartment model
- All possible tasks models written in compartment
- Works with flags/cases
- Set tasks on/off in compartment

PROs:
No connections to tasks; easier to model

CONs:
Very large model
Not easy to modify
All task variables stay in each compartment model

Option 3

- Non-generic Compartments
- Compartment only describes needed task

PROs:
Easy to model

CONs:
Not general; less flexibility

Appendix E - Verification: Analytical solution MSMPR

To verify the population balance is correctly implemented, numerical solutions of the number density crystal size distribution will be compared with the corresponding analytical solutions of the PBE for a so-called MSMPR crystallizer with simple kinetics. A MSMPR (Mixed Suspension Mixed Product Removal) crystallizer is the crystallization equivalent of the CSTR, and can be characterised as follows:

- Operation:
  - Steady state: $\partial(nV)/\partial t = 0$
  - One feed, crystal free: $n_{in}(L) = 0$
  - One product, unclassified: $n_{out}(L) = n(L)$
- Kinetics:
  - Size-independent growth: $G \neq G(L)$
  - Crystal birth at size zero: $B(L) = 0$; $B_0 \geq 0$
  - No death of crystals: $D(L) = 0$

Taking the PBE presented in chapter 1 and applying the above characteristics gives a strongly simplified PBE:

$$0 = -VG\frac{\partial n(L)}{\partial L} - \phi_{V,out} \cdot n(L)$$

This can be rewritten as:

$$\frac{dn(L)}{n(L)} = -\frac{\phi_{V,out}}{VG}dL$$

Integrating both sides from L equals zero to L and rearranging gives the analytical solution for the number density distribution in a MSMPR crystallizer:

$$n(L) = n_0 \exp\left(-\frac{L}{G\tau}\right)$$

The following is used:

- A residence time, τ, of 1000 s. ($V = 10$ [m^3], $\varphi_V = 0.01$ [m^3/s])
- A linear growth rate, $T_{G,GROWTH}$, of $2 \cdot 10^{-7}$ [m/s].
- A nucleation rate, $T_{N,PN}$, of 10^6 [#/m^{3}s].
- A linear grid with lower bound, L_{min}, of 0 [m] and upper bound, L_{max}, of $3 \cdot 10^{-3}$ [m].
- Number of grid points: 100 (and 200 to compare)
- Numerical solution using “normal” number density (not logarithm of number density)
- The runtime is multiple times the residence time to make sure steady state is reached.

The accuracy of numerically calculated partial derivatives is studied by comparing the analytical solution of the number density distribution with that obtained by numerical solution of the PBE with 100 and 200 gridpoints. In case of a steady state the logarithm of *n(L)* is a straight line. Figure D.1 depicts the results.

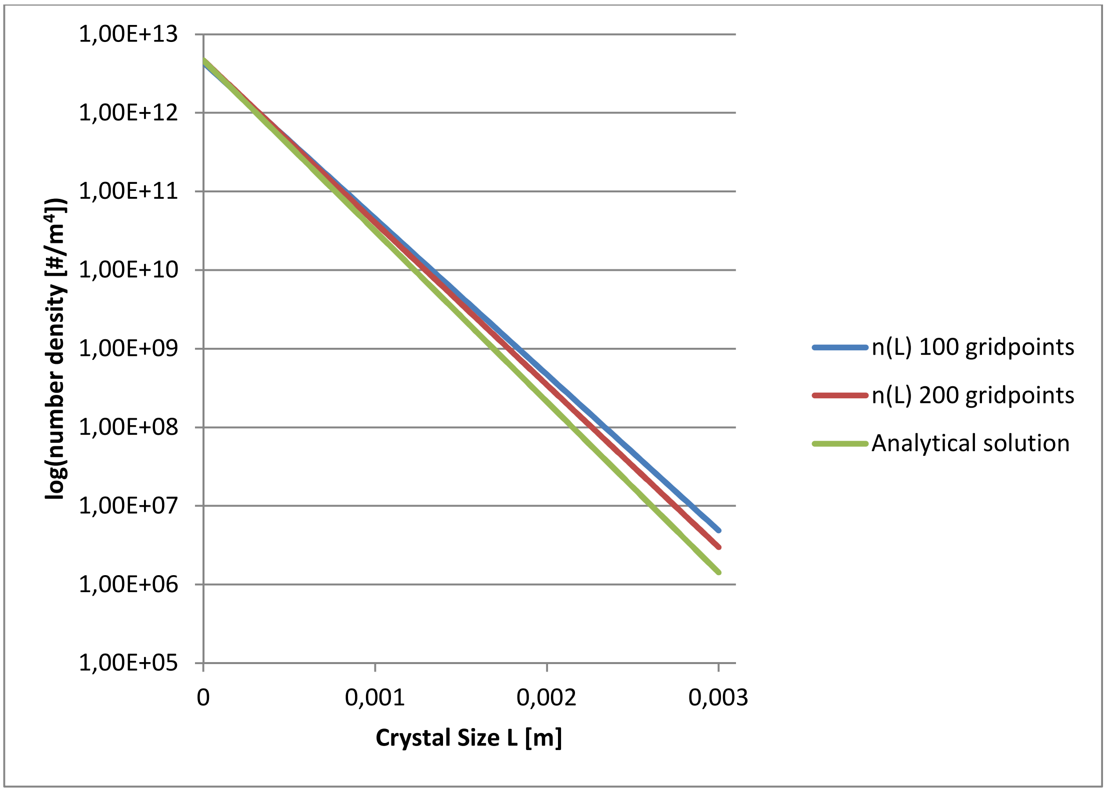

Figure D.1: Number density MSMPR - Analytical and numerical solution

It can be seen that a steady state is reached because the obtained lines are straight and the numerical solution is in agreement with the analytical solution. The influence of the discretisation resolution (100 and 200 grid points) on the accuracy of the number density distribution is also visible. As expected, the accuracy of the numerical solution increases with the number of grid points. In this study, 100 gridpoints is chosen, since the interest is in trends and not accuracy and more gridpoints increases computational time. An increase in the number of grid points causes an increase in the number of algebraic and differential variables so also an increase is seen for the simulation times.

It is also good to note that according to (Bermingham 2003) when using the same number of grid points and the same form for the number density in the PBE ("normal" number density), the accuracy of the numerical solution obtained on a linear grid is better than that obtained on a logarithmic grid. Furthermore, when using the same number of grid points and the same type of grid, the accuracy of the numerical solution obtained when using the logarithm of the number density in the PBE is better than that obtained with the "normal" number density.

This case is the same as the analytical case described in (Bermingham 2003).

Appendix F - Detailed settings for cases

Case 1

System: Ammonium Sulphate

- V_{init} = 18 L (Soare, et al. 2012)
- T_{init} = 334,65K
- W_{feed} = Saturated at 334,65 K
- Parameters with respect to the task Seeding:
  - F_1 = 1
  - L_{g1} = 125e-6
  - σ_1 = 1,3
  - L_{g2} = 93e-6
  - σ_2 = 3,3
  - Initial crystal content per cube: $x/0{,}018$ [kg/m^3] with x = 0,007; 0,02; 0,03; 0,04
- Cooling Curve implementation:
  - To reproduce the cooling curve, the following equation is implemented in the flowsheet:

    $$\frac{dT}{dt} = \Delta T$$
  - With as first part of the curve ΔT = -0,125/60, until T = 334,65 – 12,5
  - Then ΔT = -0,25/60 until T < (334,65 – 36,5)
  - So that the runtime is 11760 seconds

For calculation of ideal growth median sizes the following parameters are used:

m_seeds [g]	*C_seed [%]*	*Experiment Size [µm]*	*Ideal size [µm]*	*Model Median Size [µm]*
7	0,551989909	580	708,5924543	671,074
20	1,577114027	440	501,0575433	480,166
30	2,365671041	410	438,8438412	422,607
40	3,154228054	390	399,7372872	386,307
	w_crystals theoretical [kg]		1,268139124	
	L_seeds [µm]		125	

Case 2

System: Adipic Acid

Crystallization Compartment:

- V_{init} = 0,0015 m^3
- T = 313 K
- W_{feed} = undersaturated at 312 K

Membrane Compartment (operated under conditions of (Kuhn, et al. 2009)):

- V = 1,5 · 10^{-5} m^3
- T = 323 K
- The flowrate between the two compartments is 3,3·10^{-4} [m^3/s] (20 [L/min])
- Membrane unit operating at a pressure difference of 25 bar, for a solution saturated at 313 K, gives a total flux of 20 [kg/m^2h]
- Membrane surface area A = 0.0240 [m^2]
- So membrane solvent mass flow φ_m = (20 / 3600) * 0,0240 = 0,000133 [kg/s]

Runtime is 4000 seconds.

In case 2c at t = 2300 [s] the temperature is increased from 313 to 318 [K] for 500 seconds.

Case 3

System: Adipic Acid

Ultrasound Compartment:

- V = 0.5 L, this is chosen so that the residence time of the slurry in the ultrasound compartment is in the order of minutes, so that there is negligible growth of crystals
- T = 313 K
- Inflow:
  - $n = 0$
  - $\varepsilon = 1$
  - T =316 K
  - w_{feed} = saturated at 314,5 K, so that this is undersaturated in the feed but supersaturated under the ultrasound compartment conditions.
  - $\varphi_{V,in}$ = 9,002635·10^{-6} (determined after running case 3b)

Airlift Compartment:

- V = 18 L (Soare, et al. 2012)
- T = 313 K
- Product flow is determined by the residence time of Case 1 in the crystallizer:

$$\phi_V = \frac{V}{\tau} = \frac{0.018}{12000} = 1{,}5\cdot 10^{-6}\left[\frac{m^3}{s}\right]$$

-
- The flow from the airlift to the buffer contains no crystals (Classification) and $\varphi_{V,out}$ = 5·10^{-4}

Buffer Compartment

- V = 10 L (Kuhn, et al. 2009)
- T = 333 K, same temperature as the membrane unit
- The liquid fraction of solute, w_l, is kept saturated at 315 K. In this way the slurry is undersaturated in the buffer and membrane compartments, but is supersaturated in

the airlift compartment conditions, so that it can be used to control supersaturation in the airlift compartment.

- w_l is controlled by the solvent flow out of the membrane compartment.
- In the model, the volume of the buffer compartment is not kept constant directly by setting *dV/dt* zero. Instead, it is recognised that the total volume of the buffer + membrane should be constant, and this mass balance is used as

  $\phi_{m,in,airlift} = \phi_{m,out,airlift} - \phi_{m,out,membrane}$

Membrane Compartment (operated under conditions of (Kuhn, et al. 2009)):

- *V* = 0,18 L (arbitrarily chosen small)
- *T* = 333 K (highest possible to assure flexibility of solvent out flow)
- The flowrate between the buffer and membrane compartments is $3{,}3 \cdot 10^{-4}$ [m^3/s] (20 [L/min])
- Membrane solvent mass flow is determined by the supersaturation needed in the airlift compartment. This flow is adjusted by changing the pressure difference in the membrane unit. A relation for this can be found in (Kuhn, et al. 2009)

All temperatures are kept constant by Heat Transfer tasks in all compartments, perfect controllers are assumed.

Runtime is a multiple of the mean residence time of 12000 s, so that a steady state is reached.

In case 3b:

- In case 3b 3 airlift crystallizers with a total volume of 18L are put in series.
- In the first airlift compartment, the following is used:

  $\phi_{m,out,airlift} = \phi_{m,in,airlift} - \phi_{m,out,membrane}$
- And in airlift compartments 2 and 3:

  $\phi_{m,out,airlift} = \phi_{m,in,airlift}$ (from buffer and to buffer)
- Constant relative supersaturation σ = 0,01 [-], controlled by supersaturation controllers which set the flowrates of supersaturated flows to the airlift compartments from the buffer compartment
- Further, the same values are used as in Case 3a

Appendix G - Parameter settings for ammonium sulphate

Physical properties

M	Molecular weight	0,132134	[kg/mol]	(Westhoff 2002)
ρ_l	Density liquid phase	1248	[kg/m^3]	(Lakerveld 2010)
ρ_c	Density solid phase	1769	[kg/m^3]	(Westhoff 2002)
k_V	Volumetric shape factor	0,43	[-]	(Westhoff 2002)
dH_{crys}	Heat of crystallization	-6,8e3/0,132134	[J/kg]	(Westhoff 2002)

$$c_{p,c} = \left(1,3760 + (2,13 \cdot 10^{-2} \cdot (T - 273,15))\right) \cdot 1000$$

$$c_{p,l} = \left(4,259 - 3,0321 \cdot w_{sat} - 1,7668 \cdot 10^{-3} \cdot (T - 273,15) + 4,2874 \cdot 10^{-6} \cdot (T - 273,15)^2\right) \cdot 1000$$

(Westhoff 2002)

Kinetic properties

k_G	Growth rate constant	7,5E-05	[m/s]	(Lakerveld 2010)
δ	Growth rate factor	1,0	[-]	(Lakerveld 2010)

Solubility properties

Solubility behaviour of ammonium sulphate in water as function of temperature (range -6.55 till 90 °C) (Daudey 1987):

$$w_{sat} = 0,41179 + (9,121 \cdot 10^{-4} \cdot (T - 273,15))$$

Appendix H - Parameter settings for adipic acid

Physical properties

$C_{p,l}$	Heat capacity of the liquid phase	2420	[J/kgK]	(Kuhn, et al. 2009)
M	Molecular weight Adipic Acid	0,146	[kg/mol]	(Kuhn, et al. 2009)
ρ_l	Density liquid phase	1000	[kg/m^3]	(Kuhn, et al. 2009)
ρ_c	Density solid phase	1344	[kg/m^3]	(Kuhn, et al. 2009)
k_V	Volumetric shape factor	π/6	[-]	(Kuhn, et al. 2009)
dH_{crys}	Heat of crystallization (from water)	-265300	[J/kg]	(Invista website)
dH_{evap}	Heat of evaporation water (100C)	2257000	[J/kg]	(Janssen and Warmoeskerken 1987)
$C_{p,c}$	Heat capacity of the solid phase	1590	[J/kgK]	(Invista website)
$C_{p,w}$	Heat capacity of the solvent	4185	[J/kgK]	(Janssen and Warmoeskerken 1987)

Kinetic properties

k_G	Growth rate constant	1,27E-06	[m/s]	(Mohan, Boateng and Myerson 2000) at 313K
δ	Growth rate factor	0,85	[-]	(Mohan, Boateng and Myerson 2000) at 313K
A_{PN}	Primary Nucleation rate factor	1,126E+13	[#/m^{3}s]	(David, et al. 1991) at 313K
B_{PN}	Primary Nucleation rate factor	0,316	[-]	(David, et al. 1991) at 313K
k_{SN}	Attrition rate constant	1,9E+10	[#/mole s]	(Lakerveld 2010)
k_{DIS}	Dissolution rate constant	1,27E-06	[m/s]	chosen equal to k_G
ζ	Dissolution rate factor	1	[-]	(Lakerveld 2010)
k_{PN}	Ultrasound rate constant	2,8E+09	[#/mole s]	(Lakerveld 2010)
κ_{US}	Fraction of maximal US	1	[-]	(Lakerveld 2010)
α	Ultrasound rate factor	2	[-]	(Lakerveld 2010)

Solubility properties

Solubility behaviour of adipic acid in water as function of temperature (Kuhn, et al. 2009):

$$w_{sat} = w_{sat,\min} e^{\beta(T - T_{\min})}$$

T_{min}	Minimum temperature solubility curve	283	[K]	(Kuhn, et al. 2009)
$w_{sat,min}$	Saturated concentration at T_min	0,0108	[kg/kg]	(Kuhn, et al. 2009)
β	Exponential factor solubility curve	0,0519	[-]	(Kuhn, et al. 2009)

Appendix I - Supersaturation PI Controller

To be able to keep the supersaturation in a compartment constant, a Proportional Integral (PI) controller is implemented in the TBD model. Below the feedback control algorithm of a PI controller is given.

In feedback control, the objective is to reduce the error signal to zero where:

$$e(t) = y_{sp}(t) - y_m(t)$$

$e(t)$ = error signal

$y_{sp}(t)$ = set point

$y_m(t)$ = measured value of controlled variable

In a PI controller, integral control action is used in conjunction with proportional control. Proportional control action takes immediate corrective action as soon as an error is detected and integral control provides the elimination of offset (steady-state error) by providing automatic reset. The formula of a PI controller is:

$$p(t) = p_{bias} + K_c \left(e(t) + \frac{1}{\tau_I} \int_0^t e(t^*) dt^* \right)$$

$p(t)$ = controller output

p_{bias} = bias (steady-state) value

K_c = controller gain

τ_I = reset time

The **bias value** p_{bias} is adjusted so that the controller output and consequently the manipulated variable are at their nominal steady-state values when the error is zero. The **controller gain** K_c can be adjusted to make the controller output changes as sensitive as desired to deviations between setpoint and controlled variable. During each **reset time** τ_I, the integral term contributes the same amount to the controller output $p(t)$ as the proportional term. Reset windup occurs when the PI controller encounters as sustained error, for example during the start-up of a batch process or after a large set-point change. The undesirable effects of too much integral action can be avoided by proper tuning of controller gain and the reset time or by including derivative action.

In the TBD model, the setpoint $y_{sp}(t)$ can now be a certain supersaturation, and the output $p(t)$ can be for example the solvent flow out of the system or the temperature.

This is a shorter version of the description presented in (Seborg, Edgar and Mellichamp 2004).

Appendix J - gPROMS codes

Compartment model

```
# MODEL CompartmentModel

PARAMETER
   NoGrid            AS INTEGER
   NoFlowIn          AS INTEGER                  # no of input flows
   NoFlowOut         AS INTEGER                  # of output flows
   NoComp            AS INTEGER    DEFAULT 2     # of components

 # Tasks ON/OFF 0 or 1
   GrowthActive      AS INTEGER    DEFAULT 0
   USActive          AS INTEGER    DEFAULT 0
   EvapActive        AS INTEGER    DEFAULT 0
   HeatActive        AS INTEGER    DEFAULT 0
   BDActive          AS INTEGER    DEFAULT 0
   AttrActive        AS INTEGER    DEFAULT 0
   MembrActive       AS INTEGER    DEFAULT 0
   SeedActive        AS INTEGER    DEFAULT 0
   DisActive         AS INTEGER    DEFAULT 0
   NuclActive        AS INTEGER    DEFAULT 0

UNIT
   sd                AS  Global_SizeDomain
   sp                AS  Global_SystemProperties_Adp

   G_GRW             AS ARRAY(GrowthActive)      OF Task_Growth
   G_DIS             AS ARRAY(DisActive)         OF Task_Dissolution
   N_PN_US           AS ARRAY(USActive)          OF Task_PrimaryNucleationUS
   N_SN_ATTR         AS ARRAY(AttrActive)        OF Task_Attrition
   N_PN              AS ARRAY(NuclActive)        OF Task_PrimaryNucleation
   E_Evap            AS ARRAY(EvapActive)        OF Task_Evaporation
   Q_Heat            AS ARRAY(HeatActive)        OF Task_HeatTransfer
   Y_BD              AS ARRAY(BDActive)          OF Task_BirthDeath
   M_Mem             AS ARRAY(MembrActive)       OF Task_SolvRemovalMembr
   I_Seed            AS ARRAY(SeedActive)        OF Task_Seeding

PORT
   in                AS ARRAY (NoFlowIn)         OF SlurryConnection
   out               AS ARRAY (NoFlowOut)        OF SlurryConnection
   sp_out            AS SystemProperties
   prod_out          AS ProductConnection

VARIABLE
  T                  AS                                    Temperature
  V                  AS                                    Volume
  n                  AS ARRAY(NoGrid)                  OF NumberDensity
  h                  AS ARRAY(NoFlowOut, NoGrid)       OF Classification
  m3                 AS                                    Moment
  gm2                AS                                    Moment
```

```
 m3_out              AS ARRAY(NoFlowOut)                OF Moment
 eps                 AS                                    VolumeFraction
 w                   AS ARRAY(NoComp)                   OF WeightFraction
 w_c                 AS ARRAY(NoComp)                   OF WeightFraction
 sig                 AS                                    Supersaturation

 GG                  AS ARRAY(NoGrid)                   OF GrowthRate
 G_Gr                AS ARRAY(NoGrid)                   OF GrowthRate
 G_Ds                AS ARRAY(NoGrid)                   OF GrowthRate
 NN                  AS                                    NucleationRate
 N_US                AS                                    NucleationRate
 N_Attr              AS                                    NucleationRate
 N_B                 AS                                    NucleationRate
 YY                  AS ARRAY(NoGrid)                   OF BirthDeathRate
 EE                  AS                                    MassFlowrate
 QQ                  AS                                    HeatingRate
 MM                  AS                                    MassFlowrate
 II                  AS ARRAY(NoGrid)                   OF NumberDensity

SET
### EQUATE PARAMETERS IN SYSTEM PROPERTY CONNECTION ###
   sp_out.delta        := sp.delta ;
   sp_out.k_G          := sp.k_G ;
   sp_out.kappa_US     := sp.kappa_US ;
   sp_out.k_PN         := sp.k_PN ;
   sp_out.rho_c        := sp.rho_c ;
   sp_out.k_V          := sp.k_V ;
   sp_out.MW           := sp.MW;
   sp_out.k_SN         := sp.k_SN;
   sp_out.alpha        := sp.alpha;
   sp_out.k_DIS        := sp.k_DIS;
   sp_out.zeta         := sp.zeta;
   sp_out.A_PN         := sp.A_PN;
   sp_out.B_PN         := sp.B_PN;

TOPOLOGY
### CONNECT TASK SUBMODELS TO SYSTEM PROPERTY CONNECTION ###
 FOR i := 1 TO GrowthActive DO
          sp_out = G_GRW(i).sp_in ;
 END
 FOR i := 1 TO USActive DO
          sp_out = N_PN_US(i).sp_in;
 END
 FOR i := 1 TO NuclActive DO
          sp_out = N_PN(i).sp_in;
 END
 FOR i := 1 TO SeedActive DO
          sp_out = I_Seed(i).sp_in;
 END
 FOR i := 1 TO AttrActive DO
          sp_out = N_SN_Attr(i).sp_in;
```

```
 END
 FOR i := 1 TO DisActive DO
        sp_out = G_DIS(i).sp_in;
 END

EQUATION
  prod_out.n    = n;

#####  TASKS  #####
# GG GROWTH
  sig     = G_GRW().sig;                          # GROWTH
  sig      = G_DIS().sig;                         # DISSOLUTION
    FOR i := 1 TO NoGrid DO
        G_GR(i)           = SIGMA(G_GRW().G(i));
        G_DS(i)           = SIGMA(G_DIS().Dis(i));
        GG(i)             = G_GR(i) + G_DS(i);
    END

# NN NUCLEATION (BIRTH TERMS AT SIZE NUCLEUS)
  NN             = N_US + N_Attr + N_B;
  N_US           = SIGMA(N_PN_US().N_US);       # PRIMARY NUCLEATION ULTRASOUND
  sig            = N_PN_US().sig;
  N_B            = SIGMA(N_PN().N_B);            # PRIMARY NUCLEATION
  sig            = N_PN().sig;
  m3             = N_PN().m3;
  N_Attr         = SIGMA(N_SN_ATTR().N_Attr);   # SECUNDARY NUCLEATION ATTRITION
  sig            = N_SN_ATTR().sig;
  eps            = N_SN_ATTR().eps;

# YY BIRTH & DEATH TERMS
  YY             = SIGMA(Y_BD().Y);

# EE EVAPORATION
  EE             = SIGMA(E_Evap().E);

# QQ HEATING
  QQ             = SIGMA(Q_Heat().Q);

# MM SOLVENT REMOVAL (MEMBRANE)
  MM             =  SIGMA(M_Mem().M);

# II SEEDING
  FOR i :=1 TO NoGrid DO
        II(i)      = SIGMA(I_Seed().n_init(i));
  END

#### OTHER ####
  T              = sp.T;
  w_c            = sp.w_c;
  eps            = 1 - sp.k_V * m3 ;                # Liquid fraction
  sig            = ((w(1) - sp.w_sat) / sp.w_sat);  # Relative supersaturation
```

```
  m3              = SIGMA (n * sd.L ^ 3) * sd.dL;           # Third moment
  gm2             = 3 * SIGMA(GG * n * sd.L^2) * sd.dL;    # The growth-moment

### OUTPUT SLURRY CONNECTION ###
  FOR j := 1 TO  NoFlowOut DO
    out(j).n              = n * h(j,);                     # CLASSIFICATION
    m3_out(j)             = SIGMA (out(j).n * sd.L^3) * sd.dL;
    out(j).eps            = 1 - sp.k_V * m3_out(j);
    out(j).w(1)           =  w(1);
    out(j).T              = T;
    SIGMA(out(j).w)       = 1;
  END

##### BALANCES #####
# Total mass balance
  SIGMA(w)      = 1;
  sp.rho_l * $V = (sp.rho_l - sp.rho_c) * sp.k_V * V * gm2
                        + (SIGMA (in().phiV) - SIGMA (out().phiV)) * sp.rho_l - EE - MM;

# Component mass balances (here only for solute; w(1))
  FOR i := 1 TO NoComp-1 DO
    V * eps * sp.rho_l * $w(i) =  - sp.rho_l * w(i) * $V + (sp.rho_l * w(i)
    - sp.rho_c * w_c(i)) * sp.k_V * V * gm2 + SIGMA (in().phiV * (in().eps * sp.rho_l * in().w(i)
    + (1 - in().eps) * sp.rho_l * w(i))) - SIGMA (out().phiV * sp.rho_l * w(i)) ;
  END

# Enthalpy balance
    V * (eps * sp.rho_l * sp.cp_l + (1 - eps) * sp.rho_c * sp.cp_c) * $T
      = (sp.rho_l * sp.cp_l * T - sp.rho_c * (sp.cp_c * T + sp.dH_cryst)) * sp.k_V * V * gm2 –
         sp.rho_l * sp.cp_l * T * $V + SIGMA (in().phiV * (sp.rho_l * sp.cp_l * T
         + (in().eps * sp.rho_l * sp.cp_l + (1 - in().eps) * sp.rho_c * sp.cp_c)* (in().T - T))) –
         SIGMA (out().phiV * sp.rho_l * sp.cp_l * T) - EE * (sp.cp_w * T + sp.dH_evap) + QQ;

# Population balance: GG is size independent - solved with finite volume scheme
  IF  GG(1) > 0 OR GG(1) = 0 THEN
         $n(1) = - ( GG(1) * n(1) - NN) / sd.dL - n(1)/V * $V + YY(1)
             - SIGMA (out().phiV * out().n(1))/V + SIGMA (in().phiV  * in().n(1))/V ;
    FOR i := 2 TO  NoGrid DO
         $n(i) = - (GG(i) * n(i) - GG (i - 1) * n(i - 1)) / sd.dL - n(i)/V * $V + YY(i)
          - SIGMA (out().phiV * out().n(i))/V + SIGMA (in().phiV * in().n(i))/V ;
    END
  ELSE  # GG < 0
         $n(NoGrid) = - (0 - GG(NoGrid) * n(NoGrid)) / sd.dL - n(NoGrid)/V * $V + YY(NoGrid)
             - SIGMA (out().phiV * out().n(NoGrid))/V + SIGMA (in().phiV * in().n(NoGrid))/V ;
    FOR i := 1 TO NoGrid-1 DO
         $n(i) = - (GG (i + 1) * n (i + 1) - GG(i) * n(i)) / sd.dL - n(i)/V * $V + YY(i)
            - SIGMA (out().phiV * out().n(i))/V + SIGMA (in().phiV * in().n(i))/V ;
    END
  END
```

Process flowsheet Case 1

```
# PROCESS Flowsheet
PARAMETER
  NoGrid                   AS INTEGER
  NoComp                   AS INTEGER
  L_min, L_max             AS REAL
  V_init                   AS REAL
  T_init                   AS REAL
  w_feed                   AS REAL

UNIT
  Flowsheet                AS        Flowsheet_Case1__Amn_Airlift_Validation_Batch

SET
  NoGrid          := 100;
  NoComp          := 2;
  L_min           := 10e-6;
  L_max           := 1.5e-3;

## Initial settings
  V_init          := 0.018;
  T_init          := 334.65;
  w_feed          := 0.41179 + (9.121e-4 * (334.65 - 273.15));  #Saturated

### SEEDING ###
 WITHIN  Flowsheet.cr.I_Seed(1) DO
  L_m(1)                 :=  125e-6  ;             #  xmean log normal distribution 1
  s_d(1)                 :=  1.3  ;                #  standard deviation
  L_m(2)                 :=  93e-6  ;              #  xmean log normal distribution 2
  s_d(2)                 :=  3.3 ;                 #  standard deviation
  frac1                  :=  1;                    #  fraction of distribution 1
  seeds_density          :=  0.030 / 0.018 ;       #  initial crystal content [kg / m^3]
 END

# Start Unit Specifications
   WITHIN Flowsheet DO
      WITHIN cr DO
         AttrActive          := 0 ;
         BDActive            := 0 ;
         DisActive           := 0 ;
         EvapActive          := 0 ;
         GrowthActive        := 1 ;
         HeatActive          := 1 ;
         MembrActive         := 0 ;
         NoFlowIn            := 0 ;
         NoFlowOut           := 0 ;
         NuclActive          := 0 ;
         SeedActive          := 1 ;
         USActive            := 0 ;
      END # WITHIN cr
```

```
   END # WITHIN Flowsheet
# End Unit Specifications

ASSIGN
WITHIN Flowsheet DO
         d_T := -0.125/60;   #First part cooling curve
END

INITIAL  # Initial condition specification
  WITHIN Flowsheet.cr DO
            V               = V_init;
            T               = T_init;
         FOR i := 1 TO NoGrid DO
                  n(i)      = SIGMA(I_Seed().n_init(i));
         END
            w(1)            = w_feed;
  END

SOLUTIONPARAMETERS
   DASolver := "DASOLV" ["OutputLevel" := 2]

SCHEDULE
SEQUENCE
   CONTINUE UNTIL Flowsheet.cr.T < (334.65 - 12.5)
      RESET
         WITHIN Flowsheet DO
            d_T := -0.25/60;
         END
      END
   CONTINUE UNTIL Flowsheet.cr.T < (334.65 - 36.5)
END
```

Example task Primary Nucleation

```
# MODEL Task_PrimaryNucleation
PORT
   sp_in AS SystemProperties

VARIABLE
   N_B         AS                    NucleationRate
   sig         AS                    Supersaturation

EQUATION
IF sig < 0  OR sig = 0 THEN
         N_B      = 0;
ELSE
         N_B      = sp_in.A_PN * exp ( - sp_in.B_PN / ((log (sig+1) )^2));
END
```